Bushfire Weather in Southeast Australia: Recent Trends and Projected Climate Change Impacts

C. Lucas, K. Hennessy*, G. Mills and J. Bathols*

Bushfire CRC and Australian Bureau of Meteorology
* CSIRO Marine and Atmospheric Research

September 2007

Consultancy Report prepared for The Climate Institute of Australia

Enquiries should be addressed to:

Dr Chris Lucas
Bushfire CRC
Bureau of Meteorology Research Centre
GPO Box 1289
Melbourne 3001, Victoria
Australia
Telephone (03) 9669 4783
Fax (03) 9669 4660
E-mail c.lucas@bom.gov.au

September 2007

Executive Summary

Bushfires are an inevitable occurrence in Australia. With more than 800 endemic species, Australian vegetation is dominated by fire-adapted eucalypts. Fire is most common over the tropical savannas of the north, where some parts of the land burn on an annual basis. However, the southeast, where the majority of the population resides, is susceptible to large wildfires that threaten life and property.

A unique factor in these fires of the southeast is the climate of the region. The southeast experiences a so-called Mediterranean climate, with hot, dry summers and mild, wet winters. The winter and spring rains allow fuel growth, while the dry summers allow fire danger to build. This normal risk is exacerbated by periodic droughts that occur as a part of natural interannual climate variability.

Climate change projections indicate that southeastern Australia is likely to become hotter and drier in future. A study conducted in 2005 examined the potential impacts of climate change on fire-weather at 17 sites in southeast Australia. It found that the number of 'very high' and 'extreme' fire danger days could increase by 4-25% by 2020 and 15-70% by 2050. Tasmania was an exception, showing little increase.

This report updates the findings of the 2005 study. A wider range of observations is analysed, with additional sites in New South Wales, South Australia and southeast Queensland included. The baseline dates of the study, commencing in 1973, are extended to include the 2006-07 fire season. The estimated effects of climate change by 2020 and 2050 are recalculated using updated global warming projections from the Intergovernmental Panel on Climate Change (IPCC). Two new fire danger categories are considered: 'very extreme' and 'catastrophic'.

This study also differs from the 2005 study in that different analysis methods are used. In addition to the annual changes in fire danger estimated before, changes to individual seasons and season lengths are explicitly examined. There is also a focus on the changes to the upper extremes of fire danger. These projected changes are compared with trends over the past few decades.

Climate change projections

The primary source of data for this study is the standard observations made by the Bureau of Meteorology. The locations of the 26 selected observing stations are shown in Figure E1. At these stations, the historical record of Forest Fire Danger index (FFDI) and the likely impacts of future climate change are calculated. There are homogenization issues with the data that could affect the interpretation of the results, particularly the analysis of the current trends. However, estimates of the errors suggest that these are small enough that we can have confidence in the results.

Climate change projections over southeastern Australia were generated from two CSIRO climate simulations named CCAM (Mark2) and CCAM (Mark3). Projected changes in daily temperature, humidity, wind and rainfall were generated for the years 2020 and 2050, relative to 1990 (the reference year used by the IPCC). These projections include changes in daily variability. They are expressed as a pattern of change per degree of global warming.

The patterns were scaled for the years 2020 and 2050 using IPCC estimates of global warming for those years, i.e. 0.4-1.0ºC by 2020 and 0.7-2.9ºC by 2050. This allows for the full range of IPCC scenarios of greenhouse gas and aerosol emissions.

The modelled changes from the various scenarios are then projected onto the observed daily time series of temperature, rainfall, wind and relative humidity from 1973 to early 2007. This methodology provides an estimate, based on the observed past weather, of what a realistic time series affected by climate change may look like, assuming no change in year-to-year variability beyond that observed in the past 34 years.

For projected changes in annual cumulative FFDI (ΣFFDI), the CCAM (Mark3) high global warming scenario produces the largest changes, while the CCAM (Mark2) low global warming scenario gives the smallest changes (Figure E1). In all simulations, the largest changes are in the interior of NSW and northern Victoria. As a general rule, coastal areas have smaller changes. By 2020, the increase in ΣFFDI is generally 0-4% in the low scenarios and 0-10% in the high scenarios. By 2050, the increase is generally 0-8% (low) and 10-30% (high).

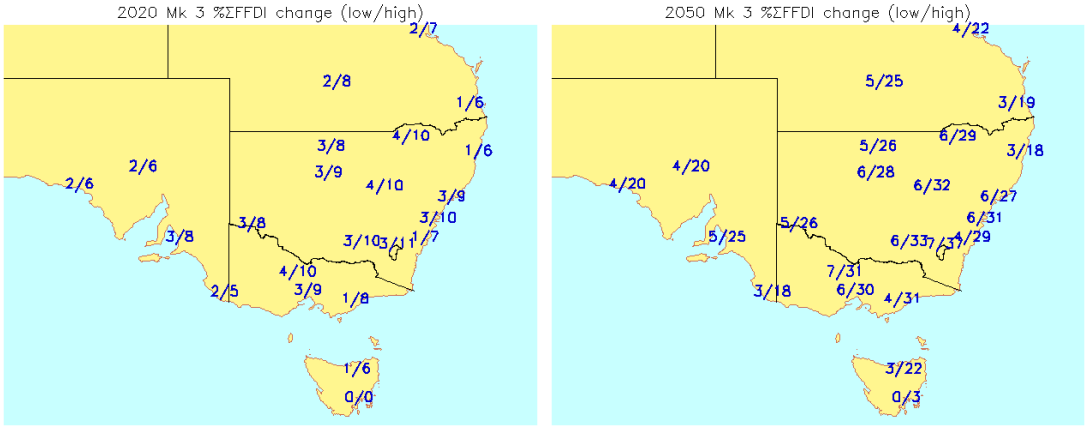

Figure E1: Percentage changes to ΣFFDI in the CCAM (Mark 3) simulations. The 2020 case is on the left; 2050 on the right. At each site, values for the 'low' scenario are to the left of slash, while values for the high scenario are to the right.

The annual cumulative FFDI values mask much larger changes in the number of days with significant fire risk. The daily fire danger rating is 'very high' for FFDI greater than 25 and 'extreme' when FFDI exceeds 50. Two new ratings have been defined for this report: 'very extreme' when FFDI exceeds 75 and 'catastrophic' when FFDI exceeds 100.

The number of 'very high' fire danger days generally increases 2-13% by 2020 for the low scenarios and 10-30% for the high scenarios (Table E1). By 2050, the range is much broader, generally 5-23% for the low scenarios and 20-100% for the high scenarios.

The number of 'extreme' fire danger days generally increases 5-25% by 2020 for the low scenarios and 15-65% for the high scenarios (Table E1). By 2050, the increases are generally 10-50% for the low scenarios and 100-300% for the high scenarios.

Table E1: Percent changes in the number of days with very high and extreme fire-weather – 2020 and 2050, relative to 1990

	2020		2050	
	Low global warming (0.4°C)	High global warming (1°C)	Low global warming (0.7°C)	High global warming (2.9°C)
Very high	+2-13%	+10-30%	+5-23%	+20-100%
Extreme	+5-25%	+15-65%	+10-50%	+100-300%

'Very extreme' days tend to occur only once every 2 to 11 years at most sites. By 2020, the low scenarios show little change in frequency, although notable increases occur at Amberley, Charleville, Bendigo, Cobar, Dubbo and Williamtown. The 2020 high scenarios indicate that 'very extreme' days may occur about twice as often at many sites. By 2050, the low scenarios are similar to those for the 2020 high scenarios, while the 2050 high scenarios indicate a four to five-fold increase in frequency at many sites.

Only 12 of the 26 sites have recorded 'catastrophic' fire danger days since 1973. The 2020 low scenarios indicate little or no change, except for a halving of the return period (doubling frequency) at Bourke. The 2020 high scenarios show 'catastrophic' days occurring at 20 sites, 10 of which have return periods of around 16 years or less. By 2050, the low scenarios are similar to those for the 2020 high scenarios. The 2050 high scenarios show 'catastrophic' days occurring at 22 sites, 19 of which have return periods of around 8 years or less, while 7 sites have return periods of 3 years or less.

Further, the projected changes vary at different times of the year. The largest changes in the seasonal median FFDI are seen in the season of highest fire danger, generally summer. A large change is also seen in the season *prior* to the peak season as well. Generally, this change is larger than that for the season immediately following the peak. The 'off season' (usually winter) tends to have the smallest increase. Taken together, the model results suggest that fire seasons will start earlier and end slightly later, while being generally more intense throughout their length. This effect is most pronounced by 2050, although it should be apparent by 2020.

Consistency between projections and recent trends

Over the recent decade or so, upward trends suggestive of increasing fire danger are seen in the median seasonal FFDI during the most active portion of the fire season and, to a lesser degree, in the surrounding seasons. The annual cumulative FFDI displays a rapid increase in the late-90s to early-00s at many locations (Figure E2). Increases of 10-40% between 1980-2000 and 2001-2007 are evident at most sites. The strongest rises are seen in the interior portions of NSW, and they are associated with a jump in the number of very high and extreme fire danger days. The strength of this recent jump at most locations equals or exceeds the changes

estimated to occur by 2050 in the different projections. Whether the recent jump will be sustained or revert to lower values remains to be seen.

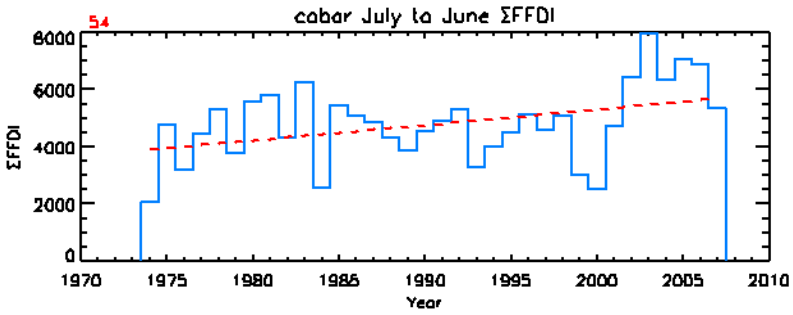

Figure E2: Time series of annual accumulated FFDI at Cobar, NSW. Trend line is shown in red. The last year, 2006-7, only extends to February.

To place these results in a broader context, data extending to 1942 are available at eight stations, allowing examination of the longer-term behaviour. Trends at these stations are generally weaker for both cumulative FFDI and the seasonal medians, and not significant at many stations (particularly for cumulative FFDI). This reflects natural long-term variability (around 20 years) in the records.

At these long-term sites, the season length is also examined by using an objectively defined start and end date of the active fire season. Four of the last five fire seasons have been among the longest on record, part of an upward swing since the early-90s (Figure E3). There is also an apparent decadal variation, with broad peaks in the 1940s, the late-70s/early-80s and in the 00s. Shorter fire seasons were generally seen in the late-50s and 60s and in the late-80s. A general upward trend is suggested, but is not statistically significant.

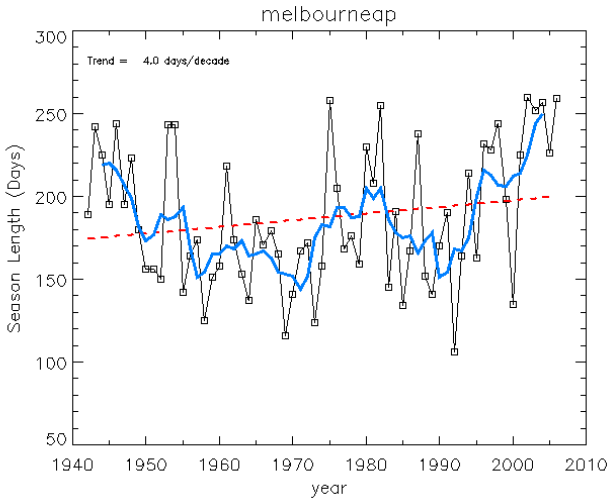

Figure E3: Estimated fire season length at Melbourne airport. The blue line is the 5-year running mean. The red dashed line is the line of best fit.

What is the driver of these recent changes in fire danger? The hypothesis posited in this study is that the naturally occurring peak in fire danger due to interdecadal variability may have been exacerbated by climate change. The test of this hypothesis comes over the next few years to decades. If correct, then it might be expected that fire-weather conditions will return to levels something more along the lines of those suggested in the 2020 scenarios. If fire danger conditions stay

this high, then the conclusion must be that the models used to make these projections are too conservative. Whatever the case, continued observation, as well as improved modelling are required to resolve this question.

What of the human impacts of these projected changes? The last few years, particularly the 2006-07 fire season, may provide an indication for the future. Early starts to the fire season suggest a smaller window for pre-season fuel-reduction burns. Logically, more frequent and more intense fires suggest that more resources will be required to maintain current levels of bushfire suppression. Shorter intervals between fires, such as those which burned in eastern Victoria during 2002-03 and 2006-07, may significantly alter ecosystems and threaten biodiversity. It is hoped that planning authorities can use this information in the development of adaptation strategies.

Introduction

Bushfires are an inevitable occurrence in Australia. With more than 800 endemic species, Australian vegetation is dominated by fire-adapted eucalypts. Fire is most common over the tropical savannas of the north, where some parts of the land burn on an annual basis. However, the southeast, where the majority of the population resides, is susceptible to large wildfires that threaten life and property.

A unique factor in these fires of the southeast is the climate of the region. The southeast experiences a so-called Mediterranean climate, with hot, dry summers and mild, wet winters. The winter and spring rains allow fuel growth, while the dry summers allow fire danger to build. This normal risk is exacerbated by periodic droughts that occur as a part of natural interannual climate variability.

The global climate is changing. The Intergovernmental Panel on Climate Change [IPCC, 2007] concluded:

- The average temperature of the Earth's surface has risen by about 0.7°C since 1900
- The 11 warmest years on record since 1850 have occurred in the past 12 years
- Global average sea-level has risen 170 mm since 1900 (1.7 mm per year), and has been rising at 3 mm per year since 1993
- The upper 3000 m of ocean has warmed, as has the lower atmosphere
- The incidence of extremely high temperatures has increased and that of extremely low temperatures has decreased
- The water vapour content of the atmosphere has increased since at least 1980, consistent with theory that warmer air can hold more moisture
- Oceans have become more acidic due to higher concentrations of carbon dioxide (CO_2)

The IPCC [2007] also concluded that it is very likely that human-induced increases in greenhouse gases have caused most of the observed increase in globally-averaged temperatures since the mid-20th century. Discernible human influences have also been found in continental-average temperatures, atmospheric circulation patterns and some types of extreme weather events. Since 1950, Australia has warmed by 0.85ºC, rainfall has increased in the north-west but decreased in the south and east, droughts have become hotter, the number of hot days and warm nights has risen and the number of cool days and cold nights has fallen [Nicholls 2006].

Climate change projections indicate that southeastern Australia is likely to become hotter and drier in future [Suppiah et al 2007]. Hennessy et al [2005] examined the potential impacts of climate change on fire-weather in southeast Australia. They found that on a broad scale, the number of very high and extreme fire danger days could increase by 4-25% by 2020 and 15-70% by 2050 across much of southeast Australia as a result of projected changes in climate due to increases in greenhouse gases. Tasmania was an exception, showing little increase.

This paper updates the findings of Hennessy et al [2005]. A wider range of observations is analysed, with additional sites in New South Wales, South Australia and southeast Queensland included. The baseline dates of the study, commencing in 1973, are extended to include the 2006-7 fire season. The estimated effects of climate change by 2020 and 2050 are recalculated using the updated global warming projections from the IPCC [2007].

This study also differs from that of Hennessy et al [2005] in that different analysis methods are utilised. In addition to the annual changes in fire danger estimated before, changes to individual seasons and season lengths are explicitly examined. There is also a focus on the changes to the upper extremes of fire danger. These projected changes are compared with the current climate and recent trends.

This update represents a resource for ongoing engagement with fire management agencies to plan for the impacts of climate change. However, the report is not intended to provide management recommendations to agencies.

Quantifying Fire Danger

Fire Weather Risk Indices

In most Australian states, fire weather risk is quantified using one of two indices: the Forest Fire Danger Index (FFDI) or the Grassland Fire Danger Index (GFDI) [Luke and McArthur 1978]. McArthur defined these indices in the late-1960s to assist foresters in relating the weather to the expected fire behaviour in the appropriate fuel type. While the details of each calculation are different, the basic ingredients are the same. Observations of temperature, relative humidity and wind speed are combined with an estimate of the fuel state to predict the fire behaviour. For forests, the fuel state is determined by the so-called 'drought factor' which depends on the daily rainfall and the period of time elapsed since the last rain. The drought factor is meant to encapsulate the effects of both slowly-varying long-term rainfall deficits (or excesses) and short-term wetting of fine fuels from recent rain [Finkele et al 2006]. For grassland, the fuel state is determined by the 'curing factor' which is the dryness of grassland from visual estimates expressed as a percentage.

Initially, these quantities were estimated using a mechanical nomogram in the form of a set of cardboard wheels (see Luke and McArthur [1978], pp 113-118), where the user 'dialled in' the observations to compute the fire danger index. Such meters are still used operationally. Noble et al [1980] reverse-engineered the meter for FFDI to derive equations suitable for use on electronic computers, i.e.

$$FFDI = 1.2753 \times \exp\left(0.987 \log DF + 0.0338T + 0.0234V - 0.0345RH\right)$$

where DF is the drought factor, T the air temperature in Celsius, V the wind speed in km/h and RH the relative humidity expressed in percent. The drought factor is calculated using the Griffiths [1999] formulation and uses the Keetch-Byram Drought Index (KBDI; Keetch and Byram [1968]) to estimate the soil moisture deficit. The Mount Soil Dryness Index [Mount 1972] is a possible alternative to KBDI, but studies suggest that it is not particularly well-suited to inland areas of Australia [Finkele et al 2006]. In the calculation of the FFDI, no allowance is made

for varying fuel loads, or for varying slopes, although these are necessary if the FFDI is to be used to estimate fire behaviour at small spatial scales.

Purton [1982] defined an equation for GFDI

$$GFDI = 10^{\wedge}(-0.6615 + 1.2705\log_{10} Q - 0.004096(100 - C)^{1.536} + 0.01201T + 0.2789\sqrt{V} - 0.09577\sqrt{RH})$$

where the variables are as above, Q is the fuel quantity in t/ha (generally assumed to be 4.5 t/ha) and C is the curing factor. The curing factor is expressed as a percentage, with a value of 100% representing fully cured grass, while 0% represents moist, green grass. Given the difficulty of accessing robust grassland curing statistics over the period of this study, we focus on the FFDI for the remainder of this report.

Fire Danger Rating

To summarize the FFDI calculation, the Fire Danger Rating (FDR) system is often used. This system is used by fire agencies to reflect the fire behaviour and the difficulty of controlling a particular fire. Table 1 shows the five categories of the FDR system and the expected fire behaviour for a standardised fuel (i.e. dry sclerophyll forest with an available fuel load of 12 t/ha) on flat ground. The fuel load in particular can have a large impact on the subsequent intensity of the fire (Fig. 1), with 'uncontrollable' fire behaviour occurring at progressively lower values of FFDI as the fuel load increases by even modest amounts.

In this report we will also examine two additional, unofficial FDR categories. We call these 'very extreme' (with FFDI in excess of 75) and 'catastrophic' (with FFDI in excess of 100). As this upper end of FFDI is poorly sampled (i.e. very rare) in terms of fire behaviour, these additional criteria are more 'numerical' in nature, and not based on many known fire behaviours or intensities. The 'catastrophic' fire weather category refers to the potential for major damage, but the actual occurrence of damage also depends on other factors such as fuel load, ignition, community actions, exposed assets and fire management.

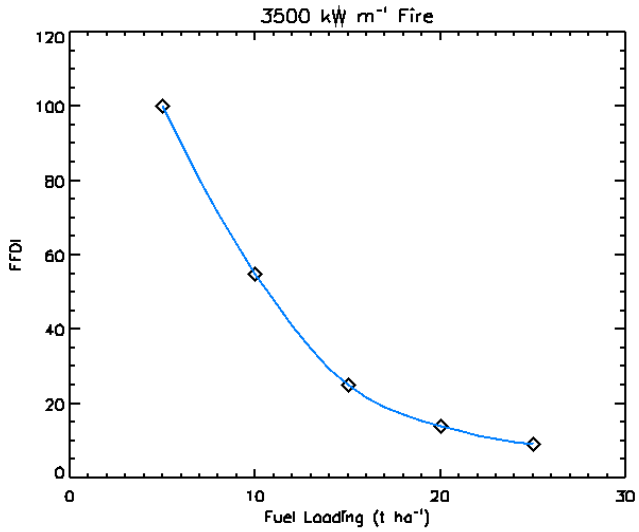

Figure 1. Effect of Fuel Load on FFDI value for a fire with an intensity of 3500 kW m^{-1}, the threshold for 'uncontrollable' fires. Adapted from data provided in Incoll [1994].

Table 1. Categories of Fire Danger Rating (FDR). Taken from Vercoe [2003].

Fire Danger Rating	FFDI range	Difficulty of suppression
Low	0-5	Fires easily suppressed with hand tools.
Moderate	5-12	Fire usually suppressed with hand tools and easily suppressed with bulldozers. Generally the upper limit for prescribed burning.
High	12-25	Fire generally controlled with bulldozers working along the flanks to pinch the head out under favourable conditions. Back burning may fail due to spotting.
Very High	25-50	Initial attack generally fails but may succeed in some circumstances. Back burning will fail due to spotting. Burning-out should be avoided.
Extreme	50+	Fire suppression virtually impossible on any part of the fire line due to the potential for extreme and sudden changes in fire behaviour. Any suppression actions such as burning out will only increase fire behaviour and the area burnt.

Multi-scale Drivers of FFDI Variability

The Forest Fire Danger Index varies on many time scales, from hourly to inter-decadal. The vagaries of daily weather and multi-year climate variability have an impact on the fire danger. To illustrate the relationships between FFDI and the weather/climate variability, we look at the case of Canberra, starting with the day of the catastrophic bushfires on 18 January 2003, and then putting the day in the context of the month, the surrounding years and finally, the 36-year climate record.

Diurnal Variability

Figure 2 shows the diurnal variation of FFDI on 18 January 2003 for Canberra. The values plotted here are derived from half-hourly measurements from the Canberra automatic weather station. The index starts to rise as the day begins, with 'very high' levels (FFDI of 25) exceeded by 9 am. 'Extreme' fire danger (FFDI of 50) is reached by 12.30 pm and fire danger peaks around 4 pm. This does not correspond to the time of maximum temperature or lowest RH, but to a peak in the wind speed. The fluctuations between 4 pm and 7 pm are associated with fluctuations in both wind speed and humidity [Mills 2005], and after 7 pm the fire danger decreases rapidly to low to moderate levels.

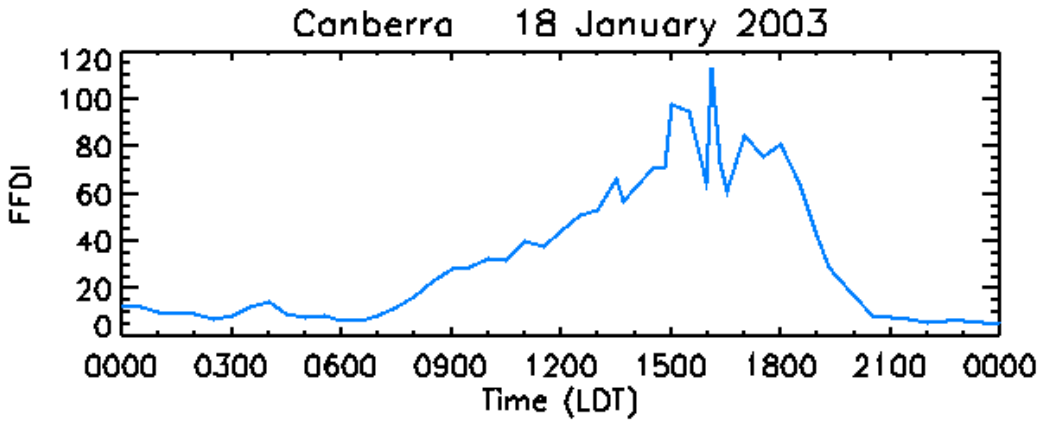

Figure 2. Time series of FFDI on 18 January 2003 at Canberra, ACT. Values are computed every 30 minutes from automatic weather station data.

Physically, short-term variations of fuel moisture content (FMC) are related to the changes in FFDI on these time scales [Luke and McArthur 1978]. The fuel moisture content of the fine fuels adjusts rapidly through adsorption and desorption of water vapour, which is a function of air temperature, relative humidity and wind speed. All three of these factors show a strong diurnal variation, resulting in FMC being higher at night and lower in the day. Lower FMC results in more flammable fuels and hence a peak in fire danger is generally found during the afternoon hours. Of course, these times can vary, with the exact details at any given location depending on microclimatic details of the site.

Synoptic Variability

Figure 3 shows the FFDI time series for Canberra during January 2003, using observations at 3 pm (see next section for more details of these data). The

variability on a day to day basis is quite high and is related to the synoptic weather situation. The values range from near zero at the beginning of the month to almost 100 on the 18th, the date of the devastating fires. The value of FFDI in this dataset agrees well with the hourly values. Looking at the month as a whole, there are 2 days with 'low' FDR, 4 days with 'moderate', 12 days with 'high', 9 days with 'very high' and 4 rated as 'extreme'.

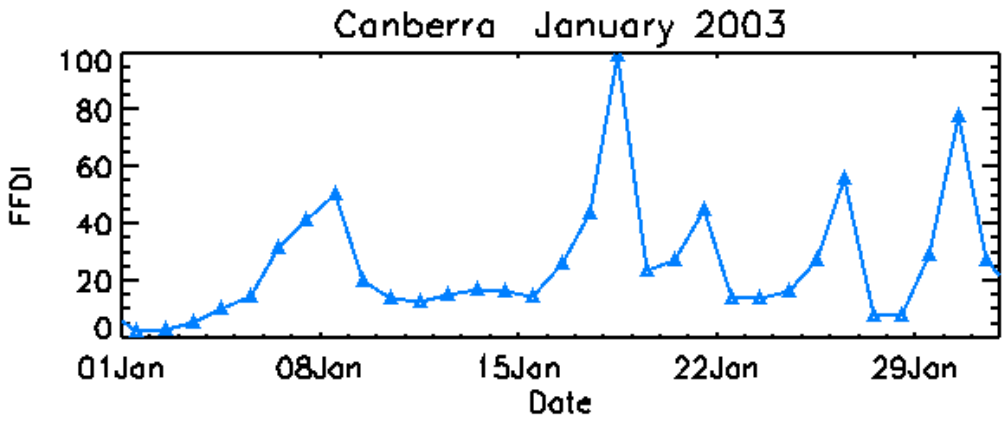

Figure 3. Time series of daily FFDI for Canberra, ACT during January 2003

A typically dangerous fire situation in southeastern Australia occurs when a vigorous cold front approaches a slow-moving high pressure system in the Tasman Sea, causing very hot and dry north-westerly winds. Figure 4 shows the situation associated with the Ash Wednesday fires in Victoria and South Australia on 16 February 1983.

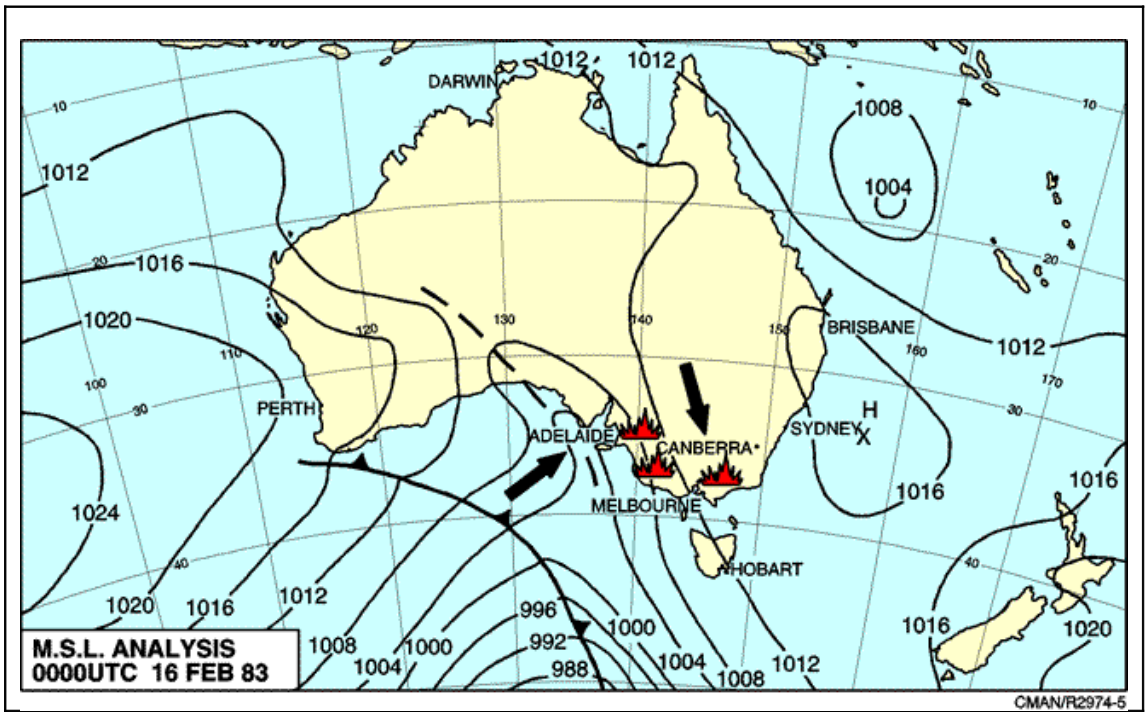

Figure 4. Mean sea level pressure contours (hPa) for 0000 UTC (11 am Australian Eastern Daylight-savings Time) 16 February 1983. Heavy arrows depict general wind direction and fire symbols denote approximate locations of bushfires observed on the day.

For most of Australia's east coast, the fire season extends from spring to mid-summer. The greatest danger occurs after the dry winter/spring period, before the onset of the rainy weather common in summer, and when deep low-pressure systems near Tasmania bring strong and dry westerly winds to the coast, as occurred in the major New South Wales fires in January 1994 (Fig. 5), and also in the 2001-02 summer.

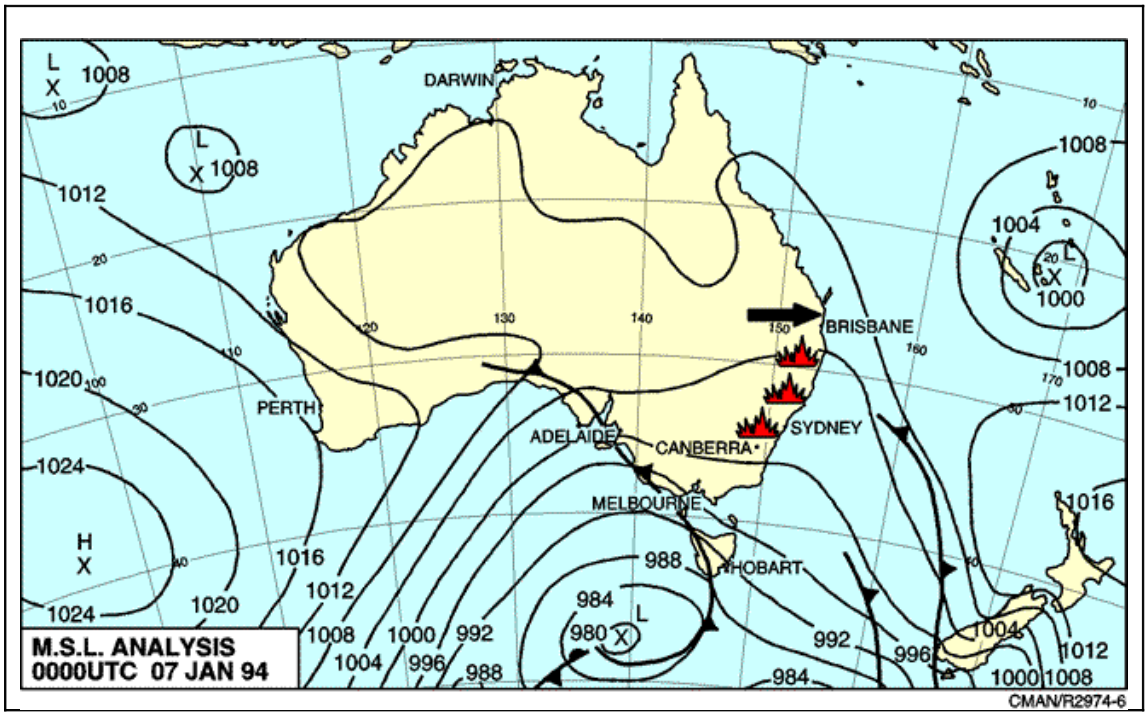

Figure 5. Mean sea level pressure contours (hPa) for 0000 UTC (11am Australian Eastern Daylight-savings Time) 7 January 1994.

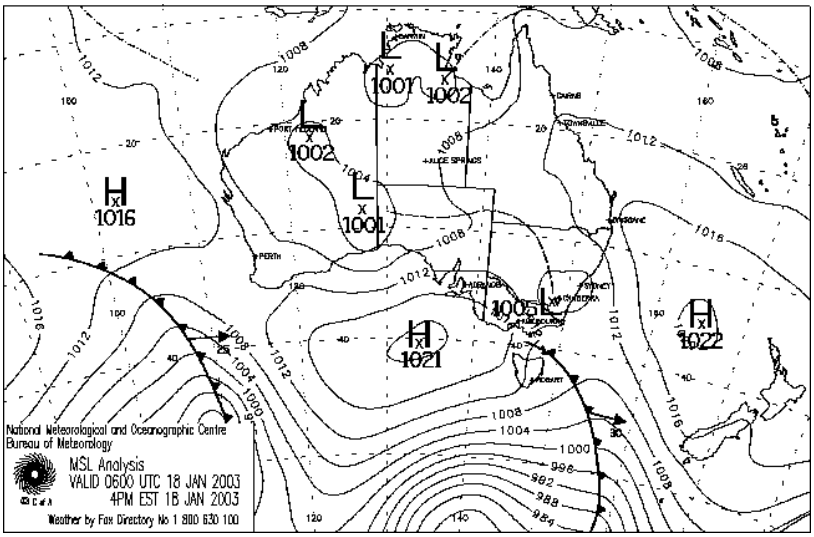

Figure 6. Mean sea level pressure analysis for 0600 UTC (5 pm Australian Eastern Daylight-savings Time) on 18 January 2003.

The synoptic situation on the day of the Canberra bushfires is shown in Figure 6. This includes features of both the weather patterns presented above, with an intense high pressure system to the east generating strong north-westerly winds ahead of an active trough-line passage. A strong cold front south of Tasmania contributes to strong westerly winds following the trough through Canberra. The

combination of these two systems produced the very high temperature and low relative humidity observed over southeastern NSW on that day.

Annual and Interannual Variability

The timing of the fire seasons varies across Australia (Fig. 7), reflecting the different weather patterns required to produce the necessary conditions (low rainfall and humidity, high temperatures and wind speeds) for higher fire dangers in the different locations. In southern Australia, the most severe fire danger occurs during summer and autumn when the highest temperatures occur and in most years the grass and forests have dried. For most of Australia's east coast, the fire season runs from spring to mid-summer. The greatest danger occurs after the dry winter and spring periods and before the onset of the rainy weather common in summer. In northern Australia, the fire season occurs during the warm, dry and sunny winter and spring, when the grasses are dead and the fuels have dried. Not every year is the same, though. Unusual rainy periods or droughts can alter the timing and severity of the fire season.

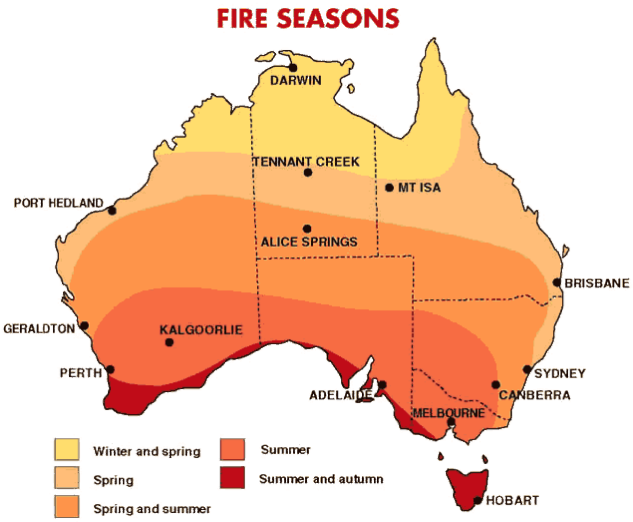

Figure 7. Map of peak fire seasons across Australia. From Luke and McArthur [1978].

Figure 8 shows a plot of the daily FFDI for Canberra for the 12 months centred on 1 January 2003. The gradual build-up of higher fire dangers can be seen from July 2002, as the temperatures rise and the rainfall begins to decline with the march of the seasons, together with the effects of the drought that year. Beginning in November 2002, an FDR of 'very high' (>25) becomes more common. This extends through to mid-late February 2003 when the values drop and tend to stay low. By the end of June 2003, the FFDI is near zero on most days.

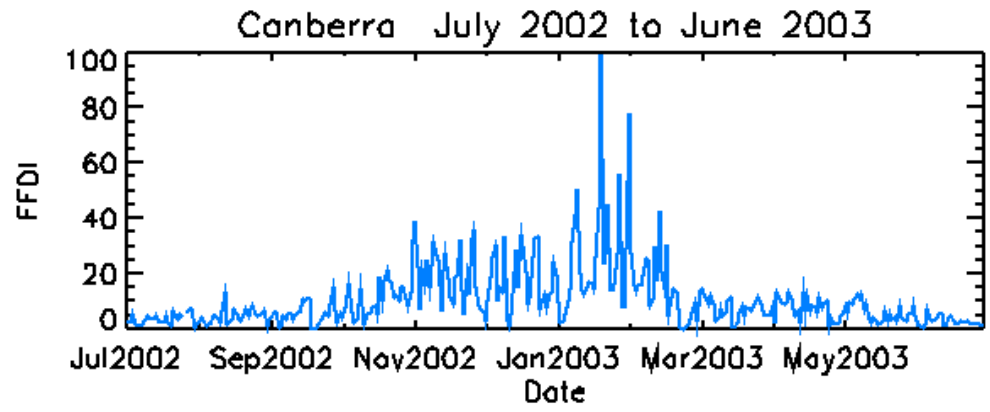

Figure 8. Time series of daily FFDI for Canberra, ACT, for the period from July 2002 through June 2003.

Moving out to a four-year window, the interannual variability becomes apparent. In Figure 9, it can be seen that the 2002-3 fire season had a different character to the years immediately surrounding it. During the 2000-01 and 2001-02 fire seasons, no 'extreme' FDR days were observed, and relatively few 'very high' days. The 2003-04 season was between these two extremes, more typical of a normal year.

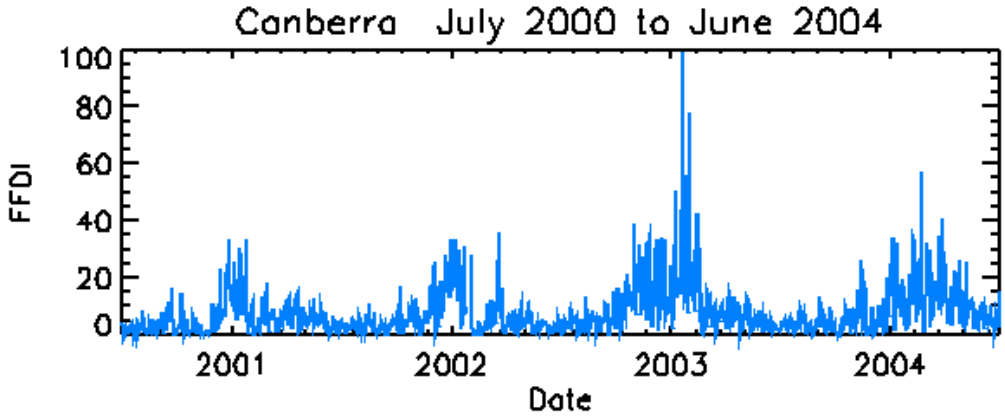

Figure 9. Time series of daily FFDI for Canberra, ACT, for the period from July 2000 through June 2004.

A primary mechanism driving this interannual variability in fire weather across Australia is the so-called El Niño-Southern Oscillation (ENSO) (Fig. 10). Briefly, ENSO is a coupled ocean-atmosphere oscillation in the equatorial Pacific Ocean, with a frequency of 2-7 years. During El Niño years, the central and eastern Pacific warms anomalously, rainfall patterns tend to shift toward the central equatorial Pacific, and Australia (particularly the east) tends to be dry and often experiences severe droughts. During the opposite phase, La Niña, the western equatorial Pacific is unusually warm and the eastern Pacific unusually cool, and Australia typically experiences above-normal precipitation.

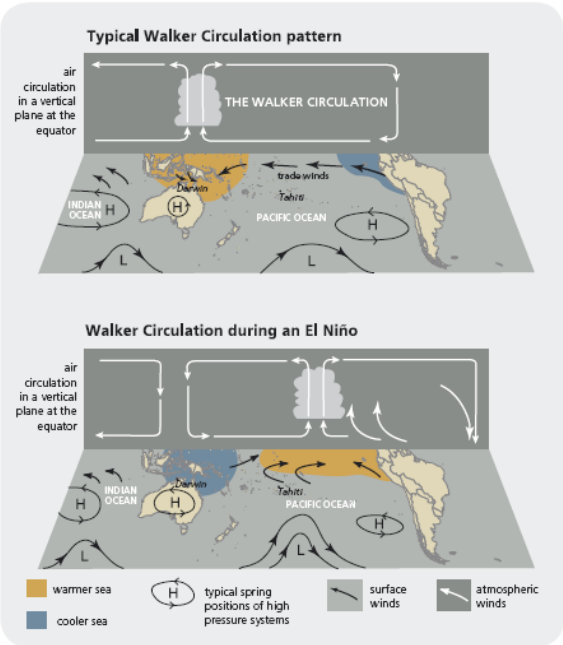

Figure 10. Schematic diagram summarizing the El Niño-Southern Oscillation phenomenon. Taken from http://www.bom.gov.au/info/leaflets/nino-nina.pdf.

Williams and Karoly [1999] first examined the impact of ENSO on fire danger in Australia. To a large degree, the severity of any given fire season can be related to the effects of El Niño. This impact at Canberra [Lucas 2005] is shown in Figure 11. During El Niño years (red line), more high, very high and extreme FDR days are observed in comparison with both neutral (green line) and La Niña (blue line) years. This effect was generally strongest in south-east Australia, inland from the coastal plains, and is particularly marked near Canberra [Lucas 2005].

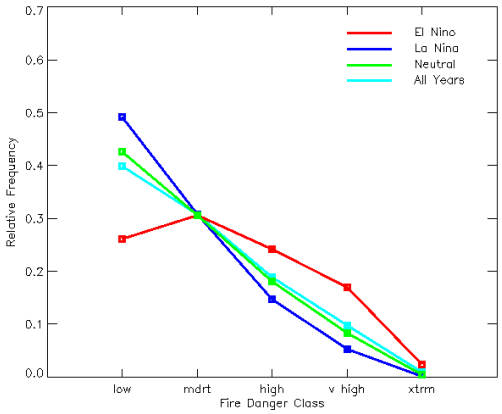

Figure 11. Relative frequency of occurrence of FDR categories during El Niño (red), neutral (green) and La Niña (dark blue) years for Canberra, ACT. Taken from Lucas [2005].

Despite the strong relationships, ENSO only explains 15-35% of the year to year variance in FFDI. For a more complete understanding of interannual variability, other potential processes must be examined, although their influences on (and their relationship to) fire weather are as yet poorly understood, and will only be mentioned briefly here.

A likely driver of fire climate variability is the Indian Ocean sea surface temperature (SST). The difference in SST between Indonesia and the central Indian

Ocean is positively correlated with rainfall in a broad northwest-southeast band across central Australia, and negatively correlated with east coast rainfall [Nicholls 1989]. This pattern of ocean temperatures is similar to the recently identified Indian Ocean Dipole [Saji et al 1999], which may be an extension of ENSO into the Indian Ocean [Allan et al 2001].

Another possible driver of variability is the Southern Hemisphere Annular Mode (SAM). The SAM is a meridional (north-south) seesaw in atmospheric pressure between the pole and the mid-latitudes, which is zonally (east-west) symmetric [Thompson and Wallace 2000]. It is an episodic phenomenon with a lifetime of about 10 days. The effect of SAM on Australia varies with the season; the positive phase of SAM corresponds with generally higher summer rainfall in north-central and south-east Australia and lower winter rainfall in south-east and south-west Australia [Hendon et al., 2007]. On longer time scales, historical records of SAM activity suggest that the strength of SAM has been increasing since the 1970s, with an associated southward shift in weather systems in the Southern Hemisphere [Marshall 2003]. A peak was also found in the late-1950s and early 1960s [Jones and Widmann, 2004].

Interdecadal Variability

All of these sources of interannual variability are subject to longer-term inter-decadal circulation variations such as the Interdecadal Pacific Oscillation (IPO) [Folland et al 1999; Power et al 1999] or other sources (follow references in Power et al 2006). The general understanding of variability at this time scale is limited. In a later section of this report, it will be shown that longer time series of observed FFDI demonstrate considerable variability on multi-decadal time scales, with significant implications.

Data

The primary source of data for this study is the standard observations made by the Bureau of Meteorology. The availability of suitable daily temperature, humidity wind and rainfall data limits the number of sites to 26, as shown in Figure 12. At these stations, the historical record of FFDI and the likely impacts of future climate change are calculated.

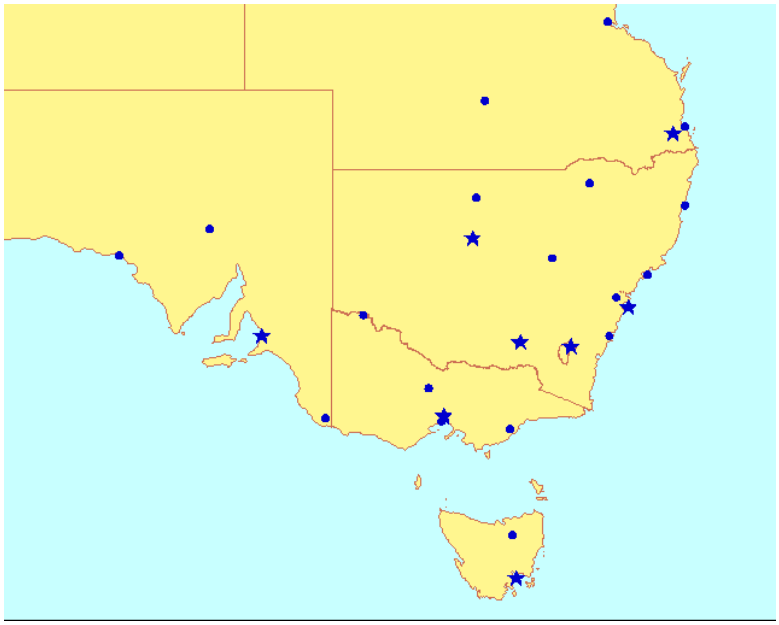

Figure 12. Map showing locations of stations used in this study. Circles represent stations with data extending to 1973. Stars represent stations where longer time series are available.

The availability of data also limits the period suitable for analysis to January 1971 through February 2007. The first two years (1971-2) are included to allow the Drought Factor time to 'spin up' to a reliable value. At 8 of these stations (indicated by stars in Fig. 12) longer-period data sets are available, extending back as far as the 1940's, and an analysis of these data is presented separately.

To calculate the daily fire danger indices, daily values of air temperature, relative humidity and wind speed, along with rainfall measurements for the KBDI, are required. For the daily FFDI calculation, the maximum air temperature, and 3 pm LST[1] values of humidity and wind speed are used. Accumulated daily rainfall is reported at 9 am LST for the preceding 24 hours. The timing of these variables is constrained by past observing practice, but results in a reasonable estimate of the maximum daily fire danger at most stations. This method of computation differs slightly from that of Hennessy et al. [2005]. In that study, so-called 'extreme FFDI' was computed using minimum daily (not necessarily 3 pm) relative humidity, along with maximum wind speed (not necessarily 3 pm) and temperature. That methodology maximizes daily FFDI. Comparison of the 'extreme FFDI' and that used here shows a high correlation, but the numbers here are about 20-30% lower [Lucas 2006c].

When examining meteorological/climate data acquired over decades, it is important to consider the homogeneity of the data. Homogeneous data are those that are free from artificial trends and/or discontinuities. These discontinuities can arise from factors such as moving the observing station, changes in instrumentation and/or changes in the observational practices. The data used in this study are generally not homogeneous. Although homogenized high-quality databases of maximum temperature, humidity and rainfall do exist at many of these stations, none of these databases has been updated to include the most recent observations. At the vast majority of the stations, a major change in the record is the introduction of the Automatic Weather Station (AWS). This generally

[1] LST=Local Standard Time. During daylight savings, subtract one hour for LST.

occurs sometime in the 1990s and is accompanied by changes in the instrumentation and, often, a site move. Particularly relevant with this change was the change in anemometer instrumentation for measuring wind (see below).

To address the lack of homogeneity, an examination of the issues in the dataset and the potential uncertainties will be discussed.

Rainfall

A homogenized time series of daily rainfall has been constructed for Australia [Haylock and Nicholls 2000]. Most of the stations in that dataset were rural rather than urban. Unfortunately, little overlap exists between the stations in the homogenized rainfall records and those used here. As the stations in our study are primarily well-staffed airports and meteorological offices, with consistent record-keeping practices, the range of errors in the data is likely to be small. Hence, negligible biases due to the rainfall data are expected in the fire-weather results.

Temperature

A homogenized daily maximum temperature database extending from 1957 (earlier in some cases) to early 1997 has been created at the Bureau of Meteorology. At the stations used in this study, most of the inhomogeneities in those time series occur before 1973. Only a very small subset occurs after. Hence, negligible biases in the FFDI calculations are likely to be introduced by the temperature records used.

Humidity

Analysis by Lucas [2006b] shows the humidity data suffer from numerous inhomogeneities. Most of these are small shifts in the dewpoint and are not biased in one way or the other. A notable exception is the change in instrumentation associated with the shift to the AWS, which generally occurred sometime in the 1990s. At many stations, the newer AWS instruments read consistently lower humidity than the original instrumentation (Lucas 2006a). The typical magnitude of this bias is -0.5ºC in dewpoint, but this amount varies with the weather conditions. The bias is hypothesized to be related to the (mis-)characterisation (and uncertainty) of a factor used in converting from wet bulb temperature to the dewpoint. For the calculations here, this bias could result in a slight over-estimation in the calculated value of FFDI. However, any potential bias introduced in the FFDI is likely to be small and, in light of the other sources of error, mostly insignificant.

Wind

The most serious homogenization issue with the FFDI calculation is due to the wind data. At some stations, the wind speeds are particularly non-homogeneous. As an example, consider Figure 13, which shows wind speed at 3 pm for Sydney airport (AP) from 1940-2007. We have rated the quality of these data as ‘Fair’, as it shows many shortcomings.

To objectively identify discontinuities in the record, monthly averages of the wind speed are computed (red lines). These monthly averages are then subjected to a multiphase regression analysis. Each segment of the multiphase regression is constrained to have a slope of zero.

The different segments show different averages, as well as different variance in the series. The first segments, pre-1955 or so, have higher maximum values than later times. From the mid-70s to the mid-90s, the averages are much lower. The peak winds are also not as high and there are numerous incidences of calm winds. In 1994 a large jump in the average speed is observed, as well as a reduction in variance, while calm winds become relatively rare.

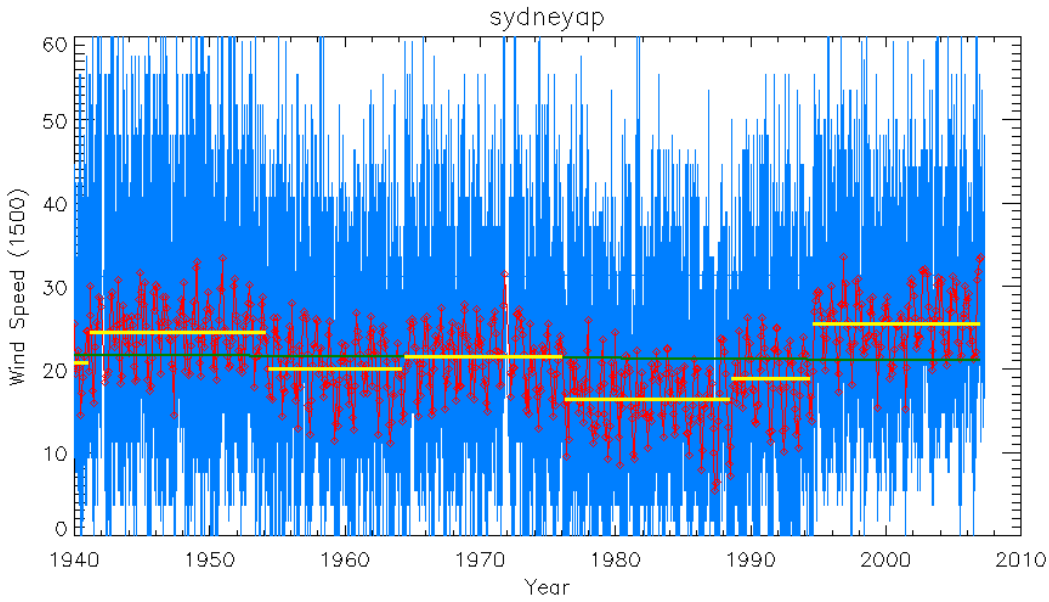

Fig. 13. Time series of 3 pm daily wind speed (blue; km h^{-1}) at Sydney airport from 1940-2007. Red lines show monthly averages and horizontal yellow lines are the separate segments in a breakpoint (multi-phase regression) analysis.

This long-term behaviour of the wind data is unrealistic. There are several reasons for this. The first is that, in many respects, wind is a very local phenomenon. The value which is measured depends heavily on the details of the local environment. For example, the growth/removal of trees or the construction/demolition of buildings can block or channel the flow, and change the measurement of the wind. This has undoubtedly been the case at Sydney AP, where several additions and expansions have been made over the years.

A second cause is the different anemometers which have been used to measure wind speeds. Before the widespread installation of AWSs, the wind speed measurements were often made from pressure (Dines) anemometers. Pressure anemometers have a relatively high start-up threshold, meaning that no wind is measured until the wind reaches a threshold. As a result, a larger number of calm and low wind speeds are seen in these observations. Wind speed measurements at the AWSs use cup anemometers. These have a low start-up threshold, but 'overspeed', with inertia preventing the cups from slowing or stopping. However, over the life of the cup anemometer, the bearings wear and increasing friction can result in gradually decreasing wind speeds. In general, when these anemometers are used, they show fewer calm/low wind speed days, and generally reduced variance in the wind speeds observed. The change in wind characteristics induced by this switch is evident in Figure 13 at the 1994 breakpoint. A similar discontinuity is present (to some degree) at the vast majority of the stations in the dataset.

At many stations located away from major urban centres or airports, and prior to the introduction of AWS, wind speeds were estimated using the visual effects of wind on vegetation and the Beaufort scale. These estimates of the wind depend on the skill of the observer and wind speeds appear to be underestimated at most times, and are generally inconsistent over longer periods. Further, the values are generally discrete, falling on the midpoints of the Beaufort categories.

The wind speed errors/inhomogeneities need to be considered when interpreting the results of the FFDI calculation. Unfortunately, a simple correction is not available. However, preliminary investigation suggests that the upper extremes of the FFDI distribution (above about the 80th percentile) are most sensitive. In some cases the monthly-averaged wind speeds in these earlier pre-AWS periods may be up to 10 km/h lower than winds in the later post-AWS periods, although differences are generally smaller than that. This can reduce the values of some of the upper percentiles by 4-5 points of FFDI (and even more above the 90th percentile). *The median value of the FFDI distribution is essentially unchanged*. Hence, the trends produced using the median values should be relatively unaffected by these errors. The bias seems to depend on factors other than the wind speed. During wet periods, the potential errors due to wind speed are apparently much smaller due to the moderating effects of the Drought Factor in the FFDI calculations. Work is continuing on understanding the effects of wind measurement errors on the distributions of FFDI.

Analysis Variables

As shown in the previous section, long time-series of daily FFDI are complex, each with uncertainties that affect its interpretation. One challenge of utilising long-term daily data like FFDI is distilling the large amount of available information into meaningful summary quantities. Visual examination time series of the daily values become less useful as the length is increased and relevant details become obscured. Several metrics are utilized in this study; each has advantages and disadvantages.

Cumulative FFDI

A useful method of examining long period variability is through the annual cumulative FFDI, denoted ΣFFDI [e.g. Beer and Williams 1995]. This variable is the summation of the daily FFDI values over an entire year. In this study, a year is defined from July through June as this better encompasses a continuous fire season in southeast Australia than the calendar year. Figure 14 shows the time series for Canberra from 1943 through to the present (note: The 2006-07 season lacks June data). Standout years are 1944-45, 1957-58, 1982-83, 1997-99 and 2006-07. The overwhelming majority of these standout years are El Niño years, further emphasizing the strong relation between El Niño and high fire danger

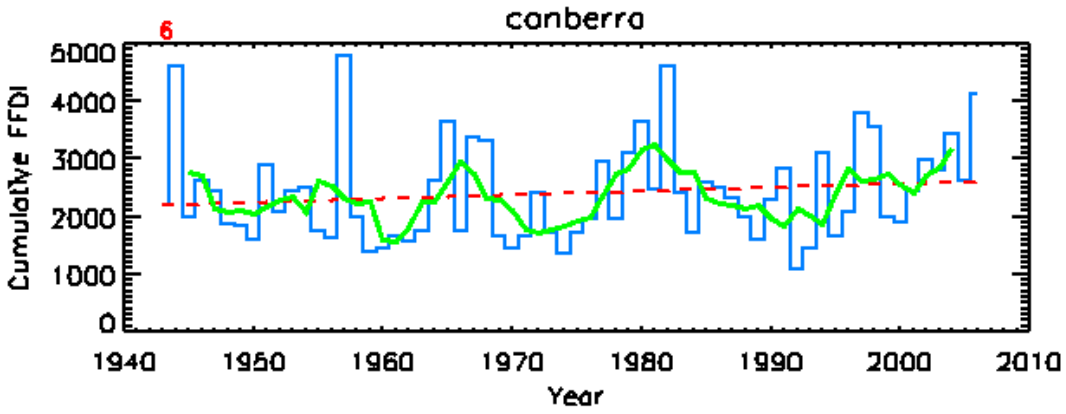

Figure 14. Annual ΣFFDI at Canberra from 1943-2007 (histogram). Also shown are the five-year running mean (green line) and the linear regression (red line). The trend (red number at top left) is +6 points per year.

The running mean in Figure 14 highlights the interdecadal nature of the variation. Numerous peaks on the order of 10-20 years apart are observed. Also apparent is a small (but statistically significant) positive trend.

There are several potential sources of error when computing cumulative FFDI at any given station. One error, resulting in an underestimate, would be due to missing days in the data set. This should be minimal at most stations, as missing days are relatively scarce at most of the stations used here. A second source of error, potentially more significant, is the wind uncertainties. Any biases introduced by incorrect wind speeds could be translated through this calculation. As suggested earlier, a consistent negative bias in wind speed would artificially lower the upper percentiles of the distribution. A simple calculation suggests that for stations with the largest wind inhomogeneities a negative bias of ~400 points (~ 10-20%) could be present.

Number of FDR Threshold Days

This is a simple metric that tabulates the number of days above a certain FFDI/FDR threshold. Most commonly, this will be expressed as the number of 'very high' and 'extreme' days (VHE days for short). Like ΣFFDI, this calculation is made over the period July through June of the following year to better encapsulate the 'natural' fire season in the southeast. Other thresholds, subsets of VHE days, are also examined. Uncertainties in this estimate should be small, with only the occasional day misclassified due to data errors.

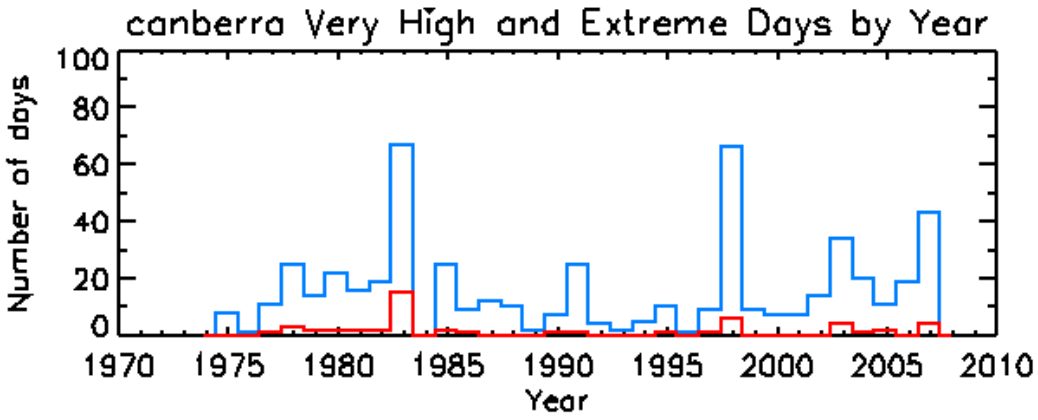

Figure 15. Number of days per year with FDR exceeding 'very high' (blue) and 'extreme' (red).

Like ΣFFDI, a considerable amount of interannual variability is seen in VHE days from Canberra (Fig. 15). The largest number of VHE days occurred in 1982-3, followed closely by 1997-8, 2006-7 and 2002-3. These are all El Niño years, consistent with the discussion of Figure 11, where a greater proportion of days were VHE days during El Niño years. The red line, only 'extreme' days, highlights the relative rarity of such days. At Canberra and other stations, the occurrence of the majority of 'extreme' days is confined to a few years.

Frequency Analysis

Frequency analysis is a highly instructive method for examining the variability of FFDI over decadal timescales. Observations over a period of interest are sorted (in ascending order) and a percentile level is assigned such that the 10th percentile value is higher than 10% of the observations, the median or 50th percentile is the value in the middle of the distribution, and the 90th percentile value is higher than 90% of the observations. Frequency analysis allows for a greater understanding of the range of variability, especially the rare extremes.

For this study, we perform a frequency analysis of daily FFDI on a seasonal basis, where observations over three-month periods are collated. Observations are grouped into December-January-February (DJF), March-April-May (MAM), June-July-August (JJA) or September-October-November (SON), giving four seasonal distributions per year. The general character of the three month season is given by the median, while the 90th (and greater) percentiles show the characteristics of the most extreme fire days.

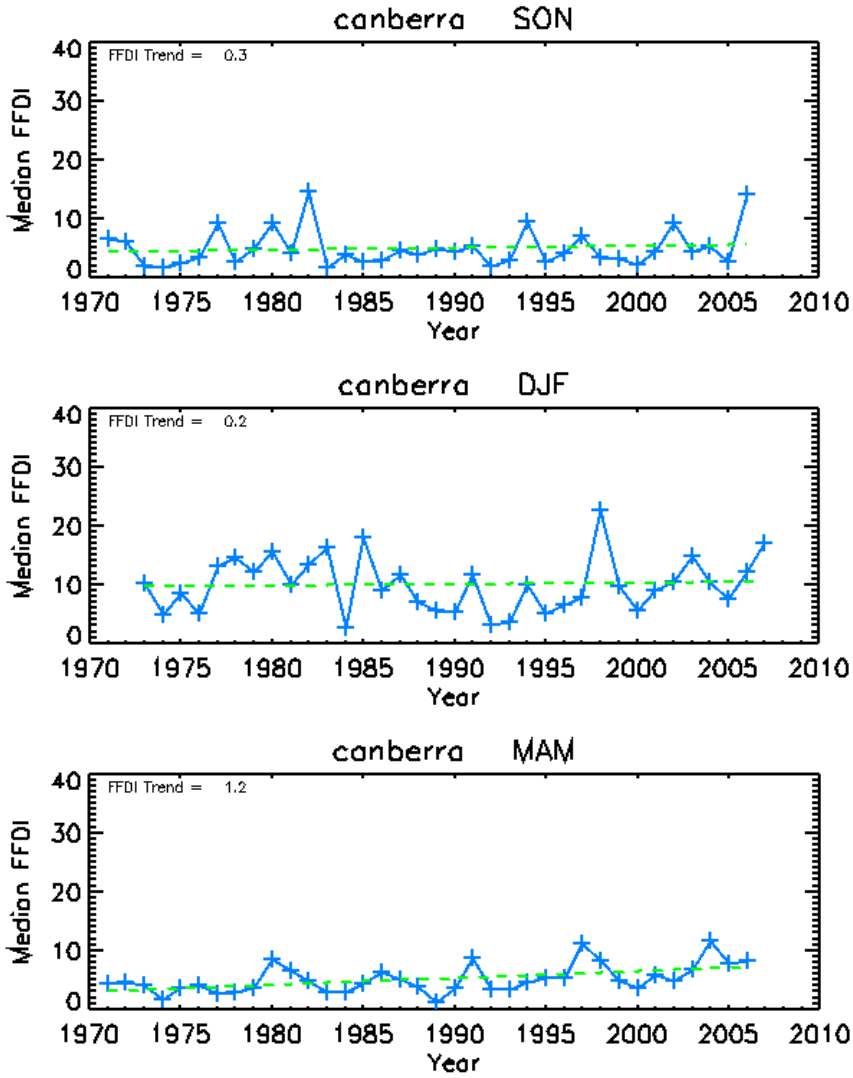

Figure 16. Seasonal median FFDI at Canberra for SON (spring, top), DJF (summer, centre) and MAM (autumn, bottom). Trend lines are shown in green. The value of the trend, in points per decade, is shown in the upper left corner of each plot.

In this study, the focus is on the median statistics. As noted earlier, the median is quite robust to the wind errors, with experiments suggesting only a minor change in its value when the wind effects are removed. The 90th percentile values are also shown in the Appendix.

Figure 16 shows time series of the median values for different seasons, plotted separately to emphasize their different character. As expected, the highest medians are observed in summer (DJF), the peak of the fire season when the highest variability is also seen. Variability is lowest in the autumn (MAM).

Fire Climate of Southeast Australia

In this section, the basic fire climate of southeast Australia is presented in terms of the three variables described above. This is done to orient the reader and provide the basis for the discussion to follow.

Figure 17 shows a map the average annual ΣFFDI from the years 1973 through 2007. The numbers are tabulated in Table 2. As noted in the Data section, these

numbers are 20-30% lower than those used in Hennessy et al [2005] due to the different methodology used in this study. Values range from 1255 at Coffs Harbour to 7249 at Woomera. Half of the 26 stations have a value of less then 2500. These are generally near the coast, from Mt Gambier to Coffs Harbour. Near the coast, the climate is moderated by the oceans and is generally more humid, resulting lower FFDI values. As one moves inland, the values rapidly increase, with averages at dry inland stations above 4500. The rapid inland increase is particularly noticeable at 'paired coastal/inland stations' (Brisbane AP/Amberley, Laverton/Melbourne AP and Sydney AP/Richmond). In all these cases, the station nearer the sea has significantly lower values than the more inland site.

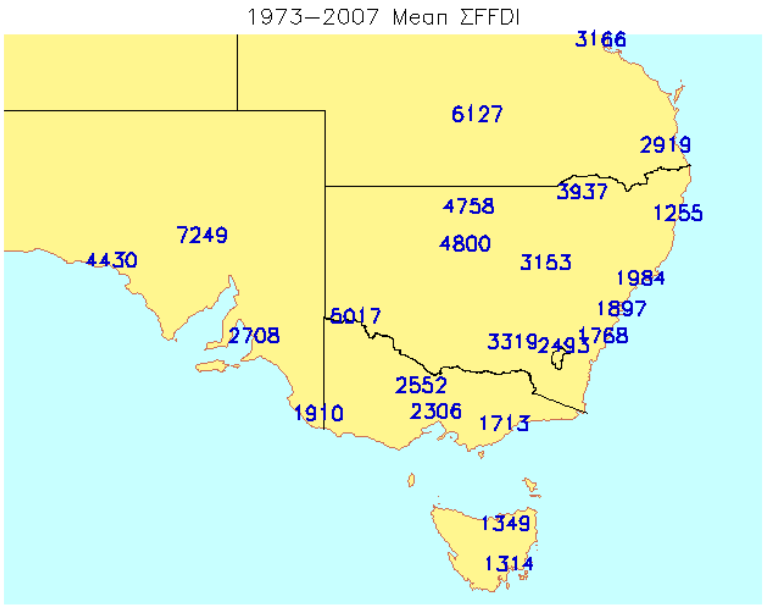

Figure 17. Average annual ΣFFDI for the 1973-74 through 2006-07 fire seasons. Brisbane, Laverton and Richmond are not shown for clarity.

Figure 18 shows maps of the number of days exceeding FDR thresholds for 'very high' (per year; upper left), 'extreme' (per decade; upper right), 'very extreme' (per decade; lower left) and 'catastrophic' (per century; lower right). Several features are evident. The first is that, at most locations, FDRs of extreme and above are relatively rare; this is particularly so in the case of 'catastrophic' (FDR>100) events. Several stations have never observed an FFDI in excess of 100[2]. A second feature is the coastal/inland disparity, as was found with ΣFFDI. Inland stations see more cases of extreme fire danger conditions. However, as was suggested by Figure 15, these occurrences are not evenly distributed throughout the year, but rather tend to either occur multiple times in a given season or not at all.

[2] In some cases, rare values of 100 exist before the beginning of the record. For example, FFDI at Hobart exceeded 100 on the 'Black Tuesday' fires of 1967. The value may also exceed 100 at times other than the 3 pm time used in this study. For example, see Figure 2.

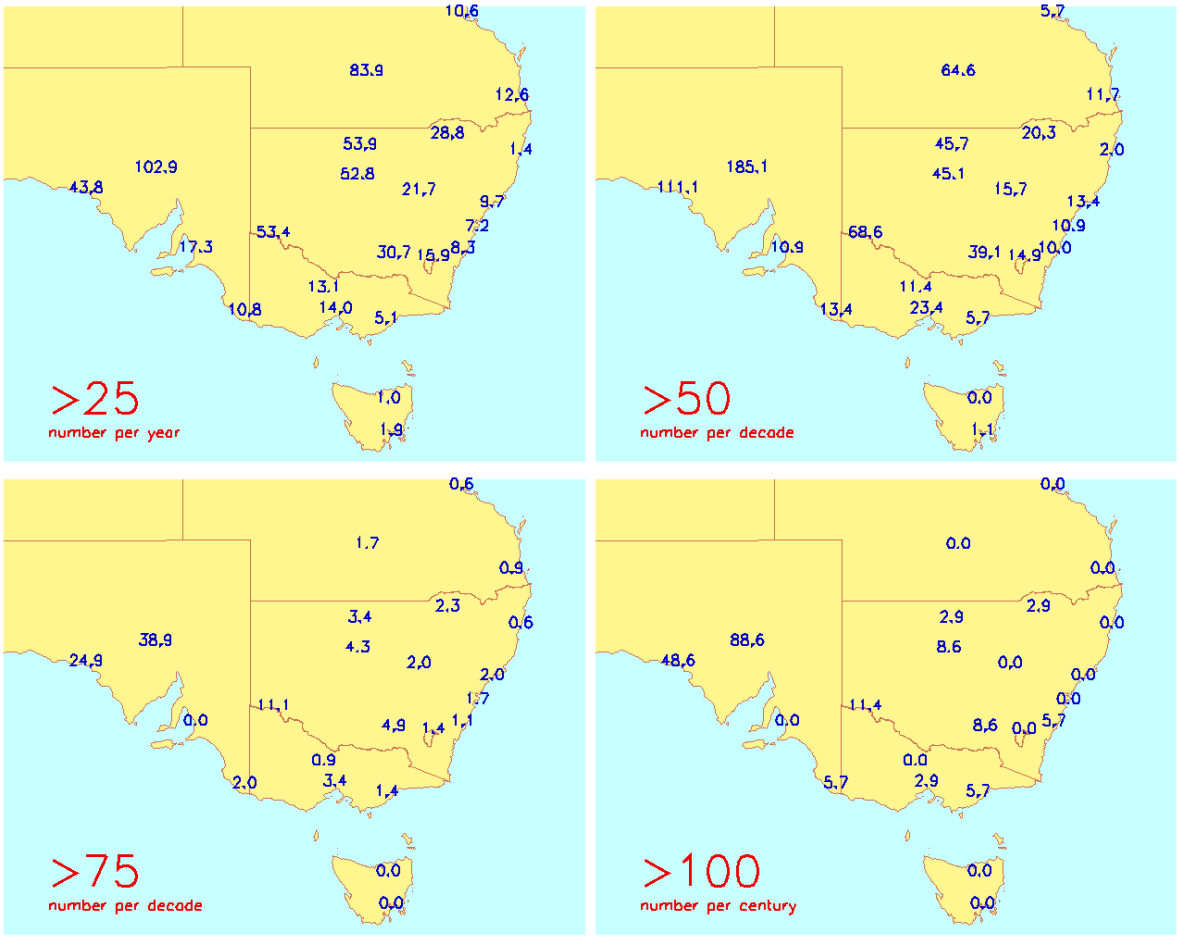

Figure 18. Average number of days exceeding a given FFDI/FDR threshold (red). Note the change in time interval over which that statistics are compiled. Based on data for 1973-2007.

Figure 19 shows the median seasonal median FFDI for each of the 4 seasons over the 36-year data period. The timing of the peak fire season as given by the median generally agrees with the schematic shown in Figure 7. Along the east coast, north from Coffs Harbour, the medians show a peak in JJA (winter) and SON (spring). From Charleville to Moree and the central NSW coastal stations, higher values are seen in SON (spring) and DJF (summer). The rest of the sites show a peak in DJF. The medians indicate that the more southerly stations tend to have a fire season biased towards summer-autumn, while the more northerly stations have a fire season biased towards spring-summer. The smallest values and weakest seasonal cycles are seen on the NSW central coast and in Tasmania.

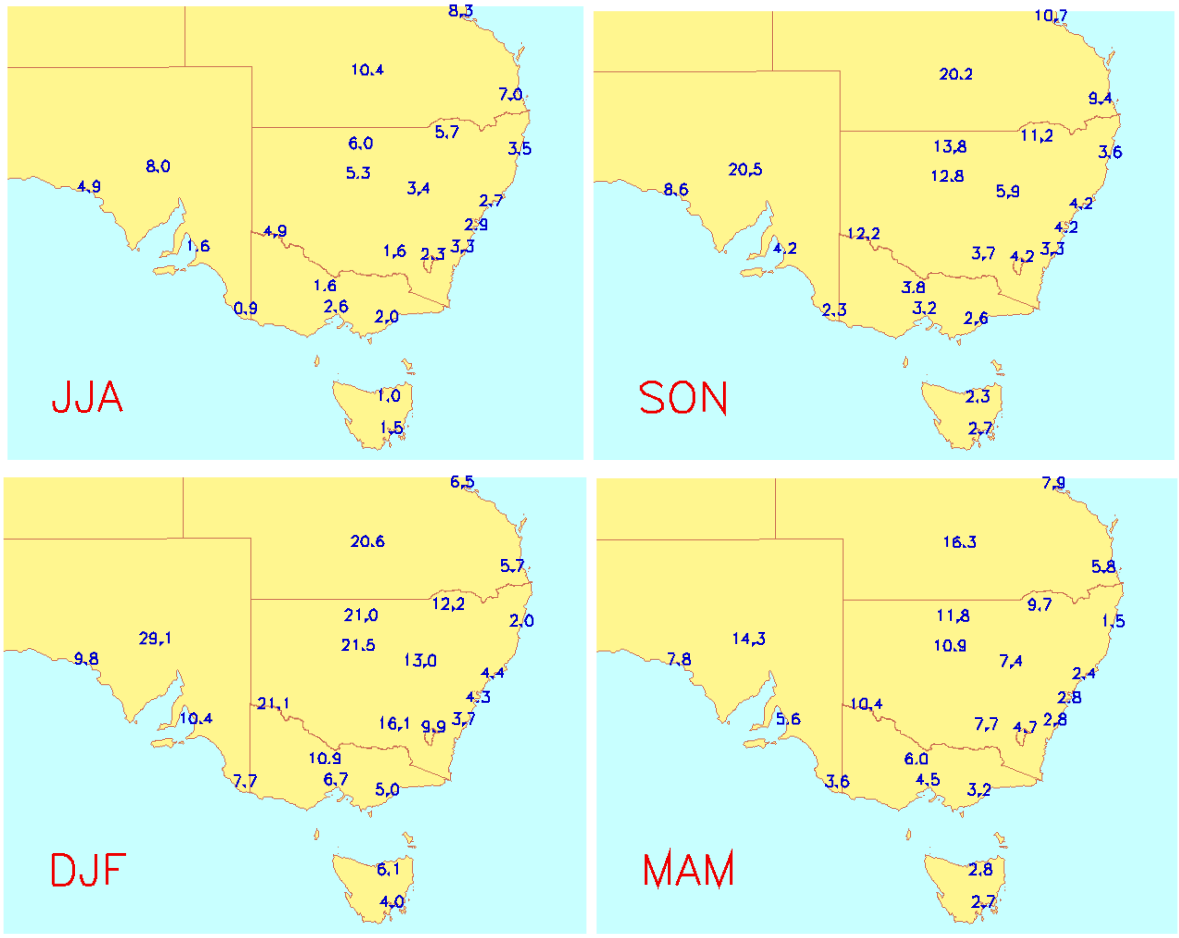

Figure 19. Map showing seasonal median FFDI values for 1973-2007. Seasons are notated in bottom left of each map. JJA = winter, SON = spring, DJF = summer and MAM = autumn.

Projected Impacts of Climate Change

Climate change can act in two ways to affect fire weather scenarios. First, it might exacerbate the fire-weather risk of any given day, leading to increased frequency or intensity of extreme fire weather days. Second, an increase in the accumulated fire risk over a year might represent a longer fire season and a reduction in the number of days suitable for controlled burning. We examine the climate change scenarios from both of these standpoints.

Creating the future scenarios

The method for creating future scenarios is described in detail in the report by Hennessy et al [2005]. A brief summary is provided here.

Climate change projections over southeastern Australia were generated from two CSIRO climate simulations named CCAM (Mark2) and CCAM (Mark3). Projected changes in daily temperature, humidity, wind and rainfall were generated for the years 2020 and 2050, relative to 1990 (the reference year used by the IPCC). These projections include changes in daily variability, computed as changes in decile values. They are expressed as a pattern of change per degree of global warming.

The patterns were scaled for the years 2020 and 2050 using estimates of global warming for those years. Hennessy et al [2005] used global warming values from the IPCC [2001] report, but in this study we use updated ranges of global warming

derived by CSIRO from the IPCC [2007] report, i.e. 0.4-1.0ºC by 2020 and 0.7-2.9ºC by 2050. This allows for the full range of SRES [2000] scenarios of greenhouse gas and aerosol emissions.

Four regional projections are given for each climate simulation: 2020 low, 2020 high, 2050 low and 2050 high. The low regional projections are based on low global warming, while high regional projections are based on high global warming.

The modelled changes from the various scenarios are then projected onto the observed time series of temperature, rainfall, wind and relative humidity from 1973 to the present. This methodology provides an estimate, based on the observed past weather, of what a realistic time series affected by climate change may look like. By using this procedure, the natural inter-relationships between the variables which make up the FFDI are maintained. The tacit assumption is that the variability observed over the past 30+ years will be maintained. With climate change, this may not be the case, and our methodology will not reproduce such a change.

In both models the largest changes to the different variables comes in the spring, although changes are observed in all seasons. There are systematic differences in the various scenarios due to differences in the two models. CCAM (Mark2) tends to have slightly higher temperature changes for a given decile/month combination. The number of rain days in both models is lower. CCAM (Mark2) generally has lower monthly average rain totals in most months. However, at many stations, CCAM (Mark3) shows an enhancement of the heaviest (decile 10) rainfalls, while showing larger decreases in rainfall in most other deciles. This often results in monthly totals which are significantly higher than the present climate. There are also differences in wind speed and relative humidity. The CCAM (Mark3) model tends to have positive (or less negative) changes in the wind speed compared to CCAM (Mark2). The signs of the change in wind are often opposite between the two models. Something similar applies to relative humidity, where CCAM (Mark3) tends to have more negative changes than CCAM (Mark2). Changes to the very low humidity deciles are especially greater in CCAM (Mark3).

Changes in cumulative FFDI

Table 2 shows the effects of climate change on the average cumulative FFDI from July to June. The CCAM (Mark3) high scenario produces the largest changes, while the CCAM (Mark2) low scenario gives the smallest changes. Figures 20 and 21 show the percentage changes in annual ΣFFDI for 2020 and 2050. In all simulations, the largest changes are in the interior of NSW and northern Victoria. As a general rule, coastal areas have smaller changes. However, the CCAM (Mark3) simulations indicate changes on the mid-NSW coast similar to that for inland NSW. At Hobart, a slight decrease is seen in the scenarios using the CCAM (Mark2) simulation.

The modelled changes are not linear; rather, there is more change between 2020 and 2050 than between 1990 and 2020. By 2020, the increase in ΣFFDI is generally 0 to 4% in the low scenarios and 0 to 10% in the high scenarios. By 2050, the increase is generally 0 to 8% (low) and 10 to 30% (high). As a rule, changes expected in the high scenario are roughly twice as large as those in the low scenario. The maximum changes in the 2020 high scenarios are about the same as in the 2050 low scenarios. Changes in Hobart are negligible.

Table 2: Annual (July to June) average cumulative FFDI for "present" (1973-2006) and changes (%) in the 2020 and 2050 scenarios, relative to 1990. The CCAM (Mark2) results are denoted "mk2" and CCAM (Mark3) results are denoted "mk3".

site	present Σ FFDI	% change							
		2020 low mk2	2020 high mk2	2020 low mk3	2020 high mk3	2050 low mk2	2050 high mk2	2050 low mk3	2050 high mk3
Adelaide	2708	2	5	3	8	3	16	5	25
Amberley	2919	2	7	1	6	4	24	3	19
Bendigo	2552	4	9	4	10	6	29	7	31
Bourke	4758	4	10	3	8	7	33	5	26
Brisbane AP	1990	1	5	0	4	3	19	2	16
Canberra	2493	3	9	3	11	6	30	7	37
Ceduna	4430	1	5	2	6	3	15	4	20
Charleville	6127	4	11	2	8	7	37	5	25
Cobar	4800	4	10	3	9	7	33	6	28
Coffs Harbour	1255	1	3	1	6	2	11	3	18
Dubbo	3153	4	11	4	10	7	34	6	32
Hobart	1314	-1	-1	0	0	-1	-1	0	3
Launceston AP	1349	0	1	1	6	0	8	3	22
Laverton	2056	1	6	2	8	4	23	5	30
Melbourne AP	2306	2	7	3	9	4	22	6	30
Mildura	5017	2	7	3	8	4	21	5	26
Mt Gambier	1910	1	3	2	5	2	11	3	18
Moree	3937	4	12	4	10	8	37	6	29
Nowra	1768	0	2	1	7	0	12	4	29
Richmond	2152	1	6	2	8	3	20	5	26
Rockhampton	3166	2	6	2	7	4	21	4	22
Sale	1713	0	5	1	8	2	19	4	31
Sydney AP	1897	1	4	3	10	2	11	6	31
Wagga	3319	3	9	3	10	6	29	6	33
Williamtown	1984	1	4	3	9	3	14	6	27
Woomera	7249	1	5	2	6	3	15	4	20

Figures 20 and 21 depict the spatial pattern of these changes. The largest changes are generally seen at the inland stations of NSW, although there are differences between the simulations. The CCAM (Mark2) simulation has larger changes in inland NSW, but in South Australia, Tasmania and Victoria CCAM (Mark3) shows larger changes. CCAM (Mark3) also depicts a significant increase on the central NSW coast compared to CCAM (Mark2).

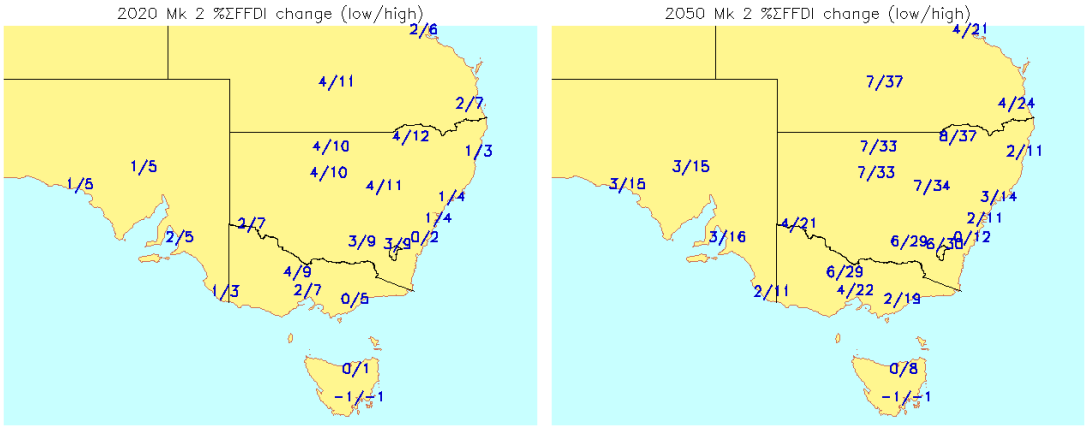

Figure 20 Changes to ΣFFDI in the CCAM (Mark2) simulations. The 2020 case is on the left; 2050 on the right. At each site, values for the low scenario are to the left of slash, while values for the high scenario are to the right.

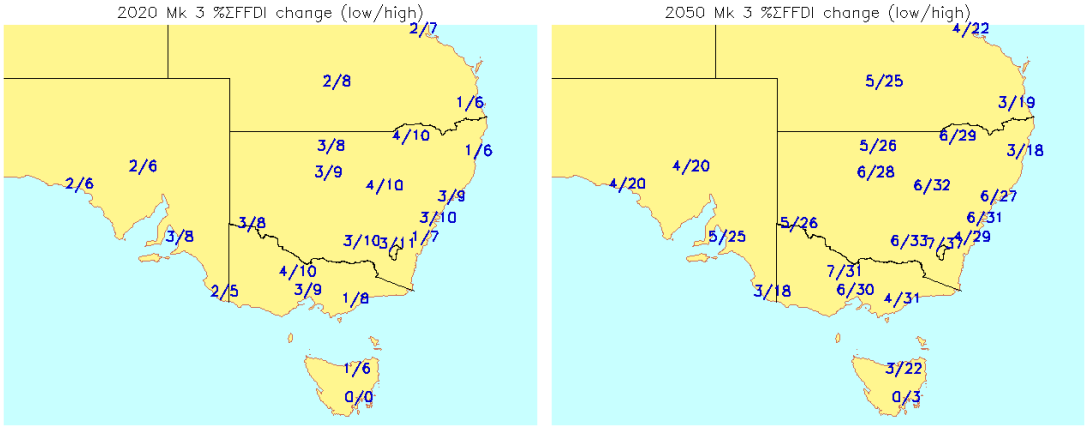

Figure 21. As in Figure 20, but for the CCAM (Mark3) scenarios.

Changes in daily fire-weather risk

The annual cumulative FFDI values mask much larger changes in the number of days with significant fire risk (Tables 3-6). Unsurprisingly, many of the characteristics are similar to what is seen with ΣFFDI.

Table 3 shows the changes in all VHE days in the different scenarios. This is the largest category, as it contains all days with FFDI in excess of 25. The increase varies at different stations. By 2020, increases are generally 2-13% for the low scenarios and 10-30% for the high scenarios. By 2050, the range is much broader, generally 5-23% for the low scenarios and from 20% to 100% for the high scenarios. The amount depends on the location and the particular model used. The number of additional VHE days this actually entails varies greatly. For example, at Cobar between 64 and 100 VHE days are expected by 2050, compared to 56 today, but at Melbourne AP, there are 16-24 VHE days by 2050, compared to only 15 today.

Table 3. Average number of days per year with FDR of 'very high' or greater (FFDI at least 25) and the percent change from the current value. Values for "present" are for 1973-2007. The CCAM (Mark2) results are denoted "mk2" and CCAM (Mark3) results are denoted "mk3".

site	now	2020				2050			
		Low mk2	Low mk3	High mk2	High mk3	Low mk2	Low mk3	High mk2	High mk3
Adelaide	18.3	19.2	19.8	20.8	22.3	19.9	20.8	26.1	30.2
%	--	5	8	13	22	9	14	43	65
Amberley	13.3	14.5	14.2	16.4	15.7	15.3	14.8	22.7	20.9
%	--	8	6	23	18	15	11	70	57
Bendigo	13.9	15.6	16.1	17.5	18.4	16.6	17.1	25.2	28.6
%	--	12	16	26	32	20	23	81	106
Bourke	57.2	62.3	61.4	71.3	68.6	66.4	64.5	103.7	91.5
%	--	9	7	25	20	16	13	81	60
Brisbane AP	5.2	5.4	5.3	5.9	5.8	5.7	5.6	8.5	7.5
%	--	4	2	14	12	9	7	63	45
Canberra	16.8	18.3	18.9	21.5	22.8	20.0	20.6	29.9	33.4
%	--	9	13	28	36	19	23	78	98
Ceduna	46.4	47.7	48.0	49.4	50.5	48.5	49.0	56.5	58.6
%	--	3	3	6	9	5	6	22	26
Charleville	89.0	95.6	93.6	108.3	102.0	101.5	97.2	147.5	126.7
%	--	7	5	22	15	14	9	66	42
Cobar	56.0	61.4	60.8	69.9	67.9	65.2	64.0	99.5	91.8
%	--	10	8	25	21	16	14	78	64
Coffs Harbour	1.5	1.6	1.6	1.8	1.8	1.8	1.8	2.3	2.5
%	--	6	6	22	20	20	18	57	71
Dubbo	23.0	25.6	25.3	30.0	29.2	27.4	27.1	45.9	43.8
%	--	11	10	30	27	19	18	100	90
Hobart	2.0	2.0	2.0	2.0	2.1	2.0	2.1	2.0	2.2
%	--	-3	-3	-2	5	-2	2	0	8
Launceston AP	1.0	1.0	1.2	1.1	1.2	1.0	1.2	1.2	2.2
%	--	-3	12	3	18	0	15	18	112
Laverton	11.8	12.0	12.3	12.8	13.6	12.4	12.8	16.7	19.2
%	--	2	4	9	15	5	9	42	63
Melbourne AP	14.8	15.7	15.9	17.0	17.6	16.2	16.5	21.2	23.6
%	--	6	7	15	19	9	12	43	59
Mildura	56.6	59.5	60.3	65.5	66.9	62.3	63.7	84.7	90.5
%	--	5	7	16	18	10	13	50	60
Mt Gambier	11.5	11.6	11.8	12.3	12.8	12.0	12.3	14.0	15.4
%	--	1	3	7	12	5	7	22	34
Moree	30.5	34.5	33.7	41.1	38.9	37.6	36.4	62.8	55.8
%	--	13	10	35	28	23	19	106	83
Nowra	8.8	8.7	9.1	9.2	10.3	8.9	9.6	10.8	14.7
%	--	-1	3	5	17	2	10	23	68
Richmond	13.3	13.8	14.2	15.2	16.3	14.5	15.1	20.3	23.6
%	--	4	6	14	23	9	13	53	77
Rockhampton	11.2	12.0	11.9	13.2	13.5	12.4	12.8	18.6	19.4
%	--	7	6	17	20	10	14	66	73
Sale	5.4	5.4	5.7	5.9	7.1	5.7	6.3	8.1	11.1
%	--	1	7	10	32	6	18	50	107
Sydney AP	7.6	7.8	8.1	8.3	9.4	8.0	8.7	9.8	14.2
%	--	2	6	9	23	4	14	28	87
Wagga	32.6	34.8	35.0	39.7	40.3	37.1	37.2	56.3	57.6
%	--	7	7	22	24	14	14	73	77
Williamtown	10.3	10.8	11.2	11.5	12.8	11.3	11.9	13.9	17.8
%	--	6	9	12	25	10	16	36	73
Woomera	109.1	112.3	112.8	118.1	119.4	115.2	115.9	135.4	139.1
%	--	2	3	8	10	6	6	24	28

Table 4 shows the number of days with an extreme or higher FDR. Overall, the spatial patterns are similar to those shown in the previous Table. By 2020, percentage increases are generally 5-25% for the low scenarios and 15-65% for the high scenarios. By 2050, the number of extreme days generally increases by 10-50% for the low scenarios and 100-300% for the high scenarios, from near zero to around 300% (quadruple the number of days). These higher percentage changes often reflect small numbers of days, but a doubling of the number of extreme days is fairly common.

Table 5 presents similar information on the occurrence of days with of very extreme (FFDI >75) or higher fire danger. As FFDIs this high are rare occurrences at most stations, the frequency is presented here in terms of the *return period*, or the typical number of years between occurrences. Very extreme days are only seen annually at Mildura, Ceduna and Woomera. At other stations, very extreme conditions occur only once every 2 to 11 years. Several stations have never observed an FFDI this high. As before, coastal stations show fewer occurrences, inland stations more. By 2020, the low scenarios show little changes in return periods at most sites, although notable decreases occur at Amberley, Charleville, Bendigo, Cobar, Dubbo and Williamtown. The 2020 high scenarios indicate that very extreme days may occur about twice as often at many sites. By 2050, the low scenarios changes are similar to those for the 2020 high scenarios, while the 2050 scenarios suggest a four- to five-fold increase in frequency at many sites.

Table 6 shows return periods for the number of 'catastrophic' (FFDI>100) days in the different scenarios. Only 12 of 26 sites have recorded 'catastrophic' fire danger days since 1973. The 2020 low scenarios indicate little or no change, except for a halving of the return period at Bourke. The 2020 high scenarios show 'catastrophic' days occurring at 20 sites, 10 of which have return periods of around 16 years or less. By 2050, the low scenarios are similar to those for the 2020 high scenarios. The 2050 high scenarios show 'catastrophic' days occurring at 22 sites, 19 of which have return periods of 8 years or less, while 7 sites have return periods of 3 years or less. For example, at Melbourne AP, the return period goes from once every 33 years at present to once every 2.4 years by 2050. Nearly all stations have some occurrence of 'catastrophic' fire danger by 2050 for the CCAM Mark3 scenario. Only four sites avoid 'catastrophic' days by 2050; Hobart, Launceston, Brisbane and Adelaide.

Changes to Median FFDI

Climate change affects the overall frequency distribution of FFDI days as well. Examining the VHE days (see above) provides information about the upper end of the distribution. As noted earlier, the median gives some indication of the overall severity of the season. A higher median may indicate a more severe fire season. Figure 22 shows a bar chart which depicts the current median value along with the changes expected in the different climate scenarios. This is analysed over individual seasons. As with the other variables, the largest changes occur in high 2050 scenarios. The 2020 changes are relatively small. As before, the changes in the 2050 low scenarios are about the same as the 2020 high scenarios. The spatial

differences in the changes are also the same, with inland locations showing greater change and coastal locales showing less.

Table 4. Average number of "extreme" fire weather days per year with FFDI > 50 and. Values for "present" are for 1973-2007. The CCAM (Mark2) results are denoted "mk2" and CCAM (Mark3) results are denoted "mk3".

site	present	2020				2050			
		Low mk2	Low mk3	High mk2	High mk3	Low mk2	Low mk3	High mk2	High mk3
Adelaide	1.2	1.4	1.5	1.5	1.8	1.4	1.5	2.3	3.8
%	--	18	26	29	55	23	32	103	234
Amberley	1.2	1.4	1.4	1.8	1.6	1.5	1.5	3.0	2.8
%	--	12	12	42	32	24	22	142	124
Bendigo	1.2	1.5	1.5	1.8	2.0	1.6	1.8	2.8	4.0
%	--	23	25	53	65	35	50	135	230
Bourke	4.8	5.6	5.6	7.3	7.2	6.2	6.3	14.6	13.9
%	--	16	16	50	48	28	31	201	188
Brisbane AP	0.5	0.5	0.5	0.6	0.6	0.6	0.5	1.0	0.9
%	--	6	6	31	31	25	6	106	88
Canberra	1.6	1.7	1.7	2.0	2.2	1.8	2.0	3.7	5.1
%	--	8	10	25	42	17	25	137	221
Ceduna	11.8	12.3	12.3	13.6	13.8	12.9	13.1	17.3	18.5
%	--	4	4	15	17	10	11	47	57
Charleville	6.8	8.2	7.9	11.3	10.2	9.5	9.1	27.5	20.9
%	--	19	15	64	50	39	33	301	205
Cobar	4.8	5.3	5.5	7.4	7.2	6.4	6.3	14.4	14.1
%	--	11	14	54	51	33	32	200	194
Coffs Harbour	0.2	0.2	0.2	0.2	0.3	0.2	0.3	0.3	0.4
%	--	0	0	14	29	0	29	43	71
Dubbo	1.7	2.0	2.1	2.8	3.1	2.5	2.6	6.3	6.7
%	--	18	27	70	83	47	55	280	303
Hobart	0.1	0.1	0.1	0.1	0.1	0.1	0.1	0.1	0.2
%	--	0	0	0	0	0	0	0	50
Launceston AP	--	0.0	0.0	0.0	0.0	0.0	0.0	0.0	0.1
%	--	--	--	--	--	--	--	--	--
Laverton	1.9	1.9	2.1	2.4	2.6	2.2	2.4	3.5	4.6
%	--	2	8	27	38	16	24	84	143
Melbourne AP	2.5	2.8	2.8	3.1	3.4	3.0	3.2	4.5	5.8
%	--	12	15	26	38	20	28	81	136
Mildura	7.3	8.0	8.3	9.1	10.0	8.6	9.0	12.8	15.9
%	--	10	14	25	38	18	24	76	120
Mt Gambier	1.4	1.5	1.6	1.6	1.8	1.6	1.7	2.2	2.9
%	--	9	13	15	26	15	17	53	104
Moree	2.2	2.5	2.4	3.6	3.4	2.8	2.7	8.5	8.0
%	--	17	13	68	60	32	27	293	273
Nowra	1.1	1.0	1.2	1.2	1.6	1.1	1.5	1.9	4.0
%	--	-3	14	14	54	3	40	83	280
Richmond	1.5	1.5	1.6	1.7	1.9	1.6	1.8	2.7	4.0
%	--	4	8	15	29	8	21	85	177
Rockhampton	0.6	0.6	0.7	0.7	0.8	0.6	0.7	1.2	1.5
%	--	5	15	20	30	5	20	105	140
Sale	0.6	0.6	0.7	0.7	0.9	0.6	0.8	1.1	1.9
%	--	5	10	15	45	5	30	80	215
Sydney AP	1.2	1.3	1.4	1.5	1.7	1.3	1.5	1.8	3.5
%	--	11	21	26	50	13	34	53	200
Wagga	4.2	4.7	4.8	5.7	5.9	5.2	5.5	9.9	11.1
%	--	14	15	37	42	26	31	138	168
Williamtown	1.4	1.6	1.7	1.7	2.3	1.6	1.9	2.4	4.1
%	--	11	17	17	62	15	36	66	189
Woomera	19.6	20.8	21.5	22.4	24.1	21.6	22.5	29.3	34.7
%	--	6	9	14	23	10	14	49	77

Table 5. Typical 'return period' for FFDI > 75 (years per occurrence) and the percentage change in the simulations. Values for "present" are for 1973-2007. The CCAM (Mark2) results are denoted "mk2" and CCAM (Mark3) results are denoted "mk3".

site	now	2020				2050			
		Low mk2	Low mk3	High mk2	High mk3	Low mk2	Low mk3	High mk2	High mk3
Adelaide	--	--	33.0	33.0	33.0	33.0	33.0	5.5	2.4
Amberley	11.0	6.6	6.6	3.7	4.7	6.6	6.6	2.5	2.1
Bendigo	11.0	8.2	8.2	6.6	5.5	8.2	6.6	3.0	1.8
Bourke	2.8	2.2	2.2	1.8	1.6	1.9	2.1	0.6	0.7
Brisbane AP	--	--	--	--	--	--	--	11.0	8.2
Canberra	6.6	6.6	6.6	6.6	4.7	6.6	6.6	2.4	1.2
Ceduna	0.4	0.4	0.4	0.3	0.3	0.3	0.3	0.2	0.2
Charleville	5.5	3.7	3.7	1.7	1.6	2.4	2.5	0.3	0.5
Cobar	2.2	1.6	1.6	1.2	1.2	1.5	1.5	0.5	0.6
Coffs Harbour	16.5	16.5	16.5	16.5	8.2	16.5	11.0	11.0	6.6
Dubbo	4.7	3.7	3.7	3.0	3.0	3.3	3.3	1.1	1.0
Hobart	--	--	--	--	--	--	--	--	--
Launceston AP	--	--	--	--	--	--	--	--	--
Laverton	3.0	2.8	2.5	2.1	1.7	2.4	2.1	1.3	0.9
Melbourne AP	2.8	2.4	2.2	1.6	1.5	1.9	1.9	1.0	0.6
Mildura	0.8	0.8	0.8	0.6	0.5	0.7	0.6	0.4	0.3
Mt Gambier	4.7	4.7	4.7	4.7	4.1	4.7	4.1	4.1	2.4
Moree	4.1	3.7	3.7	2.2	2.2	2.5	2.5	1.1	1.1
Nowra	8.2	8.2	8.2	8.2	6.6	8.2	6.6	4.7	1.6
Richmond	2.8	2.8	2.5	2.8	1.9	2.8	2.2	1.6	1.1
Rockhampton	16.5	16.5	16.5	16.5	11.0	16.5	11.0	6.6	5.5
Sale	6.6	6.6	6.6	6.6	6.6	6.6	6.6	6.6	5.5
Sydney AP	5.5	5.5	5.5	5.5	3.3	5.5	4.7	3.3	1.0
Wagga	1.9	1.6	1.5	1.1	1.1	1.3	1.3	0.4	0.4
Williamtown	4.7	3.7	3.3	3.3	2.1	3.3	2.4	1.8	0.9
Woomera	0.2	0.2	0.2	0.2	0.2	0.2	0.2	0.1	0.1

Table 6. Typical 'return period' (years) of days with 'catastrophic' fire danger (FFDI > 100). Values for "present" are for 1973-2007. The CCAM (Mark2) results are denoted "mk2" and CCAM (Mark3) results are denoted "mk3".

Site	now	2020				2050			
		low2	low3	high2	high3	low2	low3	high2	high3
Adelaide	--	--	--	--	--	--	--	--	--
Amberley	--	--	--	--	33.0	--	--	33.0	11.0
Bendigo	--	--	--	--	33.0	--	--	16.5	8.2
Bourke	33.0	16.5	16.5	8.2	8.2	11.0	11.0	4.1	2.8
Brisbane AP	--	--	--	--	--	--	--	--	--
Canberra	--	33.0	16.5	16.5	16.5	16.5	16.5	16.5	8.2
Ceduna	1.9	1.7	1.6	1.5	1.3	1.6	1.5	0.8	0.6
Charleville	--	--	--	33.0	--	--	--	3.7	5.5
Cobar	11.0	11.0	11.0	11.0	8.2	11.0	11.0	3.7	3.3
Coffs Harbour	--	--	--	--	--	--	--	33.0	33.0
Dubbo	--	33.0	33.0	16.5	16.5	16.5	16.5	6.6	4.7
Hobart	--	--	--	--	--	--	--	--	--
Launceston AP	--	--	--	--	--	--	--	--	--
Laverton	6.6	6.6	6.6	6.6	5.5	6.6	6.6	4.1	2.8
Melbourne AP	33.0	33.0	33.0	16.5	16.5	16.5	16.5	4.7	2.4
Mildura	8.2	6.6	4.7	3.0	2.1	4.1	3.3	1.4	0.8
Mt Gambier	16.5	16.5	16.5	16.5	11.0	16.5	16.5	16.5	5.5
Moree	33.0	33.0	33.0	33.0	33.0	33.0	33.0	4.7	3.7
Nowra	16.5	16.5	16.5	16.5	16.5	16.5	16.5	16.5	8.2
Richmond	--	--	--	--	33.0	--	33.0	16.5	4.1
Rockhampton	--	--	--	33.0	33.0	--	33.0	33.0	16.5
Sale	16.5	16.5	16.5	16.5	16.5	16.5	16.5	16.5	6.6
Sydney AP	--	--	33.0	--	33.0	--	33.0	--	4.1
Wagga	11.0	11.0	11.0	11.0	6.6	11.0	11.0	3.0	1.8
Williamtown	--	16.5	16.5	16.5	16.5	16.5	16.5	16.5	3.3
Woomera	1.1	1.0	0.9	0.8	0.7	0.8	0.8	0.5	0.3

By performing a seasonal analysis, an estimate of changes in the timing of fire seasons can be made. The greatest changes in the median FFDI are seen in the season of highest fire danger, generally summer (DJF). A large change is also seen in the season prior to the peak season as well. Generally, this change is larger than that for the season immediately following the peak. The 'off season' (usually winter (JJA)) tends to have the smallest increase.

Taken together, these results suggest that fire seasons will start earlier and end slightly later, while being generally more intense throughout their length. This effect is most pronounced by 2050, although it should be apparent by 2020.

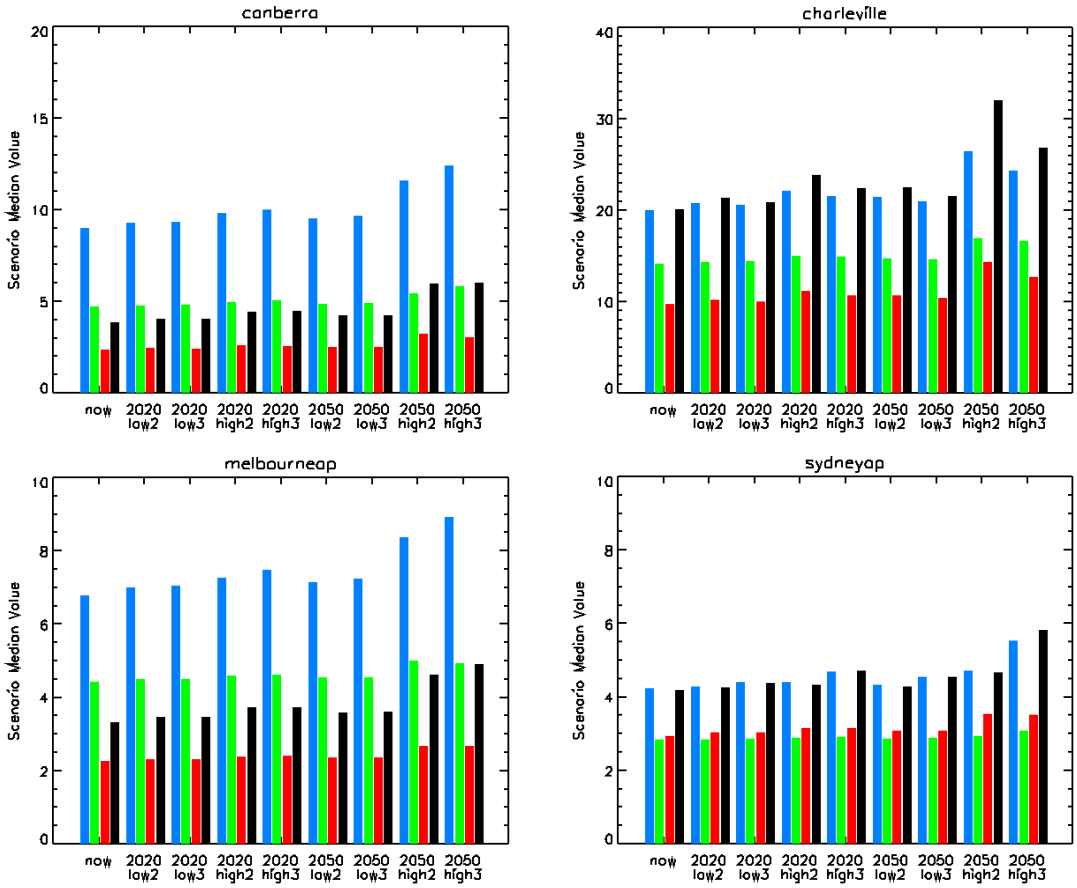

Figure 22. Changes in the median FFDI at Canberra, Charleville, Melbourne AP and Sydney AP under the various climate scenarios. All four seasons are shown, with summer (DJF) in blue, autumn (MAM) in green, winter (JJA) in red and spring (SON) in black. Note that the vertical scale on each plot varies.

Table 7 estimates the average trend associated with this change in median FFDI. This is computed by taking the difference in the medians and dividing by the number of decades (3 or 6) between 1990 and either 2020 or 2050. The trends are generally quite small, only a few tenths of a point per decade. However, even these small trends should be detectable at most stations assessed in this report. The trends computed in this table are used to provide a base for comparing the observed trends in a later section. The current trends are presented in Figure 25 and Table 8.

Table 7.Expected trends in median FFDI over summer (DJF; points/decade) from model simulations

Site	2020 Low Mk2	2020 High Mk2	2020 Low Mk3	2020 High Mk3	2050 Low Mk2	2050 High Mk2	2050 Low Mk3	2050 High Mk3
Adelaide	0.2	0.2	0.1	0.1	0.2	0.2	0.1	0.1
Amberley	0.2	0.1	0.0	0.0	0.3	0.2	0.1	0.0
Bendigo	0.3	0.4	0.1	0.2	0.5	0.6	0.1	0.1
Bourke	0.6	0.6	0.3	0.3	0.9	0.9	0.2	0.2
Brisbane AP	0.1	0.1	0.0	0.0	0.2	0.1	0.0	0.0
Canberra	0.3	0.3	0.1	0.1	0.4	0.6	0.1	0.1
Ceduna	0.1	0.2	0.0	0.1	0.1	0.2	0.0	0.1
Charleville	0.7	0.5	0.2	0.2	1.1	0.7	0.2	0.2
Cobar	0.6	0.6	0.2	0.2	0.9	0.9	0.2	0.2
Coffs Harbour	0.1	0.1	0.0	0.0	0.1	0.1	0.0	0.0
Dubbo	0.4	0.4	0.2	0.2	0.6	0.6	0.1	0.1
Hobart	-0.0	0.0	-0.0	-0.0	0.0	0.0	-0.0	0.0
Launceston AP	0.0	0.1	-0.0	0.0	0.1	0.2	0.0	0.0
Laverton	0.1	0.2	0.0	0.1	0.2	0.3	0.0	0.1
Melbourne AP	0.2	0.2	0.1	0.1	0.3	0.4	0.1	0.1
Mildura	0.4	0.6	0.1	0.2	0.6	1.0	0.1	0.2
Mt Gambier	0.5	0.3	0.2	0.1	0.7	0.4	0.2	0.1
Moree	0.1	0.2	0.0	0.1	0.2	0.2	0.0	0.0
Nowra	0.0	0.1	-0.0	0.0	0.1	0.2	0.0	0.0
Richmond	0.1	0.2	0.0	0.1	0.2	0.3	0.0	0.1
Rockhampton	0.2	0.2	0.1	0.1	0.2	0.3	0.0	0.1
Sale	0.1	0.2	0.0	0.0	0.1	0.3	0.0	0.0
Sydney AP	0.1	0.2	0.0	0.1	0.1	0.2	0.0	0.1
Wagga	0.6	0.6	0.2	0.2	0.8	0.9	0.2	0.2
Williamtown	0.1	0.2	0.0	0.1	0.1	0.2	0.0	0.1

Table 8. Trends in the seasonal median (50th percentile) FFDI for spring (SON), summer (DJF) and autumn (MAM) from 1973-2007. Trends in 90th percentile are also shown. Values significant at the 90% level are underlined. Values significant at the 95% level are in bold. Units are 'points' per decade

Site	50% SON	50% DJF	50% MAM	90% SON	90% DJF	90% MAM
Adelaide	0.5	**0.9**	**0.7**	1.4	**2.4**	**1.3**
Amberley	**1.4**	**1.4**	**1.3**	**3.4**	**2.1**	**1.9**
Bendigo	**1.0**	**2.2**	**1.4**	**3.1**	**4.3**	**3.2**
Bourke	**3.7**	**5.1**	**2.6**	**5.9**	**6.8**	**4.5**
Brisbane AP	0.2	0.3	0.3	-0.2	0	0.2
Canberra	0.3	0.2	**1.2**	0.7	0.4	**2.6**
Ceduna	**0.9**	**1.1**	**1.2**	**3.4**	**3.2**	**3.8**
Charleville	**2.1**	1.0	**1.8**	**3.0**	1.9	**2.9**
Cobar	1.7	**2.5**	0.9	**2.9**	2.8	1.0
Coffs Harbour	0.3	0.3	0.2	0.5	**0.8**	0.3
Dubbo	1.3	**3.5**	**1.5**	3.0	**6.2**	**2.9**
Hobart	**0.3**	0.3	**0.3**	**0.7**	0.8	0.6
Launceston AP	**0.3**	0.5	**0.5**	**0.6**	0.5	**1.0**
Laverton	**0.5**	0.1	0.1	1.5	1.2	0.3
Melbourne AP	**0.7**	0.5	0.3	**2.2**	**2.7**	0.8
Mildura	**1.9**	**2.3**	**1.3**	**3.4**	**3.3**	**2.4**
Mt Gambier	0.2	0.1	0.3	**1.0**	0.7	0.8
Moree	**1.7**	1.3	**1.3**	**3.7**	**3.0**	**2.1**
Nowra	0.5	0.4	**0.6**	1.8	0.6	**1.6**
Richmond	0.7	0.5	0.9	1.7	0.7	1.2
Rockhampton	**1.2**	**1.3**	**1.1**	**2.3**	**1.9**	**2.3**
Sale	0.5	0.6	**0.5**	1.2	0.9	**1.3**
Sydney AP	**0.6**	**0.6**	0.4	1.9	**1.3**	**1.1**
Wagga	1.2	**2.2**	**1.7**	2.5	3.3	**2.7**
Williamtown	0.3	0.6	-0.2	1.8	0.8	0.3
Woomera	**2.9**	**3.4**	**1.9**	**6.1**	**4.9**	**3.5**

Year to year variability

The changes to the fire season suggested in this study do not represent a uniform shift across all years. Rather, the fire seasons shift by different amounts in different years. Figure 23 illustrates this, where the various climate change scenarios are applied to the historic record for Canberra. Some change in the number of VHE days is seen in most years, suggesting that in most years some increase in fire danger will be observed. In many cases, the largest increases are seen in years that are already more extreme in the current climate (e.g. 1982-83, 1997-98, 2006-07). By 2050, the scenarios suggest that what were more 'marginal' years, such as the late-70s/early-80s become equivalent to (or exceed) what are the more extreme years in the current climate. However, many of the less extreme years, which show few VHE days, remain so in the projections, with little increase expected.

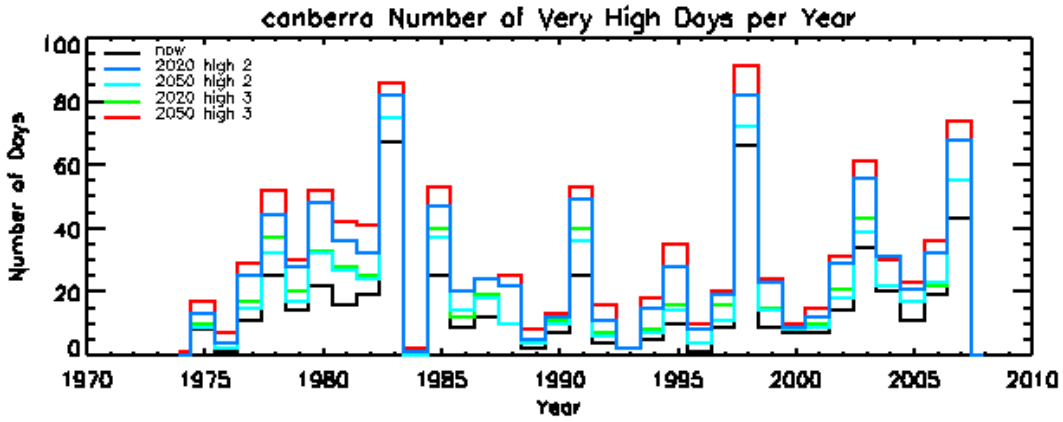

Figure 23. Time series showing changes in VHE fire danger days at Canberra for 'now' (1973-2006) and the equivalent days for the 2020 and 2050 'high' scenarios in CCAM (Mark2) and CCAM (Mark3).

The broad conclusion from this is that dangerous fire seasons will become more common. The more extreme years will become even worse, 'marginal' years will become more dangerous and the infrequent less extreme years will remain so.

Evaluating the current climate: Where are we today?

The analysis in the preceding section is based on projections in changes in model distributions for periods centred on 2020 and 2050, relative to a period centred on 1990. As we are more than halfway to 2020, some effect on FFDI should be discernable by this time. In this section, we will evaluate this case.

Over the last few years, there has been a growing awareness of bushfires in Australia. Several high-impact events, including the Sydney 'Black Christmas' bushfires beginning in late-2001, the Canberra bushfires in January 2003 and the eastern Victorian fires in early 2003 and 2007, have hastened this trend. Along with this awareness has come the general perception that bushfire seasons are becoming more extreme, with an increase in the number of 'very high' and 'extreme' days, inferring larger, more-frequent and less controllable bushfires. There are many ways to evaluate claims that seasons are getting worse.

Trends in the Median

A simple, non-quantitative method of examining the claim is to rank the medians of the individual summer seasons. (Recall, the median can be used as a proxy for the overall season strength). Figure 24 shows the years of the three highest summer median FFDI from 1973-74 through the 2006-07 seasons at each station. While individual years do vary to some degree at each station, 50 out of the 69 possible 'slots' on the map have occurred since 2000, and 59 of the 69 have occurred since 1996. **All** stations have one post-2000 year in their strongest three during summer, and at many stations all three have occurred since 2000. The latter is particularly marked in the northern plains of NSW and at many stations in SA. A similar tendency, albeit not as marked, is seen for autumn to spring (not shown). The overwhelming majority of stations have at least one of their top three medians after 2000. For spring, the worst years were 1982, 2006, 2002 and 1994. In autumn, these years are 2005, 2004 and 2002, although there is larger variety of years during this season.

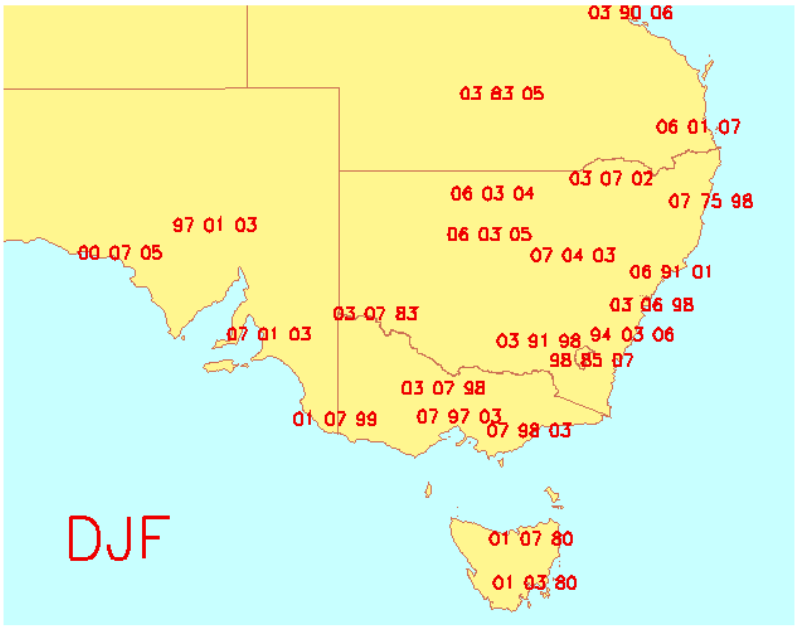

Figure 24. Map showing years with the three highest ranking summer (DJF) median FFDI. In this example 2006-7 would be noted with an '07'. Brisbane, Laverton and Richmond not shown for clarity.

These results suggest a positive trend in the summer median at most stations. This is evaluated directly by computing the trend over the 1973-74 to 2006-07 summer seasons. The results are shown on the map in Figure 25. Red numbers indicate trends significant at the 95% level. Trends exceeding 1.0 FFDI point per decade are seen at most inland stations on the mainland. The trend at Bourke, in northern NSW, exceeds 5 points per decade. The majority of these trends are significant at the 95% level. Trends at coastal stations and in Tasmania are lower and generally not significant. (In the figure, non-significant trends at Laverton, Brisbane AP and Richmond are not shown for clarity.)

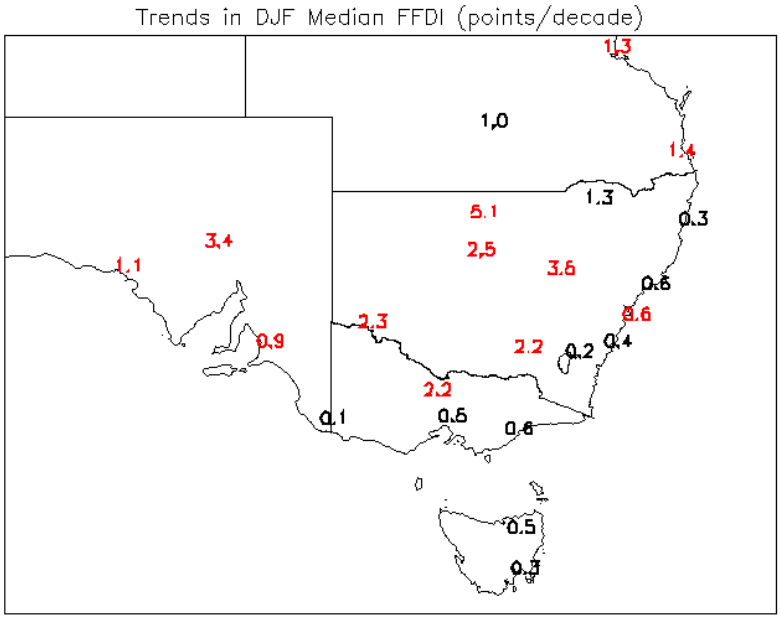

Figure 25. Map of observed trends in summer (DJF) median FFDI. Units are points per decade. Red numbers are significant at the 95% level.

Table 8 shows the trends and their significance at these stations for the other seasons. Significant trends are seen at many stations in both spring and autumn. Again, the stronger trends tend to be at the inland stations, although this is not always the case. Some stations (e.g. Canberra) have strong trends in just one season. This variability across seasons suggests that the timing and or length of the active fire seasons may be changing, and that these changes vary geographically. Also shown in Table 8 are trends in the less reliable (due to data inhomogeneities) 90th percentile of FFDI. In general, these trends are much larger than those in the median, with about the same levels of significance.

Comparing these results with Table 7 is revealing. In general, the trends seen to date in the observations are very much higher, up to 5 or 6 times so in some cases, than the trends projected in the model simulations.

Trends in ΣFFDI

At all the stations in the study, the linear trends of ΣFFDI have been computed (Table 9). The trends are similar to those for the medians, with most stations showing a significant positive trend. The exceptions are a few stations near the coast and Canberra. As with the medians, the largest trends are found in the interior of NSW and other inland areas. Units are points per year.

Table 9. Trends in cumulative FFDI from 1973-74 to-2006-07. Units are points per year. Significance indicated as in Table 8.

Site	Trend	Site	Trend
Adelaide	**18**	Laverton	8
Amberley	**56**	Melbourne AP	**23**
Bendigo	**51**	Mildura	**51**
Bourke	**121**	Mt Gambier	8
Brisbane AP	4	Moree	**54**
Canberra	20	Nowra	**21**
Ceduna	**49**	Richmond	**84**
Charleville	**52**	Rockhampton	**46**
Cobar	**54**	Sale	**24**
Coffs Harbour	9	Sydney AP	**26**
Dubbo	**72**	Wagga	**46**
Hobart	**10**	Williamtown	**17**
Launceston AP	**11**	Woomera	**95**

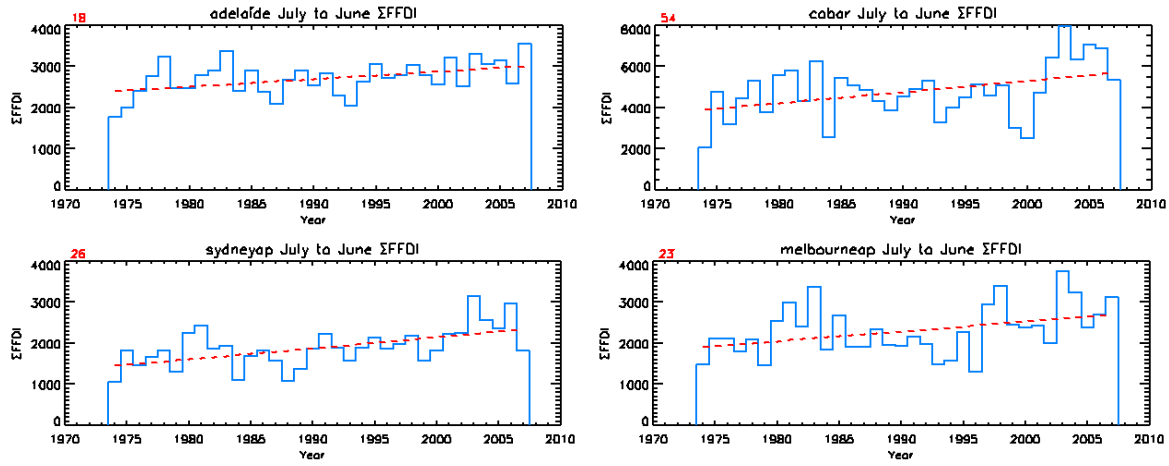

Figure 26. Time series plots of ΣFFDI at (clockwise from upper left) Adelaide, Cobar, Sydney AP and Melbourne AP. Linear regression line is shown in red. The trend, in points per year, is given by the red number at the top left of each figure. Refer to Table 9 for significance of trend.

Examining individual time series plots (Fig. 26, see also Fig. 14) of ΣFFDI reveals some interesting behaviour in the trends. Rather than being a smooth, continuous increase, the ΣFFDI displays a jump in the late-90s to early-00s at many locations. The strongest jumps are seen in the interior portions of NSW. Table 10 shows the average annual ΣFFDI from 1980-2000 and from 2001 to 2007, along with the percent change between these two periods[3]. Increases of 10-40% are evident at most sites. The changes observed thus far in the 21st century are equal to or

[3] The separation point is somewhat arbitrary. It was chosen based on a visual examination of the plots. The start date for the first period (1980) was chosen to eliminate the particularly low values observed in the early to mid-70s, when a strong La Niña brought an extended period of abnormally high precipitation and low fire danger to much of the region.

exceed the changes predicted to occur by 2050 in the different modelling scenarios (see Table 2). This tendency is particularly pronounced in interior NSW. The changes in ΣFFDI at these stations are associated with an increase in the number of VHE days.

Data inhomogenities cannot be absolutely excluded as the source of this apparent jump in fire danger. However, several factors suggest that this is a real phenomenon. As noted earlier, a statistical analysis of the wind uncertainties suggests that the medians of the distributions are not seriously affected by the errors. Hence, the medians should be relatively homogeneous and computed trends should be realistic. Another factor is the timing and spatial coherence of the jump. In interior NSW, the large jump begins in 2001-02 across a wide area. It seems unlikely that all the sensors would malfunction simultaneously across a broad region of the country.

Table 10. Average ΣFFDI from 1980 to 2000 and from 2001 to 2007. The percentage change between the two is also shown.

site	1980-2000 ΣFFDI	2001-07 ΣFFDI	%change	site	1980-2000 ΣFFDI	2001-07 ΣFFDI	%change
Adelaide	2671	3051	14	Laverton	2065	2268	9
Amberley	2805	3885	38	Melbourne AP	2274	2805	23
Bendigo	2400	3439	43	Mildura	5095	5898	15
Bourke	4346	7375	69	Mt Gambier	1932	2004	3
Brisbane AP	1970	2139	8	Moree	3753	5159	37
Canberra	2484	2925	17	Nowra	1718	2242	30
Ceduna	4444	5114	15	Richmond	2452	3099	26
Charleville	6215	7065	13	Rockhampton	3125	3878	24
Cobar	4519	6388	41	Sale	1639	2175	32
Coffs Harbour	1205	1490	23	Sydney AP	1812	2475	36
Dubbo	2914	4662	59	Wagga	3130	4451	42
Hobart	1339	1424	6	Williamtown	1950	2425	24
Launceston AP	1397	1488	6	Woomera	7478	8244	10

Analysis of Long Time Series

The use of 36-year series to estimate trends may not give a true representation of the variability in the data. At eight stations, longer records exist that can be used to test the robustness of these trends. Trends in both the seasonal median FFDI and in annual cumulative FFDI for the eight 'long' time series are shown in Table 11. In general, the trends are much weaker than seen in the shorter time series, and in some cases, not significant. The weaker trends in the longer time series are a result of inter-decadal variability (see Figs 14 and 27), with extended periods of higher and lower ΣFFDI. The five-year running-mean helps highlight these periods. Periods of approximately 20 years are particularly noticeable by inspection. Spectral analysis (not shown) also suggests similar results, with low-frequencies dominating. There is a peak at the highest (2 year) frequencies, but not as strong.

Table 11. Trends from the 'long' time series for annual cumulative FFDI (points/year) and seasonal median FFDI (points per decade). Significance indicated as in Table 8.

Site	Start Year	ΣFFDI	Spring median	Summer median	Autumn median
Adelaide	1955	7	0.1	0.3	0.2
Amberley	1953	**22**	**0.6**	**0.4**	**0.5**
Canberra	1942	6	0.2	0.1	**0.3**
Cobar	1942	13	0.4	0.5	**0.5**
Hobart	1942	6	**0.1**	**0.2**	**0.1**
Melbourne AP	1942	8	0.2	**0.2**	**0.4**
Sydney AP	1942	5	0.2	**0.2**	0
Wagga	1942	16	0.2	**0.8**	**0.7**

Figure 27 is for Wagga, but shares the same characteristics as the other series. All show high periods of ΣFFDI in the 1940s, 60s, early-80s and 2001-07. The early-70s and early-to mid-90s are generally periods of low ΣFFDI. The magnitude and prominence of the individual peaks varies at the different stations. However, at all stations with long time series, the most recent seasons show the highest observed ΣFFDI in the record.

The median statistics in the long time series show an upward trend. As with ΣFFDI, the trend in the long time series is generally not as large as those found in the shorter series. In the median time series, the inter-decadal variation in the medians is much less pronounced. However, the upper percentiles (not shown) indicate a much stronger inter-decadal variation.

As noted earlier, changes are also suggested in the length and timing of the active fire season. This is examined using a simple metric of the time series extending back to the 1940s and 1950s. For this purpose, the start (end) of the active fire season is objectively defined as the average date of the first (last) three occurrences of an FFDI of at least 25 after 1 July of a given year. From these start and end dates, the length of the season can be determined. These dates are computed at Adelaide, Canberra, Wagga and Melbourne. This simple methodology fails at Hobart and Sydney. Figure 28 shows the season length time series from the four stations. To highlight the general behaviour, a five-year running mean is also shown. Several features are readily apparent. In most cases, the last few years have been among the longest on record, part of an upward swing since the early-90s. There is also an apparent decadal variations, with broad peaks in the 1940s, the late-70s/early-80s and in the present. Shorter fire seasons were generally seen in the late-50s and 60s and in the late-80s. A general upward trend is suggested, but is not statistically significant. This broad behaviour is similar at each of the other long-period stations.

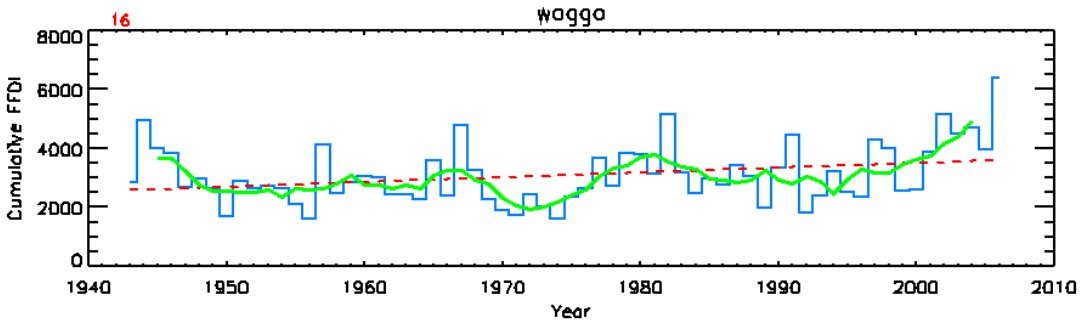

Figure 27. Time series of ΣFFDI at Wagga. The red line is based on linear regression and the red number at the top left indicates the trend. The green line is the 5-year running mean.

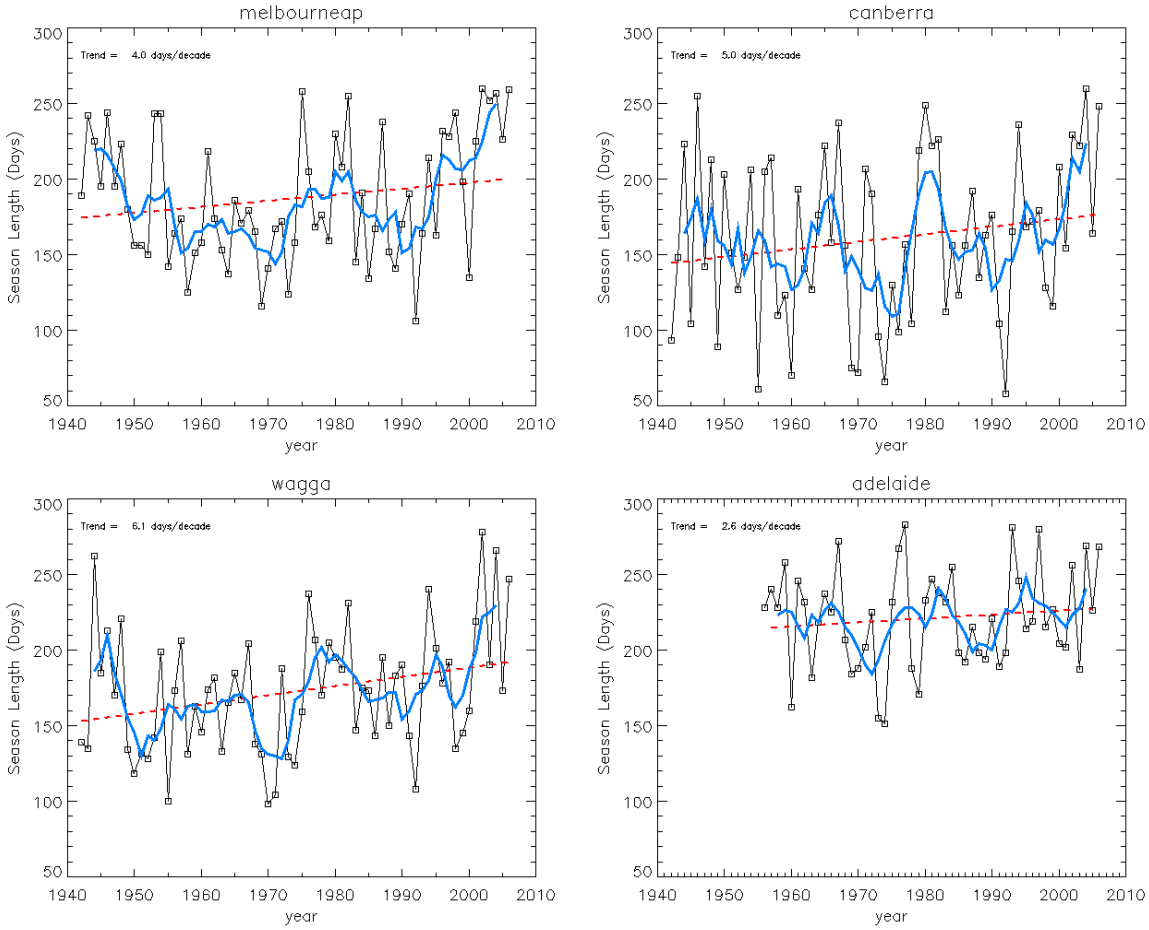

Figure 28. Estimated season length (days) at Melbourne AP, Canberra, Wagga and Adelaide calculated as described in the text. The blue line is the 5-year running mean. The red dashed line is the trend.

Interdecadal Variability and Climate Change

An important question is raised by these findings: Is the apparent recent increase in fire weather due to climate change or is it simply the reflection of some natural (and unforseen) interdecadal change? Unfortunately, it is not possible to answer this question unequivocally at this time. Some insight is available, though. The relative merits of these positions will be examined below.

Historically, Australia has undergone boom and bust years in rainfall. The 20th century saw numerous, long-lasting periods of drought, including the late-30s and

early 40s and the early to mid-60s. A 'short, sharp drought' was seen in 1982-83. The early 90s also saw an extended drought.

Over the period June 2004 to May 2007, rainfall has been below-average to very much below average over much of south-eastern Australia (Fig. 30) and the rainfall deficiencies likely extend further back, as the 2002-03 El Niño also brought severe drought to eastern Australia [BoM 2006]. In fact, much of Australia, particularly the southeast portion, has been in the grip of an extended drought from 1996-2007.

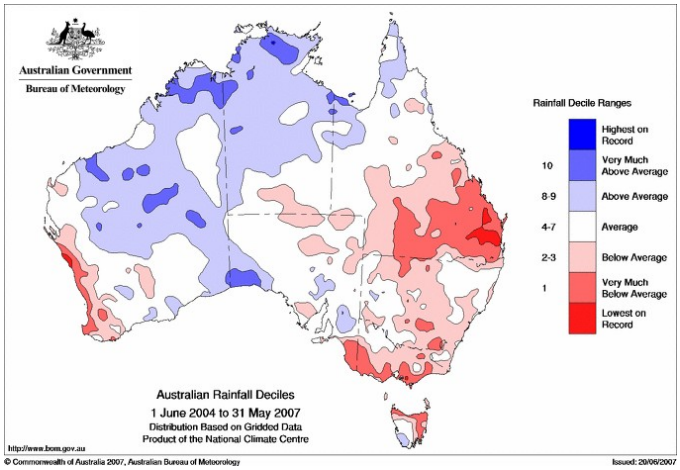

Figure 30. Rainfall deciles for Australia from June 2004 through May 2007. From http://www.bom.gov.au/cgi-bin/silo/rain_maps.cgi

Comparison of these times of drought with the FFDI time series shows that there is (unsurprisingly) a strong correlation, with the 'high' periods of ΣFFDI (or longer fire season length or larger values of the 90th-percentile FFDI) corresponding to drought episodes. These droughts, in turn, are often associated with El Niño events (Fig. 31). However, the relationships between ENSO and rainfall (and hence droughts) are not necessarily related in some simple, linear way (e.g. Power et al 1998). Droughts can often last longer than a single El Niño event. Even a weak El Niño event (e.g. 2002-03) can have a large impact on rainfall and vice versa (1997-98).

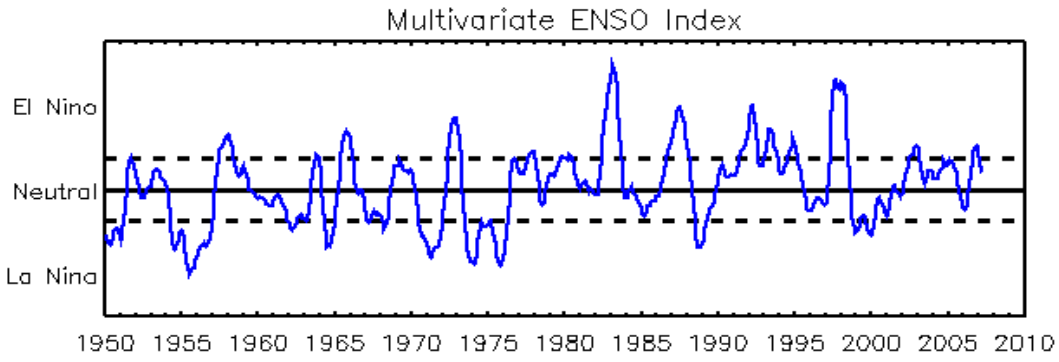

Figure 31. Time series of Multivariate ENSO Index showing occurrences of El Niño and La Niña. Data courtesy of Klaus Wolter at http://www.cdc.noaa.gov/people/klaus.wolter/MEI/mei.html.

ENSO itself is also subject to inter-decadal (and perhaps longer) variations. Some periods are dominated by La Niña, others by El Niño. The longer time-scale drivers

are a poorly-understood but apparently natural part of the climate system. Whether these variations are due to longer-period circulation anomalies such as the Interdecadal Pacific Oscillation (IPO, e.g. Power et al 1999) or other mechanisms is still an active area of research at this time. However, the longer-time variations of climate are a reality and are clearly visible in the historical records of fire weather presented above.

A shift in the behaviour of ENSO and the subsequent response of the atmosphere was observed in 1976 (see Diaz et al 2001 for review, the shift is also apparent in Fig 31). Since that time, the La Niña phase of ENSO has occurred less frequently and been weaker. Several unusual extended El Niño episodes have also occurred (e.g. early-90s). The question of whether the trends in ENSO are the result of anthropogenic climate change or a reflection of some other natural variability has been the subject of intense debate in recent years [Trenberth and Hoar 1997, Rajagopalan et al 1997]. Current thinking suggests, albeit with very low confidence, that little change is expected in ENSO due to climate change [Cane 2005, IPCC 2007]. Regardless, given the nature of the variations, the available time series are likely too short to make the determination with any statistical certainty at this time [Wunsch 1999].

As noted earlier, the drought of the previous few years has been particularly severe. Several studies [Karoly et al. 2003, Nicholls 2004] have suggested that anthropogenic climate change is at least partially to blame for this. During the 2002-03 El Niño, temperatures were particularly high, likely exacerbated by global warming. This, in turn, results in enhanced evaporation, worsening the drought. Such a mechanism would also be present in the most recent years, and is consistent with the apparent jump in fire-weather danger noted at many of the sites in the study.

In summary, the longer time records clearly show evidence of ongoing interdecadal variation, with recent years showing an apparent jump in fire danger. However, careful examination of the records suggests that climate change may be playing a role as well. The available data indicate that the fire seasons we have been experiencing for the last few years have been longer and, in many ways, stronger than any observed dating back to the 1940s. It is not that a given day has a higher FFDI value; rather, there are more VHE days and fewer low-to-medium FFDI days. A reasonable hypothesis for this behaviour is that we a currently experiencing an upswing in fire danger due to some natural forcing with an interdecadal time scale, and that this is being exacerbated by the subtle, ongoing effects of climate change.

Future Improvements

As with any scientific study, there are limitations imposed by the analysis method and the available data. The given framework of a study also imposes shortcomings on the results. In this section, some of these are briefly discussed to provide a guide for future directions in research on this topic.

The basis of the analysis here is the observed weather data. These data are adjusted using projections of change based on two climate model simulations. Results from other models should be considered in any updated assessment of fire-weather risk.

Given the influence of ENSO on the climate of Australia, and particularly the southeast, understanding any changes which may occur in its behaviour is paramount for understanding future fire danger. Unfortunately, the current generation of climate models do not simulate ENSO particularly well. As noted earlier, there is a low-confidence projection that ENSO will likely stay the same [Cane 2004, IPCC 2007]. Any future changes in ENSO will likely affect the results presented here.

The problems with the data noted earlier remain a significant issue for this study. The wind data in particular are a problem. An initial effort to homogenize the wind data has been made by D. Jakob, now in the Bureau's Hydrology section. The problem is very difficult and may actually be intractable. The differences in instrumentation may simply be too large to overcome. An alternate recourse is to regenerate the historical wind data using a numerical model that assimilates other variables which have been reliably. Such a project represents a significant outlay of resources and is in the very-early planning phase.

The results of this project could be vastly improved if climate-vegetation interactions were explicitly taken into account. Vegetation (fuel) is not a static quantity; rather it varies with both the climate and the land-use. Changes in the vegetation density and type can be expected as the climate changes, partly due to "fertilization" effect of higher carbon dioxide levels. These changes will lead to a change in the fire regime of a given area and correspondingly have a large impact on the fire behaviour. To address this in the future, observations of vegetation-climate interactions must continue. The next generation of global climate models will begin to incorporate dynamic vegetation effects. These initial efforts will provide some insight, but eventually the development of the model parameterizations specific to the vegetation of the Australian region is necessary for a greater understanding of fire in this region.

Fire impact assessments are needed at finer spatial scales (10-100 m), allowing for differing terrain and vegetation, property types and fire management techniques. The FIRESCAPE model [Cary 1997] provides some of these features and is being used in a climate change study for Sydney. Similar studies should be considered for other areas.

Concluding Remarks

In this study, the potential impact of climate change on southeast Australia is estimated. Simulations from two CSIRO climate models using two greenhouse gas and aerosol emissions scenarios are combined with historical weather observations to assess the changes to fire weather expected by 2020 and 2050. In general, fire weather conditions are expected to worsen. By 2020, the increase in ΣFFDI is generally 0-4% in the low scenarios and 0-10% in the high scenarios. By 2050, the increase in generally 0-8% (low) and 10-30% (high). The largest changes are expected in northern New South Wales. Little change is expected in Tasmania. With this increase in ΣFFDI, a larger number of days with a Fire Danger Rating of 'very high' or 'extreme' are also expected. The number of 'extreme' fire danger days generally increases 5-25% for the low scenarios and 15-65% for the high scenarios. By 2050, the increases are generally 10-50% in the low scenarios and100-

300% for the high scenarios. The seasons are likely to become longer, starting earlier in the year.

These results are placed in the context of the current climate and its tendencies. During the last several years in southeast Australia, including the 2006-07 season, particularly severe fire weather conditions have been observed. In many cases, the conditions far exceed the projections in the high scenarios of 2050. Are the models (or our methodology) too conservative or is some other factor at work?

Examining longer-term observations at eight stations, back to the early 1940s in many cases, reveals considerable inter-decadal variability. Periods of increasing and decreasing fire weather danger are apparent in the record. The peaks of these 'cycles' occur roughly every 20 years and the time series might suggest that we are at (or near) a peak, although there is no physical basis on which to estimate when or to what extent a decrease might occur.

There is also evidence for anthropogenic climate change being a driver of this upswing. The current peaks in ΣFFDI are much higher than observed in past instances. There are also a greater number of VHE days at many locales. There is also the suggestion that the fire season is starting earlier. Finally, the severity and length of the recent drought [e.g. Nicholls 2006] and the associated fire danger has not been seen in the available records.

The hypothesis posited in this study is that the naturally occurring peak in fire danger due to interdecadal variability may have been exacerbated by climate change. The test of this hypothesis comes over the next few years to decades. If correct, then it might be expected that fire weather conditions will return to levels something more along the lines of those suggested in the 2020 scenarios. If fire danger conditions stay this high, then the conclusion must be that the models used to make these projections are too conservative. Whatever the case, continued observation, as well as improved modelling are required to resolve this question.

What of the human impacts of these projected changes? The last few years, particularly the 2006-07 fire season, may provide an indication for the future. Early season starts suggest a smaller window for pre-season fuel-reduction burns. Logically, more frequent and more intense fires suggest that more resources will be required to maintain current levels of bushfire suppression. Shorter intervals between fires, such as those which burned in eastern Victoria during 2002-03 and 2006-07, may significantly alter ecosystems and threaten biodiversity. It is hoped that planning authorities can use this information in the development of adaptation strategies.

References

Allan, R. and others, 2001: Is there an Indian Ocean dipole and is it independent of the El Nino-Southern Oscillation? *CLIVAR exchanges*, 6 (3), 18-22. Available from www.clivar.org.

Beer, T. and A. Williams, 1995: Estimating Australian forest fire danger under conditions of doubled carbon dioxide concentrations. *Climatic Change*, **29**, 169-188.

Bureau of Meteorology, 2006: *Special Climate Statement 9: An exceptionally dry decade in parts of southern and eastern Australia: October 1996-September 2006*. Issued 10 October 2006, National Climate Centre, Australian Bureau of Meteorology, Melbourne.

Cane, M. A., 2005: The evolution of El Niño, past and future. *Earth and Planetary Science Letters*, **230**, 227-240

Cary, G. J., 1997: FIRESCAPE – a model for simulation of theoretical long-term fire regimes in topographically complex landscapes. In: Australian Bushfire Conference: Bushfire '97, Australian Bushfire Association, Darwin, pp. 45–67

Diaz, H. F., M. P. Hoerling and J. K. Eischeid, 2001: ENSO variability, teleconnections and climate change. *Int. J. Climotol.*, **21**, 1845-1862.

Finkele, K., G. A. Mills, G. Beard, and D. Jones, 2006: National daily grided soil moisture deficit and drought factors for use in prediction of Forest Fire Danger Index in Australia. *Aust. Meteor. Mag.* **55**, 183-197.

Folland, C. K., D. E. Parker, A. W. Colman and R. Washington, 1999: Large scale modes of ocean surface temperatures since the late nineteenth century. *Beyond El Niño: Decadal and interdecadal Climate Variability*. A. Navarra, Ed., Springer-Verlag, 73-102.

Griffiths, D., 1999: Improved formula for the drought factor in McArthur's Forest Fire Danger Meter. *Australian Forestry*, **62**(2):202-206.

Haylock, M. and N. Nicholls, 2000: Trends in extreme rainfall indices for an updated high quality data set for Australia, 1910-1998. *J. Int. Climotol.*, **20**, 1533-1541.

Hennessy, K., C. Lucas, N. Nicholls, J. Bathols, R. Suppiah and J. Ricketts, 2005: *Climate change impacts on fire-weather in south-east Australia*. Consultancy report for the New South Wales Greenhouse Office, Victorian Dept. of Sustainability and Environment, ACT Government, Tasmanian Department of Primary Industries, Water and Environment and the Australian Greenhouse Office. CSIRO Marine and Atmospheric Research and Australian Government Bureau of Meteorology, 88 pp, http://www.cmar.csiro.au/e-print/open/hennessykj_2005b.pdf

Hendon H. H., D. W. J. Thompson, M. Wheeler, 2007: Australian rainfall and surface temperature variation associated with the Southern Hemisphere Annular Mode. *J. Climate*, **20**, 2452-2467.

Incoll, R., 1994: Asset protection in a fire prone environment. Biodiversity Series

Paper no. 8, Available from http://www.environment.gov.au/biodiversity/publications/series/paper8/paper17.html.

IPCC, 2001. *Climate Change 2001: The Scientific Basis*. Summary for Policymakers. Contribution of Working Group I to the Third Assessment Report of the Intergovernmental Panel on Climate Change, in Houghton, J.T., Ding, Y., Griggs, D.J., Noguer, M., Van Der Linden, P.J. and Xioaosu, D (eds) Cambridge University Press, Cambridge, UK, 944 pp. www.ipcc.ch

-----, 2007: *Climate change 2007: The physical science basis*. Summary for Policymakers. Contribution of Working Group I to the Fourth Assessment Report of the Intergovernmental Panel on Climate Change , in Solomon, S., D. Qin, M. Manning, Z. Chen, M. Marquis, K.B. Averyt, M. Tignor and H.L. Miller (eds.)]. Cambridge University Press, Cambridge, UK, 21 pp. www.ipcc.ch

Jones, J.M. and M. Widmann, 2004: Early peak in the Antarctic oscillation index. *Nature*, **432**, 290-291.

Karoly, D., Risbey, J. and Reynolds, A., 2003: *Climate Change - Global Warming Contributes to Australia's Worst Drought*, World Wildlife Fund Australia, Sydney, New South Wales.

Keetch, J. J. and Byram, G. M., 1968: *A drought index for forest fire control*. USDA Forest Service Research Paper SE-38, 32 pp.

Lucas, C., 2005: Fire climates of Australia: Past, present and future. Proceedings, 6th Symposium on Fire and Forest Meteorology, Canmore, Alberta, Canada, 25-27 October 2005. Available from http://ams.confex.com/ams/pdfpapers/97592.pdf.

-----, 2006a: An examination of dewpoint biases introduced by different instrumentation. *BMRC Res. Lett.*, **4**, Available from http://www.bom.gov.au/bmrc/pubs/researchletter/reslett_04/reslett_04.pdf.

-----, 2006b: A high-quality humidity dataset for Australia. *Proceedings, 17th Australia New Zealand Climate Forum, Canberra, ACT*, p.33.

-----, 2006c: An Australian fire weather data set: 1957-2003. Poster, The Joint AFAC/IFCAC/Bushfire CRC conference 2006. Melbourne, Australia, August 2006. Available from http://www.bushfirecrc.com/documents/poster_proga%20-%20Lucas1.pdf.

Luke, R.H. and McArthur, A.G., 1978: *Bushfires in Australia*. Australian Government Publishing Service, Canberra. 359pp.

Marshall, G.J., 2003: Trends in the southern annular mode from observations and reanalyses. *J. Climate*, **16**, 4134-4143.

McArthur, A.G., 1967: Fire behaviour in eucalypt forest. *Comm. Aust. Timb. Bur. leaflet 107*, 25 pp.

McBride, J.M. and N. Nicholls, 1983: Seasonal relationships between Australian rainfall and the Southern Oscillation. *Mon. Wea. Rev.*, **111**, 1998-2004.

Mills, G.A., 2005: On the sub-synoptic scale meteorology of two extreme fire weather days during the Eastern Australian fires of January 2003. *Aust. Meteor. Mag.*_**54**, 265-290.

Mount, A.B., 1972: *The derivation and testing of a soil dryness index using run-off data*. Tasmanian Forestry Commission, Bulletin No. 4, Hobart.

Nicholls, N., 1989: Sea surface temperature and Australian winter rainfall. *J. Climate*, **2**,965-973.

-----, 2004: The changing nature of Australian droughts. *Climatic Change*, **63**, 323-336.

-----, 2006: Detecting and attributing Australian climate change: a review. *Aus. Meteorol. Mag.*, **55**, 199-211.

Noble, I.R., Bary, G.A.V. Bary and A.M. Gill, 1980: McArthur's fire-danger meters expressed as equations. *Australian Journal of Ecology*, **5**, 201-203.

Power, S. B., F. Tseitkin, S. Torok, B. Lavery, R. Dahni and B. McAveney, 1998: Australian temperature, Australian rainfall and the Southern Oscillation, 1910-1992: Coherent variability and recent changes. *Aust. Meteor. Mag.*, **47**, 85-101.

-----, T. Casey, C. Folland, A. Colman and V. Mehta, 1999: Interdecadal modulation of the impact of ENSO on Australia. *Clim. Dyn.*, **15**, 319-324.

-----, M. Haylock, R. Colman and X. Wang, 2006: The predictability of interdecadal changes in ENSO activity and ENSO teleconnections. *J. Climate*, **19**, 4755-4771.

Purton, C. M., 1982: *Equations for the McArthur Mk 4 Grassland fire danger meter*. Bureau of Meteorology Meteorological Note no. 147, 12 pp.

Rajogopalan, B., U. Lall and M. A. Cane, 1997: Anomalous ENSO occurrences: An alternative view. *J. Climate*, **10**, 2351-2357.

Saji, N.H., B.N. Goswami, P.N. Vinayachandran and T. Yamagata, 1999: A dipole mode in the tropical Indian ocean. *Nature*, **401**,360-363.

SRES, 2000: *Special Report on Emission Scenarios: Summary for Policymakers*. A

Special Report of Working Group III of the Intergovernmental Panel on Climate Change. Cambridge University Press, Cambridge, UK, 27 pp. Available from http://www.ipcc.ch/pub/sres-e.pdf.

Suppiah, R., K.J. Hennessy, P.H. Whetton, K. McInnes, I. Macadam, J. Bathols and J. Ricketts, 2007: Australian climate change projections derived from simulations performed for the IPCC 4th Assessment Report. *Aust. Meteorol. Mag.*, accepted.

Suppiah, R., B. Preston, P. H. Whetton, K. L. McInnes, R. N. Jones, I. Macadam, J. Bathols and D. Kirono, 2006: Climate change under enhanced greenhouse conditions in South Australia. CSIRO consultancy report for the South Australian Government, 64 pp.

Thompson, D.W.J. and J.M. Wallace, 2000: Annular modes in the extratropical circulation: Part I: month-to-month variability. *J. Climate*, **13**, 1000-1016.

----- and S. Solomon, 2002: Interpretation of recent southern hemisphere climate change. *Science*, **296**,895-899.

Trenberth, K. E. and T. J. Hoar, 1997: El Nino and climate change. *Geophys. Res. Lett.*, **24**, 3057-3060.

Vercoe, T. 2003: *'Whoever owns the fuel owns the fire' -- Fire management for forest growers*. AFG Special Liftout no. 65, 26(3), 8pp. Available from http://www.coagbushfireenquiry.gov.au/subs_pdf/57_2_ragg_afg.pdf

Williams, A.A.J and Karoly, D.J., 1999: Extreme fire weather in Australia and the impact of the El Nino-Southern Oscillation. *Aust. Met. Mag.*, **48**, 15-22.

Wunsch, C., 1999: The interpretation of short climate records, with comments on the North Atlantic and Southern Oscillations. *Bull. Amer. Meteor.Soc.*, **80**, 245-255.

Appendix

This section represents a site-by-site summary of the key changes at each study location in the report. The information provided here, with one exception, is provided in the main body of the report. Here, it is summarized by individual station.

Each section consists of 1 page: A large table and two figures. The table shows the projected model changes for all eight scenarios, as well as the current values. Shown are annual cumulative FFDI (ΣFFDI), the number of VHE, 'extreme', 'very extreme' and 'catastrophic' days expressed as both the raw numbers (days per year) and as a percentage increase over the current value. Also shown are the seasonal median FFDI and 90th percentile values for each season.

The top figure shows the time series of annual cumulative FFDI. The line of best fit is shown in red (trends are quantified in Table 9). The numerical value of the trend ('points' per year) is given by the red number on the upper left. The last year on the record is incomplete. It is missing the period from March to June, so the numbers are lower than they should be.

The bottom plot shows the time series of DJF (summer) median FFDI value. The line of best fit is shown in green. Units of the trend line (upper left) in this case are given in points per decade.

Adelaide

variable	now	2020				2050			
		low2	low3	high2	high3	low2	low3	high2	high3
ΣFFDI	2708	2	3	5	8	3	5	16	25
VHE	18.3	19.2	19.8	20.8	22.3	19.9	20.8	26.1	30.2
%	0.0	5.1	7.9	13.4	21.9	8.8	13.7	42.5	64.9
xtrm	1.2	1.4	1.5	1.5	1.8	1.4	1.5	2.3	3.8
%	0.0	18.4	26.3	28.9	55.3	23.7	31.6	102.6	234.2
vxtrm	0.0	0.0	0.0	0.0	0.0	0.0	0.0	0.2	0.4
cata	0.0	0.0	0.0	0.0	0.0	0.0	0.0	0.0	0.0
DJF50	10.1	10.3	10.3	10.6	10.6	10.4	10.5	11.4	11.5
MAM50	5.7	5.8	5.8	5.9	5.9	5.8	5.8	6.2	6.2
JJA50	1.8	1.9	1.9	1.9	1.9	1.9	1.9	2.1	2.1
SON50	4.1	4.3	4.3	4.6	4.4	4.4	4.3	5.4	5.1
DJF90	27.6	28.1	28.2	29.2	29.3	28.6	28.7	31.7	32.4
MAM90	16.9	17.1	17.2	17.4	17.5	17.3	17.3	18.4	18.3
JJA90	5.6	5.7	5.8	5.9	6.0	5.8	5.9	6.5	6.6
SON90	14.8	15.4	15.3	16.2	15.9	15.8	15.6	19.3	18.3

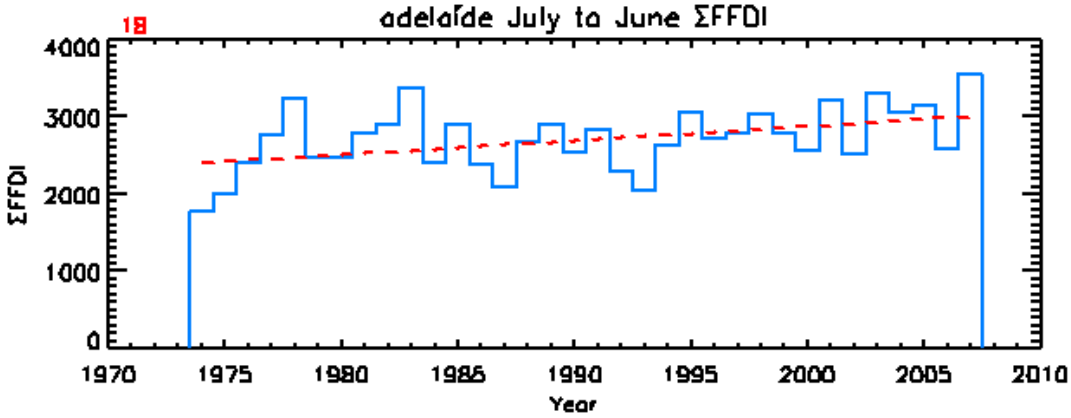

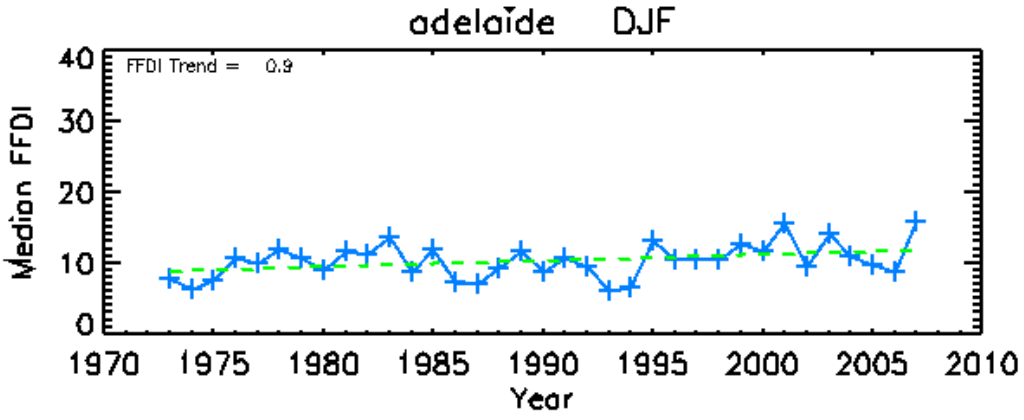

Amberley

variable	now	2020				2050			
		low2	low3	high2	high3	low2	low3	high2	high3
ΣFFDI	2919	2	1	7	6	4	3	24	19
VHE	13.3	14.5	14.2	16.4	15.7	15.3	14.8	22.7	20.9
%	0.0	8.4	6.4	23.0	18.0	14.5	10.7	70.0	56.8
xtrm	1.2	1.4	1.4	1.8	1.6	1.5	1.5	3.0	2.8
%	0.0	12.2	12.2	41.5	31.7	24.4	22.0	141.5	124.4
vxtrm	0.1	0.2	0.2	0.3	0.2	0.2	0.2	0.4	0.5
cata	0.0	0.0	0.0	0.0	0.0	0.0	0.0	0.0	0.1
DJF50	5.1	5.2	5.2	5.6	5.5	5.4	5.3	6.9	6.2
MAM50	5.5	5.6	5.6	5.8	5.8	5.7	5.7	6.6	6.5
JJA50	7.0	7.2	7.0	7.7	7.3	7.4	7.2	9.1	8.0
SON50	8.8	9.1	9.1	9.5	9.6	9.3	9.4	11.0	11.2
DJF90	14.4	14.8	14.7	15.6	15.3	15.2	15.0	18.2	17.3
MAM90	13.6	13.8	13.8	14.2	14.2	14.0	14.1	15.5	15.6
JJA90	17.7	18.2	17.8	19.3	18.4	18.6	18.1	22.5	20.0
SON90	22.4	22.8	22.8	23.7	23.8	23.3	23.1	27.2	26.9

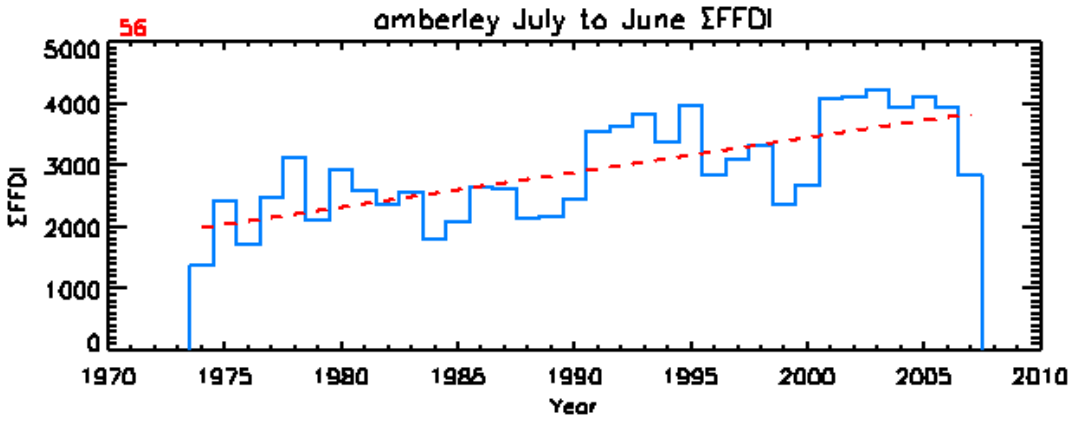

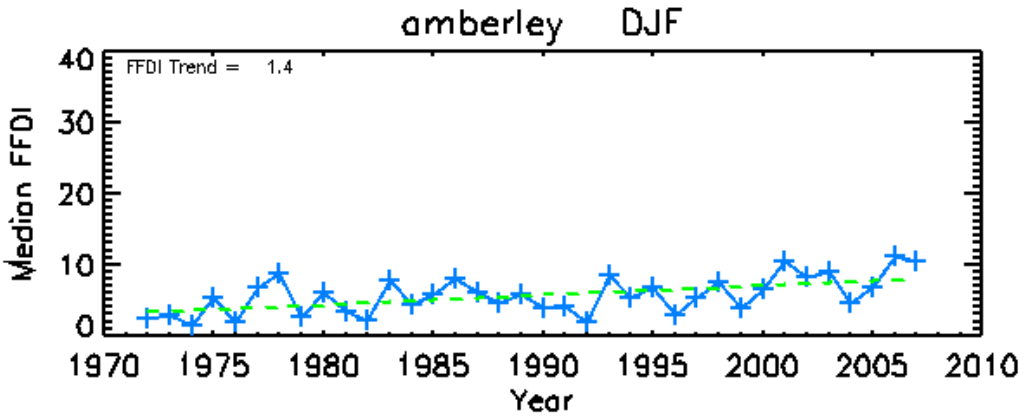

Bendigo

variable	now	2020				2050			
		low2	low3	high2	high3	low2	low3	high2	high3
ΣFFDI	2552	4	4	9	10	6	7	29	31
VHE	13.9	15.6	16.1	17.5	18.4	16.6	17.1	25.2	28.6
%	0.0	12.4	15.7	26.1	32.0	19.6	22.7	81.0	105.9
xtrm	1.2	1.5	1.5	1.8	2.0	1.6	1.8	2.8	4.0
%	0.0	22.5	25.0	52.5	65.0	35.0	50.0	135.0	230.0
vxtrm	0.1	0.1	0.1	0.2	0.2	0.1	0.2	0.3	0.5
cata	0.0	0.0	0.0	0.0	0.0	0.0	0.0	0.1	0.1
DJF50	11.4	11.8	11.9	12.3	12.5	12.0	12.2	14.3	14.8
MAM50	5.7	5.9	5.9	6.0	6.1	5.9	5.9	6.6	6.6
JJA50	1.6	1.7	1.7	1.8	1.8	1.7	1.7	2.1	1.9
SON50	3.7	4.0	4.0	4.5	4.4	4.3	4.1	6.5	6.0
DJF90	25.4	26.0	26.3	27.3	27.9	26.6	26.9	31.0	32.9
MAM90	15.1	15.4	15.3	15.9	15.7	15.6	15.5	17.1	16.5
JJA90	4.5	4.6	4.7	4.8	5.0	4.7	4.8	5.5	5.9
SON90	12.8	13.6	13.7	15.0	15.1	14.3	14.3	20.3	20.6

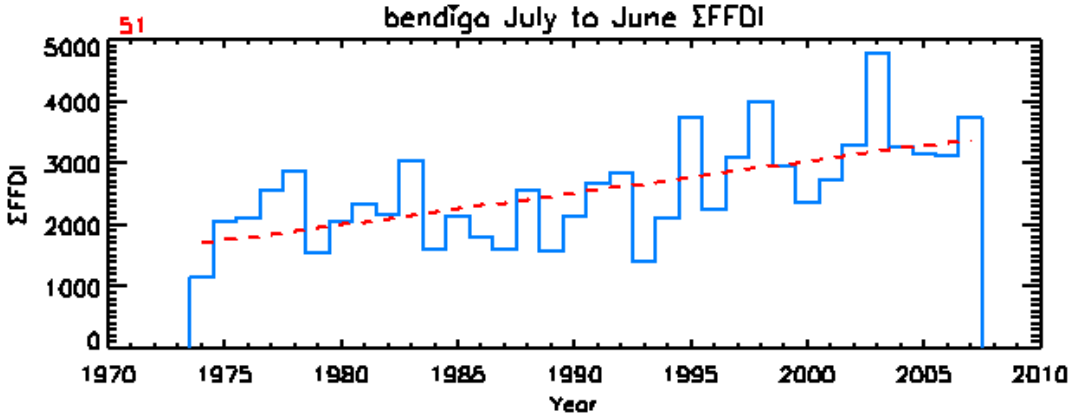

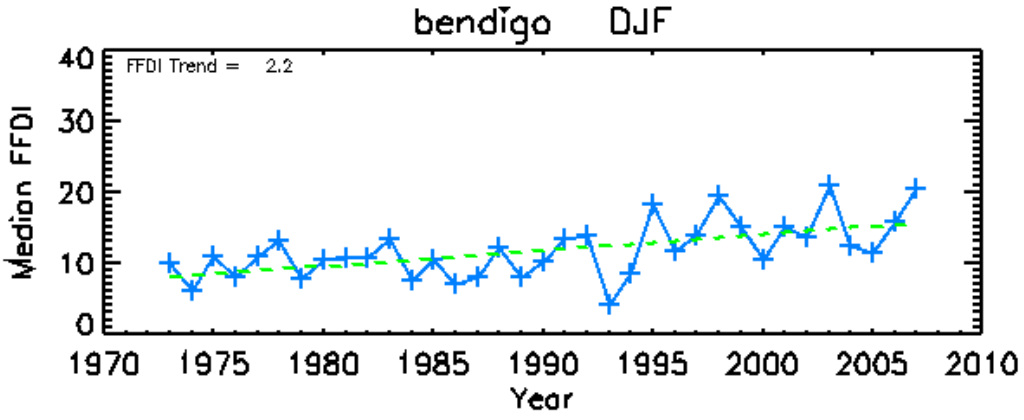

Bourke

variable	now	2020				2050			
		low2	low3	high2	high3	low2	low3	high2	high3
ΣFFDI	4758	4	3	10	8	7	5	33	26
VHE	57.2	62.3	61.4	71.3	68.6	66.4	64.5	103.7	91.5
%	0.0	9.0	7.3	24.7	19.9	16.0	12.8	81.2	59.9
xtrm	4.8	5.6	5.6	7.3	7.2	6.2	6.3	14.6	13.9
%	0.0	16.2	16.2	50.0	48.1	28.1	30.6	200.6	187.5
vxtrm	0.4	0.5	0.5	0.5	0.6	0.5	0.5	1.5	1.5
cata	0.0	0.1	0.1	0.1	0.1	0.1	0.1	0.2	0.4
DJF50	21.9	22.7	22.7	23.8	23.7	23.2	23.2	27.5	27.4
MAM50	10.7	11.0	10.9	11.4	11.2	11.2	11.0	12.8	12.2
JJA50	5.7	6.0	6.0	6.4	6.4	6.2	6.2	7.9	7.7
SON50	14.7	15.8	15.5	17.6	16.7	16.6	16.0	23.8	20.6
DJF90	41.5	42.4	42.5	43.9	44.3	43.1	43.4	49.1	49.9
MAM90	23.5	24.1	23.7	25.0	23.9	24.6	23.8	27.9	25.1
JJA90	13.2	13.9	13.8	15.0	14.6	14.4	14.2	19.3	17.8
SON90	31.9	33.7	33.5	36.7	36.0	35.1	34.7	46.4	44.5

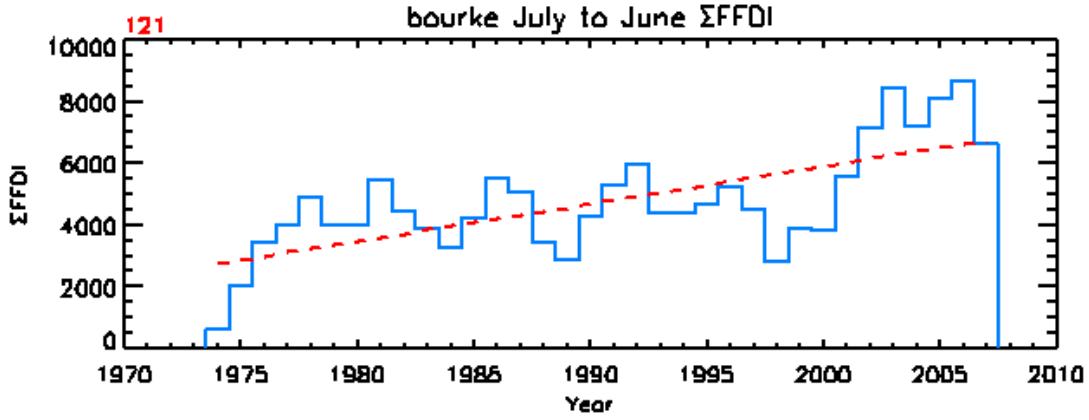

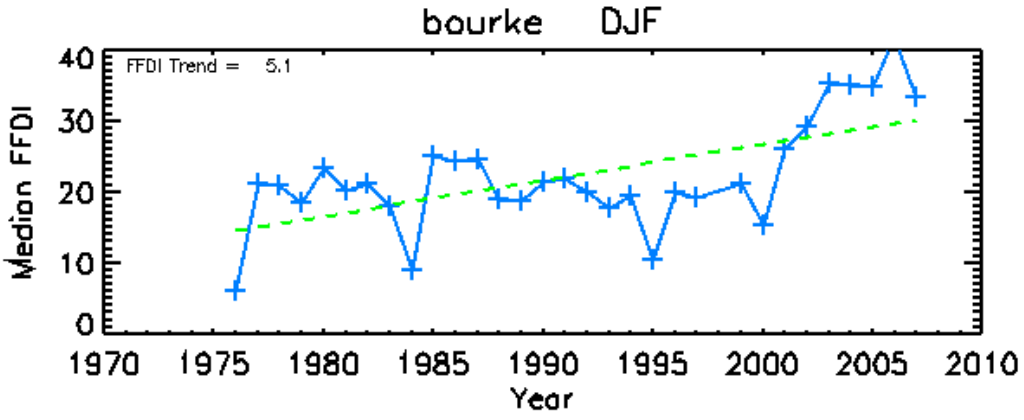

Brisbane AP

variable	now	2020				2050			
		low2	low3	high2	high3	low2	low3	high2	high3
ΣFFDI	1990	1	0	5	4	3	2	19	16
VHE	5.2	5.4	5.3	5.9	5.8	5.7	5.6	8.5	7.5
%	0.0	4.1	2.3	14.0	12.2	9.3	7.0	63.4	44.8
xtrm	0.5	0.5	0.5	0.6	0.6	0.6	0.5	1.0	0.9
%	0.0	6.2	6.2	31.2	31.2	25.0	6.2	106.2	87.5
vxtrm	0.0	0.0	0.0	0.0	0.0	0.0	0.0	0.1	0.1
cata	0.0	0.0	0.0	0.0	0.0	0.0	0.0	0.0	0.0
DJF50	3.7	3.8	3.8	4.0	4.0	3.9	3.9	4.7	4.5
MAM50	3.9	3.9	3.9	4.1	4.0	4.0	4.0	4.5	4.4
JJA50	5.2	5.2	5.2	5.5	5.3	5.3	5.3	6.3	5.8
SON50	5.7	5.7	5.8	5.9	6.1	5.8	5.9	6.5	6.9
DJF90	8.7	8.8	8.8	9.2	9.1	9.0	8.9	10.4	10.1
MAM90	8.8	8.8	8.9	9.1	9.1	9.0	9.0	9.7	9.8
JJA90	13.2	13.5	13.3	14.1	13.6	13.8	13.4	16.6	14.5
SON90	12.5	12.6	12.8	13.0	13.4	12.7	13.0	14.2	15.4

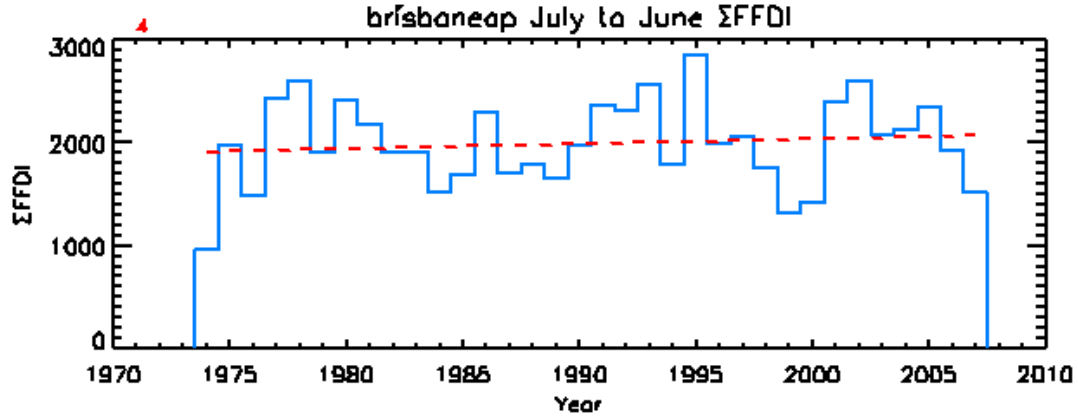

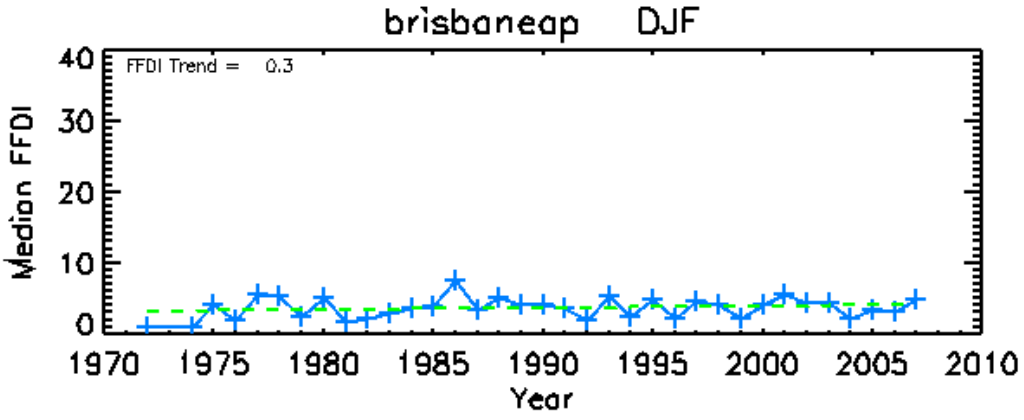

Canberra

variable	now	2020				2050			
		low2	low3	high2	high3	low2	low3	high2	high3
ΣFFDI	2493	3	3	9	11	6	7	30	37
VHE	16.8	18.3	18.9	21.5	22.8	20.0	20.6	29.9	33.4
%	0.0	9.0	12.6	28.1	35.7	19.1	22.7	78.0	98.4
xtrm	1.6	1.7	1.7	2.0	2.2	1.8	2.0	3.7	5.1
%	0.0	7.7	9.6	25.0	42.3	17.3	25.0	136.5	221.2
vxtrm	0.2	0.2	0.2	0.2	0.2	0.2	0.2	0.4	0.8
cata	0.0	0.0	0.1	0.1	0.1	0.1	0.1	0.1	0.1
DJF50	9.0	9.3	9.3	9.8	10.0	9.5	9.7	11.6	12.4
MAM50	4.7	4.8	4.8	5.0	5.1	4.8	4.9	5.4	5.8
JJA50	2.3	2.4	2.4	2.6	2.6	2.5	2.5	3.2	3.0
SON50	3.8	4.0	4.0	4.4	4.5	4.2	4.2	6.0	6.0
DJF90	27.0	27.8	28.0	29.2	30.0	28.4	28.9	33.9	36.4
MAM90	14.2	14.4	14.4	14.9	14.8	14.7	14.6	16.4	16.3
JJA90	5.6	5.8	5.9	6.2	6.3	6.0	6.1	7.6	7.9
SON90	14.0	14.7	15.0	16.1	16.9	15.4	15.7	20.9	24.2

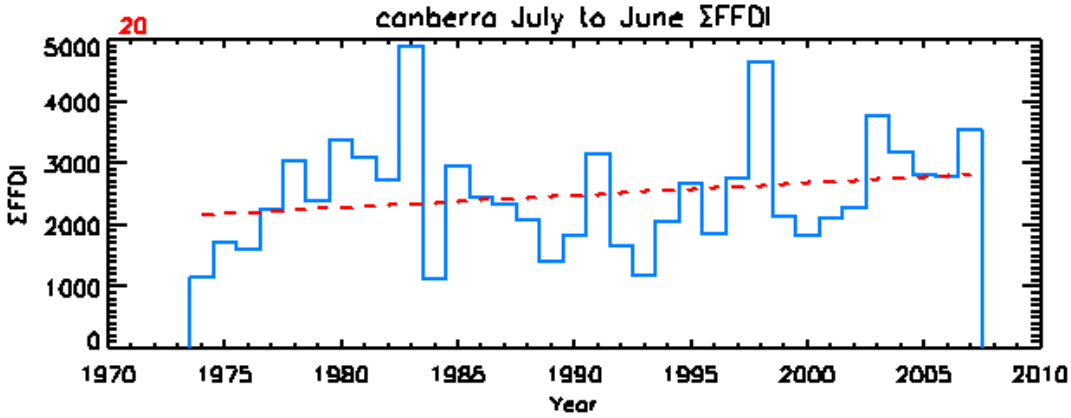

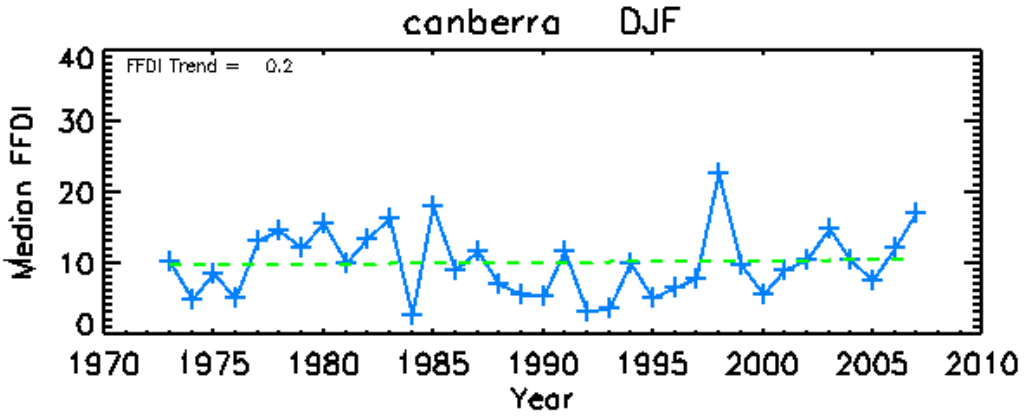

Ceduna

variable	now	2020				2050			
		low2	low3	high2	high3	low2	low3	high2	high3
ΣFFDI	4430	1	2	5	6	3	4	15	20
VHE	46.4	47.7	48.0	49.4	50.5	48.5	49.0	56.5	58.6
%	0.0	2.7	3.4	6.4	8.7	4.5	5.6	21.6	26.3
xtrm	11.8	12.3	12.3	13.6	13.8	12.9	13.1	17.3	18.5
%	0.0	4.4	4.4	15.4	16.7	9.8	11.1	46.5	57.3
vxtrm	2.6	2.7	2.8	3.2	3.5	3.0	3.2	4.8	5.5
cata	0.5	0.6	0.6	0.7	0.8	0.6	0.7	1.2	1.6
DJF50	10.1	10.2	10.3	10.4	10.6	10.3	10.4	10.9	11.6
MAM50	7.9	8.0	8.0	8.1	8.2	8.0	8.1	8.4	8.4
JJA50	4.9	5.0	5.1	5.1	5.3	5.1	5.2	5.5	5.9
SON50	8.0	8.2	8.2	8.6	8.7	8.4	8.4	9.9	10.3
DJF90	39.3	39.7	40.0	41.3	41.9	40.5	40.9	44.8	47.0
MAM90	26.8	26.9	27.1	27.2	27.8	27.0	27.4	28.6	29.5
JJA90	17.1	17.7	17.7	18.6	18.7	18.1	18.2	21.0	21.6
SON90	34.0	34.8	35.4	36.7	37.6	35.6	36.3	42.6	45.9

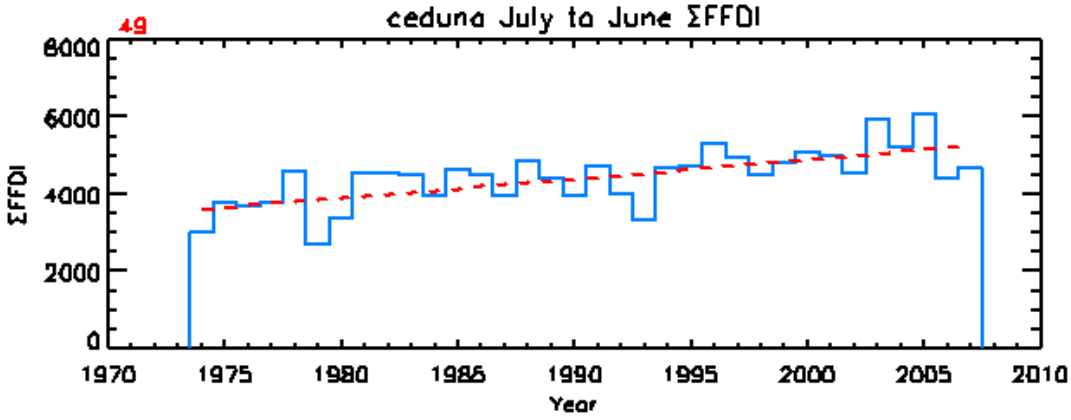

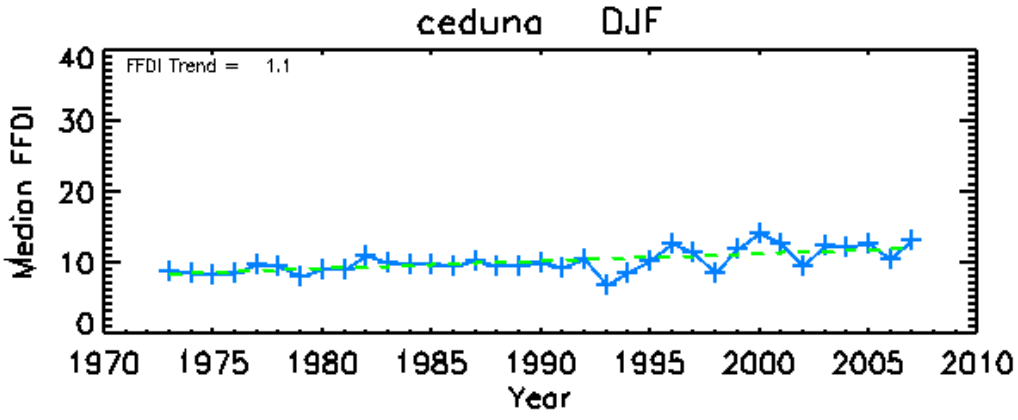

Charleville

variable	now	2020				2050			
		low2	low3	high2	high3	low2	low3	high2	high3
ΣFFDI	6127	4	2	11	8	7	5	37	25
VHE	89.0	95.6	93.6	108.3	102.0	101.5	97.2	147.5	126.7
%	0.0	7.4	5.1	21.6	14.6	14.0	9.2	65.7	42.3
xtrm	6.8	8.2	7.9	11.3	10.2	9.5	9.1	27.5	20.9
%	0.0	19.0	15.0	64.6	49.6	39.4	33.2	300.9	204.9
vxtrm	0.2	0.3	0.3	0.6	0.6	0.4	0.4	2.9	2.0
cata	0.0	0.0	0.0	0.0	0.0	0.0	0.0	0.3	0.2
DJF50	20.0	20.8	20.5	22.1	21.5	21.4	21.0	26.4	24.3
MAM50	14.1	14.4	14.4	15.0	14.9	14.7	14.6	16.9	16.7
JJA50	9.7	10.2	10.0	11.2	10.7	10.6	10.4	14.3	12.7
SON50	20.1	21.4	20.9	23.9	22.4	22.5	21.6	32.0	26.9
DJF90	41.5	42.7	42.6	44.8	44.6	43.5	43.5	51.0	50.9
MAM90	28.6	29.1	29.0	30.0	29.8	29.5	29.5	33.6	32.5
JJA90	18.9	19.9	19.5	21.8	20.6	20.8	20.0	28.4	23.7
SON90	38.6	40.5	40.0	44.3	42.3	42.2	41.0	57.0	50.9

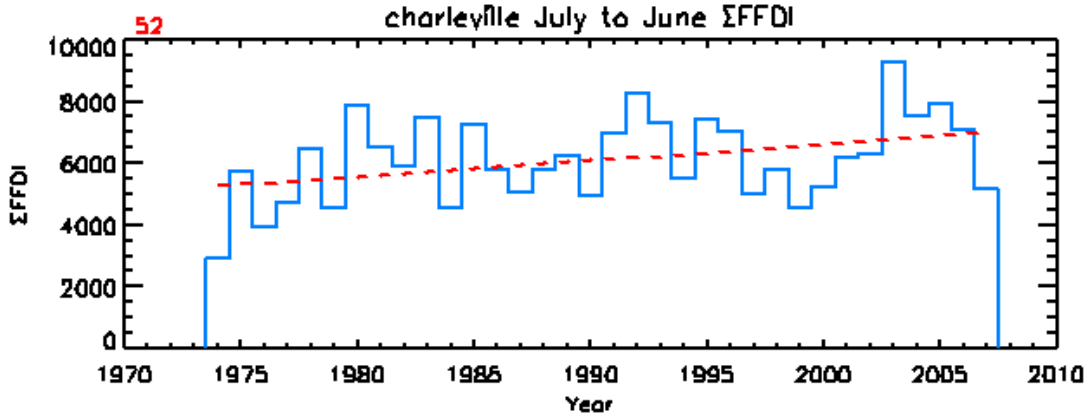

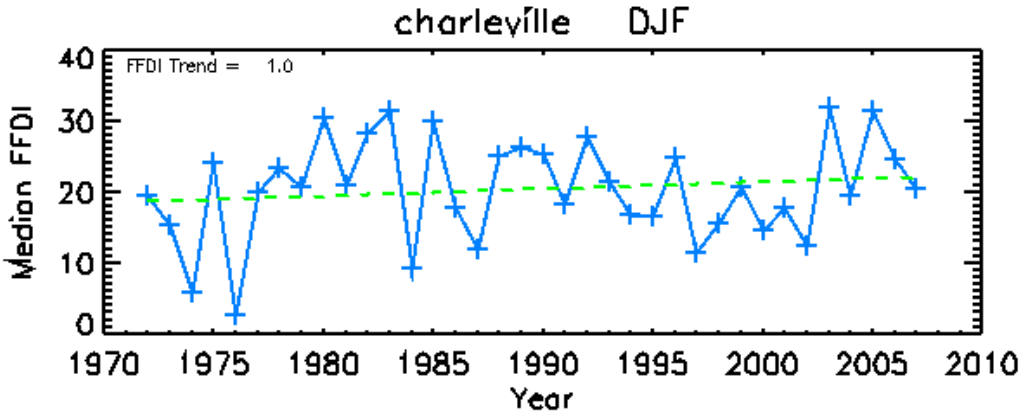

Cobar

variable	now	2020				2050			
		low2	low3	high2	high3	low2	low3	high2	high3
ΣFFDI	4800	4	3	10	9	7	6	33	28
VHE	56.0	61.4	60.8	69.9	67.9	65.2	64.0	99.5	91.8
%	0.0	9.6	8.5	24.9	21.3	16.4	14.3	77.7	63.9
xtrm	4.8	5.3	5.5	7.4	7.2	6.4	6.3	14.4	14.1
%	0.0	11.4	13.9	54.4	50.6	32.9	31.6	200.0	193.7
vxtrm	0.5	0.6	0.6	0.8	0.8	0.7	0.7	1.9	1.8
cata	0.1	0.1	0.1	0.1	0.1	0.1	0.1	0.3	0.3
DJF50	20.7	21.3	21.3	22.4	22.5	21.9	21.9	25.9	26.3
MAM50	10.3	10.6	10.5	11.1	10.8	10.8	10.6	12.6	11.6
JJA50	4.8	5.0	5.0	5.3	5.3	5.1	5.1	6.2	6.3
SON50	12.3	13.2	13.0	14.8	14.1	13.9	13.5	20.2	18.0
DJF90	39.9	41.0	41.1	42.7	42.8	41.8	42.0	48.0	48.5
MAM90	22.5	23.1	22.7	23.9	22.9	23.5	22.8	26.8	23.9
JJA90	11.6	12.1	12.1	13.1	12.9	12.6	12.5	16.3	16.1
SON90	30.0	31.6	31.4	34.5	33.9	33.0	32.6	44.5	42.2

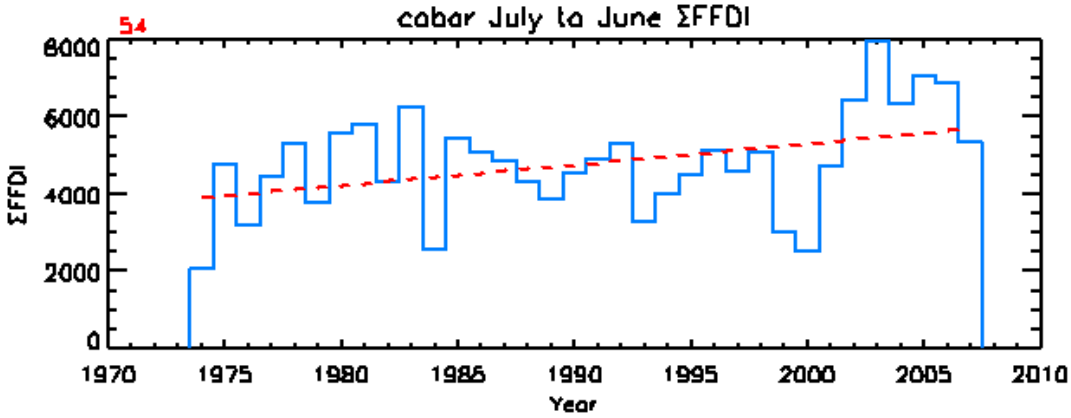

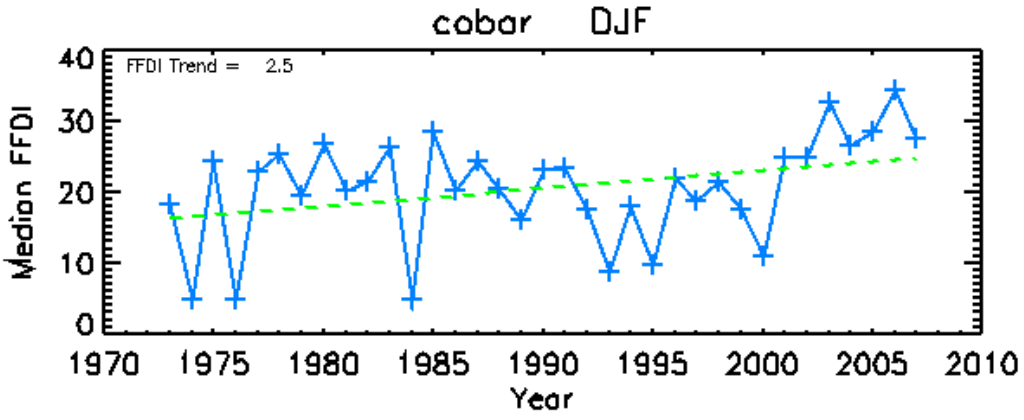

Coffs Harbour

variable	now	2020				2050			
		low2	low3	high2	high3	low2	low3	high2	high3
ΣFFDI	1255	1	1	3	6	2	3	11	18
VHE	1.5	1.6	1.6	1.8	1.8	1.8	1.8	2.3	2.5
%	0.0	6.1	6.1	22.4	20.4	20.4	18.4	57.1	71.4
xtrm	0.2	0.2	0.2	0.2	0.3	0.2	0.3	0.3	0.4
%	0.0	0.0	0.0	14.3	28.6	0.0	28.6	42.9	71.4
vxtrm	0.1	0.1	0.1	0.1	0.1	0.1	0.1	0.1	0.2
cata	0.0	0.0	0.0	0.0	0.0	0.0	0.0	0.0	0.0
DJF50	2.1	2.1	2.1	2.3	2.3	2.2	2.2	2.8	2.8
MAM50	1.4	1.5	1.5	1.5	1.5	1.5	1.5	1.7	1.6
JJA50	3.4	3.4	3.4	3.5	3.5	3.5	3.5	3.8	3.7
SON50	3.5	3.5	3.6	3.5	3.7	3.5	3.6	3.5	4.1
DJF90	6.7	6.8	6.9	7.0	7.2	6.9	7.1	7.7	8.5
MAM90	5.3	5.3	5.4	5.4	5.5	5.3	5.4	5.5	6.0
JJA90	8.6	8.7	8.6	8.9	8.9	8.8	8.8	9.7	9.6
SON90	9.0	9.0	9.1	9.1	9.7	9.0	9.4	9.1	11.2

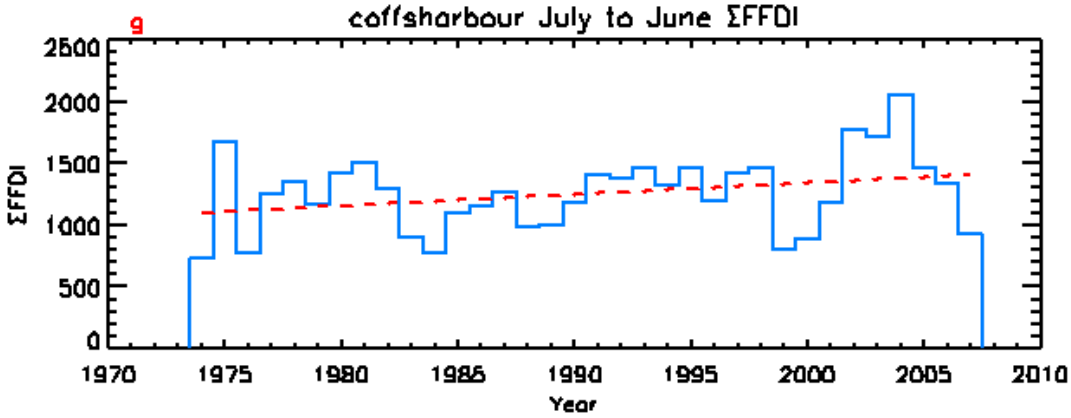

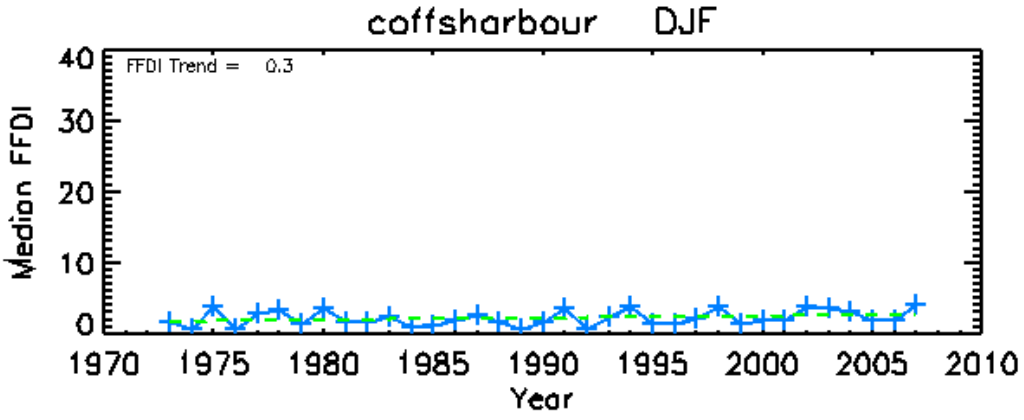

Dubbo

variable	now	2020				2050			
		low2	low3	high2	high3	low2	low3	high2	high3
ΣFFDI	3153	4	4	11	10	7	6	34	32
VHE	23.0	25.6	25.3	30.0	29.2	27.4	27.1	45.9	43.8
%	0.0	11.3	9.7	30.3	26.6	18.9	17.8	99.5	90.0
xtrm	1.7	2.0	2.1	2.8	3.1	2.5	2.6	6.3	6.7
%	0.0	18.2	27.3	70.9	83.6	47.3	54.5	280.0	303.6
vxtrm	0.2	0.3	0.3	0.3	0.3	0.3	0.3	0.9	1.0
cata	0.0	0.0	0.0	0.1	0.1	0.1	0.1	0.2	0.2
DJF50	12.9	13.4	13.5	14.2	14.2	13.8	13.8	16.5	16.6
MAM50	7.2	7.5	7.5	7.9	7.7	7.7	7.6	9.1	8.5
JJA50	3.0	3.1	3.2	3.3	3.4	3.2	3.3	4.0	4.0
SON50	6.2	6.6	6.6	7.3	7.2	6.9	6.9	10.1	9.6
DJF90	29.0	30.1	30.1	31.7	31.7	30.7	30.8	36.6	36.7
MAM90	18.2	18.8	18.4	19.6	18.5	19.1	18.5	22.1	19.2
JJA90	7.7	8.1	8.0	8.7	8.7	8.3	8.3	10.4	10.8
SON90	21.4	22.8	23.0	25.2	25.8	24.0	24.3	33.7	35.3

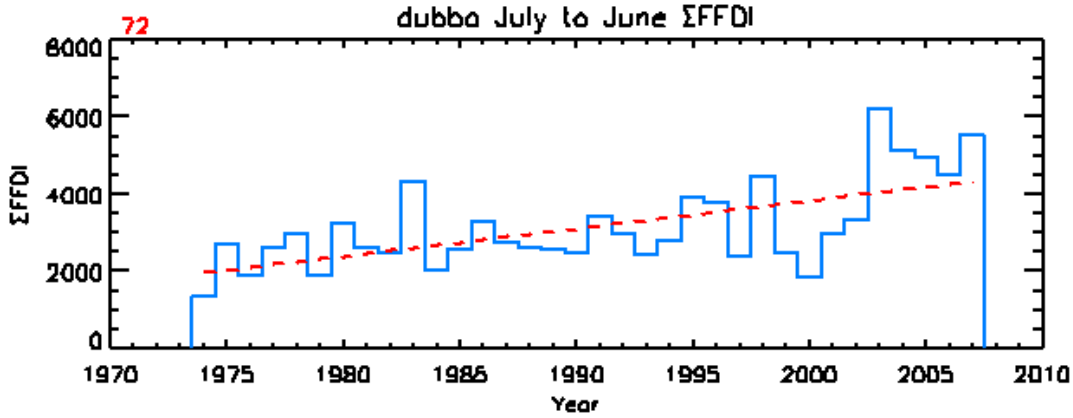

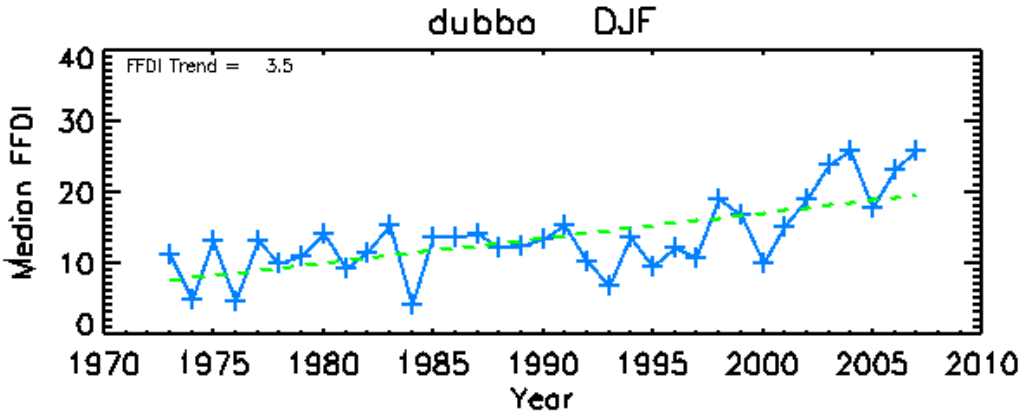

Hobart

variable	now	2020				2050			
		low2	low3	high2	high3	low2	low3	high2	high3
ΣFFDI	1314	-1	0	-1	0	-1	0	-1	3
VHE	2.0	2.0	2.0	2.0	2.1	2.0	2.1	2.0	2.2
%	0.0	-3.0	-3.0	-1.5	4.5	-1.5	1.5	0.0	7.5
xtrm	0.1	0.1	0.1	0.1	0.1	0.1	0.1	0.1	0.2
%	0.0	0.0	0.0	0.0	0.0	0.0	0.0	0.0	50.0
vxtrm	0.0	0.0	0.0	0.0	0.0	0.0	0.0	0.0	0.0
cata	0.0	0.0	0.0	0.0	0.0	0.0	0.0	0.0	0.0
DJF50	4.1	4.1	4.1	4.1	4.2	4.1	4.1	4.2	4.3
MAM50	2.8	2.7	2.8	2.8	2.8	2.8	2.8	2.9	3.0
JJA50	1.6	1.6	1.6	1.6	1.6	1.6	1.6	1.6	1.6
SON50	2.6	2.5	2.5	2.5	2.5	2.5	2.5	2.5	2.5
DJF90	10.7	10.6	10.6	10.6	10.6	10.6	10.6	10.6	10.7
MAM90	7.6	7.4	7.5	7.4	7.7	7.4	7.6	7.3	8.2
JJA90	4.0	3.9	3.9	3.8	4.0	3.8	4.0	3.6	4.1
SON90	6.9	6.8	6.9	6.8	6.9	6.8	6.9	6.6	6.9

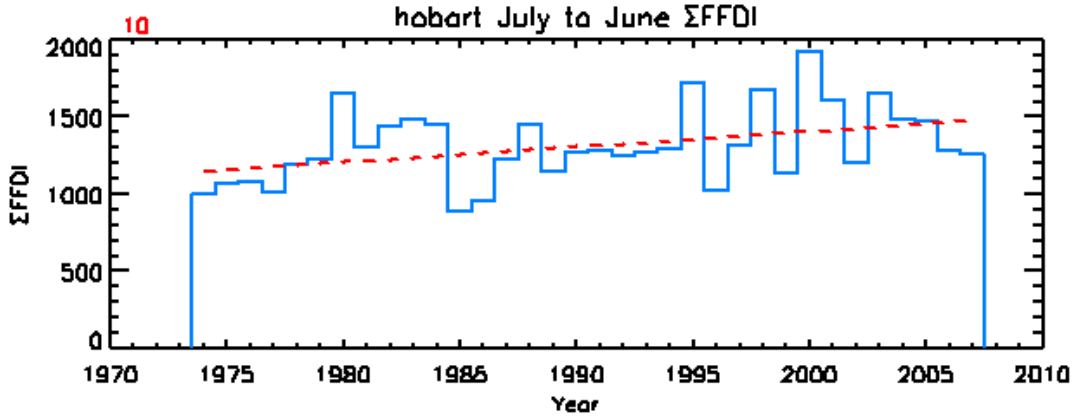

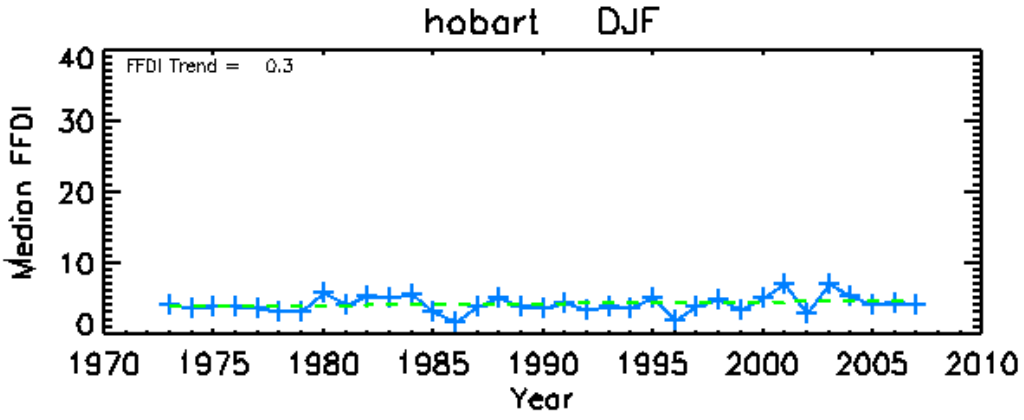

Launceston AP

variable	now	2020				2050			
		low2	low3	high2	high3	low2	low3	high2	high3
ΣFFDI	1349	0	1	1	6	0	3	8	22
VHE	1.0	1.0	1.2	1.1	1.2	1.0	1.2	1.2	2.2
%	0.0	-2.9	11.8	2.9	17.6	0.0	14.7	17.6	111.8
xtrm	0.0	0.0	0.0	0.0	0.0	0.0	0.0	0.0	0.1
%	--	--	--	--	--	--	--	--	--
vxtrm	0.0	0.0	0.0	0.0	0.0	0.0	0.0	0.0	0.0
cata	0.0	0.0	0.0	0.0	0.0	0.0	0.0	0.0	0.0
DJF50	6.1	6.1	6.2	6.2	6.5	6.1	6.3	6.7	7.5
MAM50	3.0	3.0	3.0	3.0	3.1	3.0	3.1	3.2	3.6
JJA50	1.0	1.0	1.0	1.0	1.1	1.0	1.0	1.0	1.2
SON50	2.3	2.4	2.4	2.4	2.5	2.4	2.5	2.6	2.9
DJF90	13.3	13.3	13.5	13.5	14.0	13.4	13.7	14.2	16.1
MAM90	8.7	8.6	8.7	8.7	9.1	8.6	8.9	9.0	10.1
JJA90	2.3	2.3	2.3	2.3	2.5	2.3	2.4	2.5	2.8
SON90	5.9	6.0	6.1	6.2	6.5	6.1	6.3	6.9	7.9

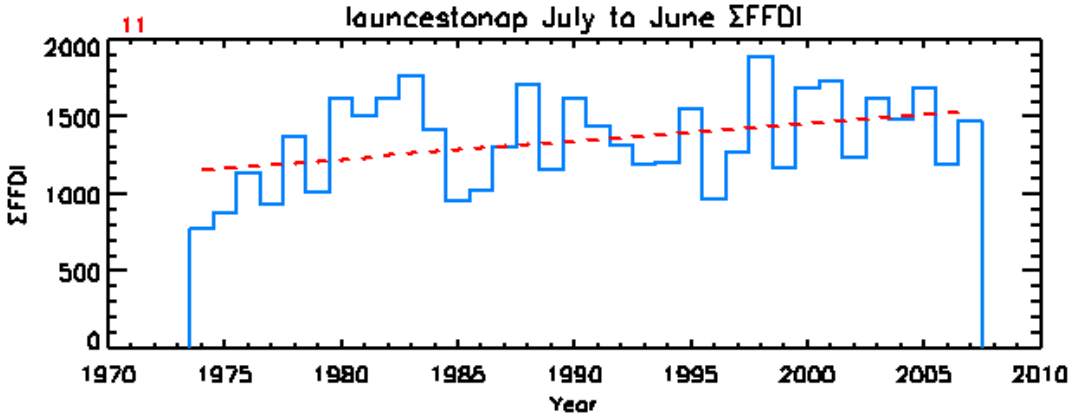

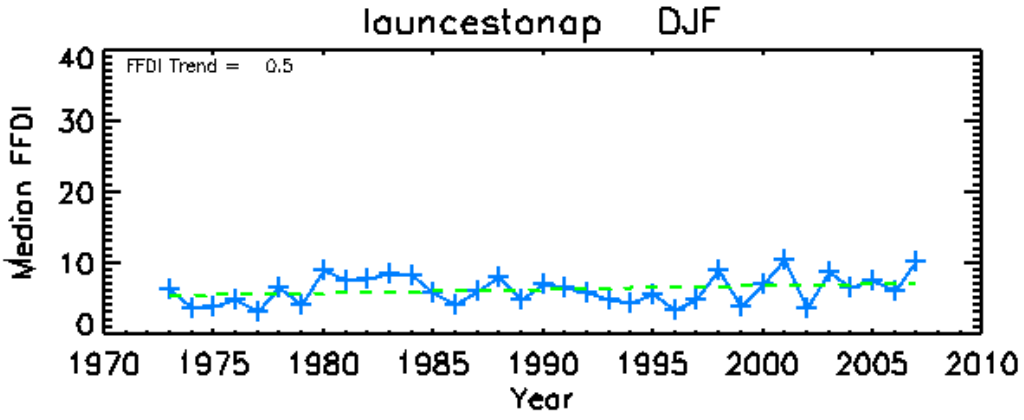

Laverton

variable	now	2020				2050			
		low2	low3	high2	high3	low2	low3	high2	high3
ΣFFDI	2056	1	2	6	8	4	5	23	30
VHE	11.8	12.0	12.3	12.8	13.6	12.4	12.8	16.7	19.2
%	0.0	1.8	4.1	9.0	15.4	5.4	8.5	41.9	63.2
xtrm	1.9	1.9	2.1	2.4	2.6	2.2	2.4	3.5	4.6
%	0.0	1.6	7.9	27.0	38.1	15.9	23.8	84.1	142.9
vxtrm	0.3	0.4	0.4	0.5	0.6	0.4	0.5	0.8	1.2
cata	0.2	0.2	0.2	0.2	0.2	0.2	0.2	0.2	0.4
DJF50	5.6	5.7	5.7	5.9	6.1	5.8	5.9	6.8	7.2
MAM50	3.9	3.9	3.9	4.0	4.0	4.0	4.0	4.4	4.4
JJA50	2.2	2.3	2.3	2.4	2.3	2.3	2.3	2.6	2.6
SON50	3.0	3.1	3.2	3.4	3.5	3.3	3.3	4.3	4.4
DJF90	21.1	21.3	21.5	22.1	22.8	21.7	22.1	25.0	27.4
MAM90	12.4	12.4	12.4	12.9	12.9	12.7	12.6	14.0	14.1
JJA90	5.8	5.9	5.9	6.2	6.2	6.0	6.1	7.1	7.4
SON90	10.9	11.4	11.6	12.4	13.0	11.8	12.2	15.9	18.0

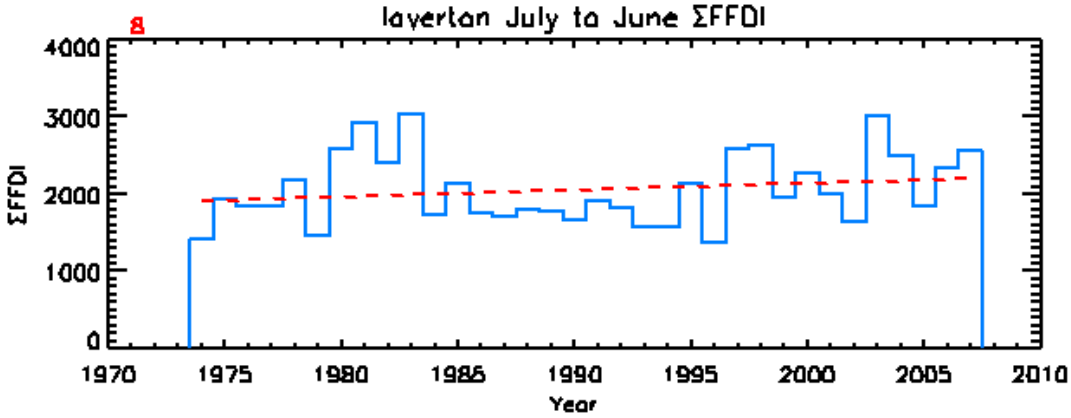

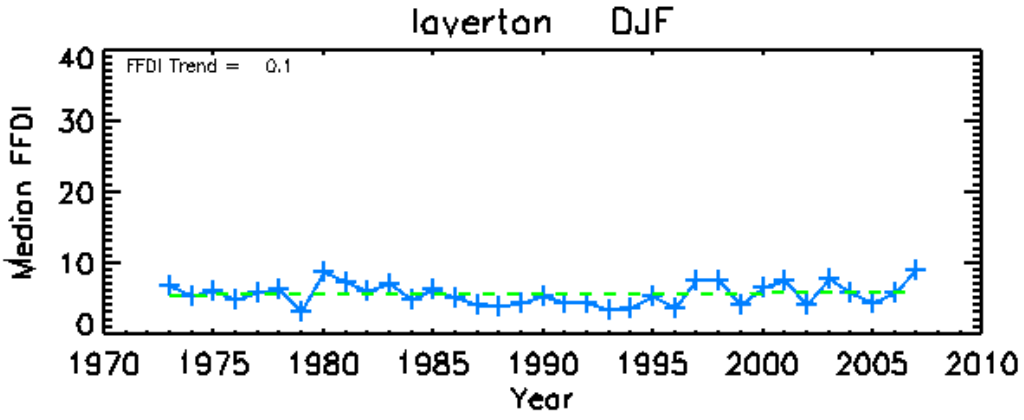

Melbourne AP

variable	now	2020				2050			
		low2	low3	high2	high3	low2	low3	high2	high3
ΣFFDI	2306	2	3	7	9	4	6	22	30
VHE	14.8	15.7	15.9	17.0	17.6	16.2	16.5	21.2	23.6
%	0.0	5.7	7.2	14.7	19.0	9.2	11.5	42.7	59.3
xtrm	2.5	2.8	2.8	3.1	3.4	3.0	3.2	4.5	5.8
%	0.0	12.2	14.6	25.6	37.8	19.5	28.0	80.5	135.4
vxtrm	0.4	0.4	0.5	0.6	0.7	0.5	0.5	1.0	1.6
cata	0.0	0.0	0.0	0.1	0.1	0.1	0.1	0.2	0.4
DJF50	6.8	7.0	7.1	7.3	7.5	7.1	7.2	8.4	8.9
MAM50	4.4	4.5	4.5	4.6	4.6	4.5	4.6	5.0	4.9
JJA50	2.3	2.3	2.3	2.4	2.4	2.3	2.4	2.7	2.7
SON50	3.3	3.5	3.5	3.7	3.7	3.6	3.6	4.6	4.9
DJF90	24.8	25.5	25.8	26.5	27.3	26.0	26.4	30.3	33.0
MAM90	14.0	14.3	14.2	14.8	14.6	14.5	14.4	16.0	15.8
JJA90	5.6	5.7	5.7	5.9	6.1	5.8	5.9	6.6	7.3
SON90	12.0	12.6	12.8	13.5	14.2	13.0	13.5	16.5	18.9

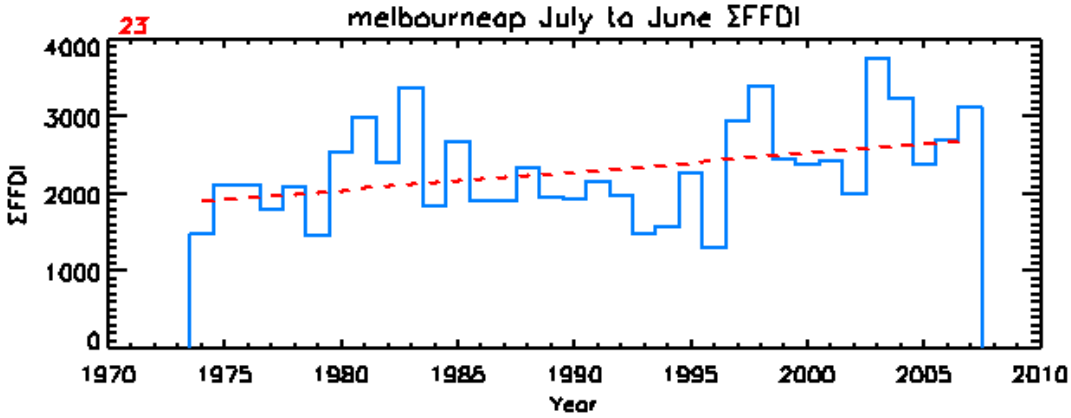

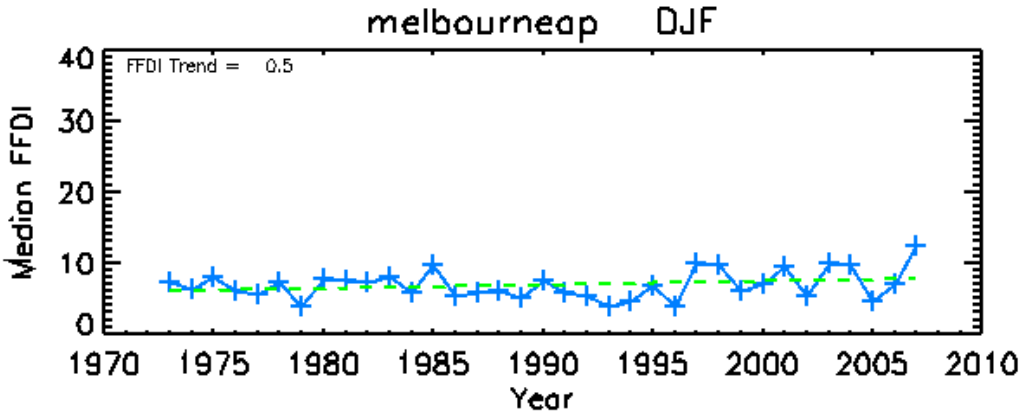

Mildura

variable	now	2020				2050			
		low2	low3	high2	high3	low2	low3	high2	high3
ΣFFDI	5017	2	3	7	8	4	5	21	26
VHE	56.6	59.5	60.3	65.5	66.9	62.3	63.7	84.7	90.5
%	0.0	5.0	6.5	15.7	18.2	10.0	12.5	49.6	59.9
xtrm	7.3	8.0	8.3	9.1	10.0	8.6	9.0	12.8	15.9
%	0.0	10.0	14.2	25.0	37.5	17.9	24.2	75.8	119.2
vxtrm	1.2	1.2	1.3	1.7	1.8	1.4	1.6	2.6	3.9
cata	0.1	0.2	0.2	0.3	0.5	0.2	0.3	0.7	1.2
DJF50	20.2	20.6	20.9	21.4	22.1	20.9	21.4	23.7	26.1
MAM50	10.2	10.3	10.4	10.6	10.8	10.5	10.6	11.2	12.0
JJA50	4.7	4.9	4.9	5.0	5.1	4.9	5.0	5.5	5.9
SON50	12.0	12.6	12.5	13.8	13.3	13.1	12.8	17.8	16.3
DJF90	39.4	40.2	40.6	41.5	42.4	40.8	41.4	45.1	49.4
MAM90	24.0	24.3	24.2	24.7	24.5	24.5	24.4	26.2	25.7
JJA90	11.9	12.3	12.3	12.9	13.0	12.6	12.7	15.0	15.3
SON90	30.7	31.9	32.0	33.9	34.4	32.8	33.0	40.3	41.6

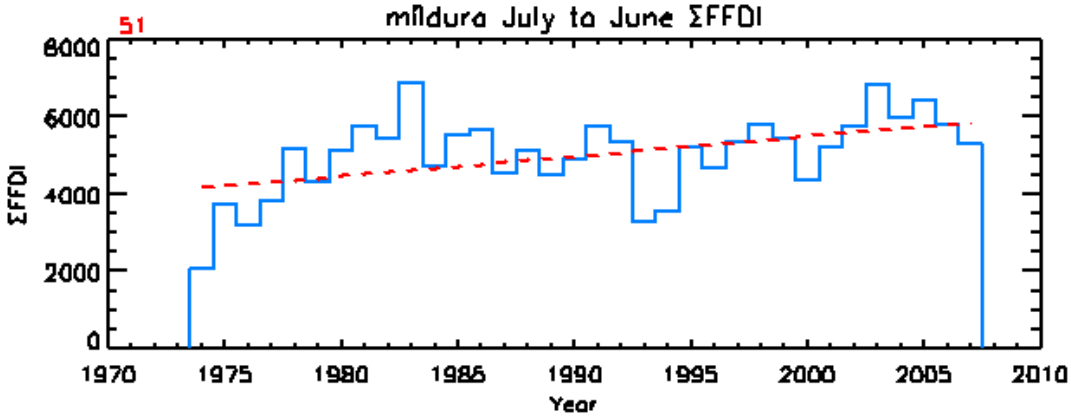

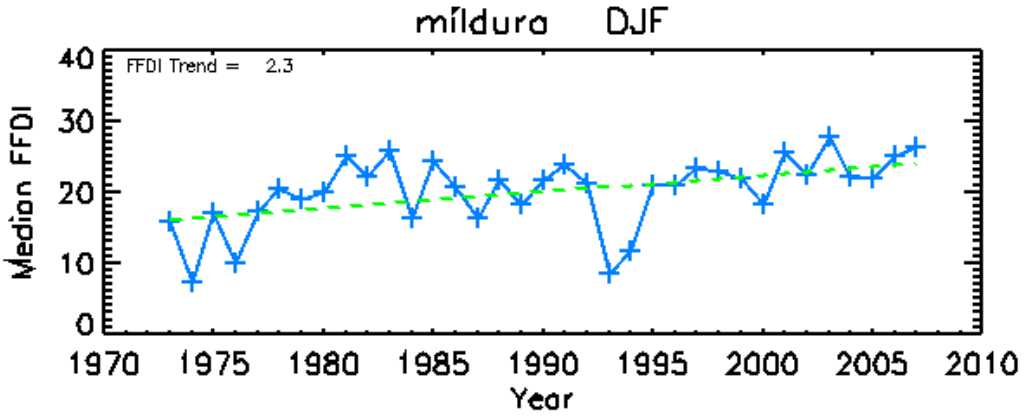

Moree

variable	now	2020				2050			
		low2	low3	high2	high3	low2	low3	high2	high3
ΣFFDI	3937	4	4	12	10	8	6	37	29
VHE	30.5	34.5	33.7	41.1	38.9	37.6	36.4	62.8	55.8
%	0.0	13.1	10.2	34.5	27.5	23.1	19.1	105.6	82.7
xtrm	2.2	2.5	2.4	3.6	3.4	2.8	2.7	8.5	8.0
%	0.0	16.9	12.7	67.6	59.2	32.4	26.8	293.0	273.2
vxtrm	0.2	0.3	0.3	0.5	0.5	0.4	0.4	0.9	0.9
cata	0.0	0.0	0.0	0.0	0.0	0.0	0.0	0.2	0.3
DJF50	7.7	7.8	7.9	8.1	8.2	7.9	8.0	8.7	9.1
MAM50	3.7	3.8	3.8	3.9	3.9	3.8	3.8	4.1	4.3
JJA50	0.9	0.9	0.9	0.9	1.0	0.9	0.9	1.0	1.1
SON50	2.1	2.2	2.2	2.2	2.3	2.2	2.3	2.5	2.7
DJF90	22.3	22.6	22.6	23.1	23.0	22.9	22.8	25.1	25.7
MAM90	13.3	13.5	13.4	13.7	13.7	13.6	13.6	14.2	14.4
JJA90	2.6	2.6	2.6	2.6	2.7	2.6	2.7	2.7	3.2
SON90	7.4	7.6	7.8	7.8	8.3	7.7	8.0	8.8	10.4

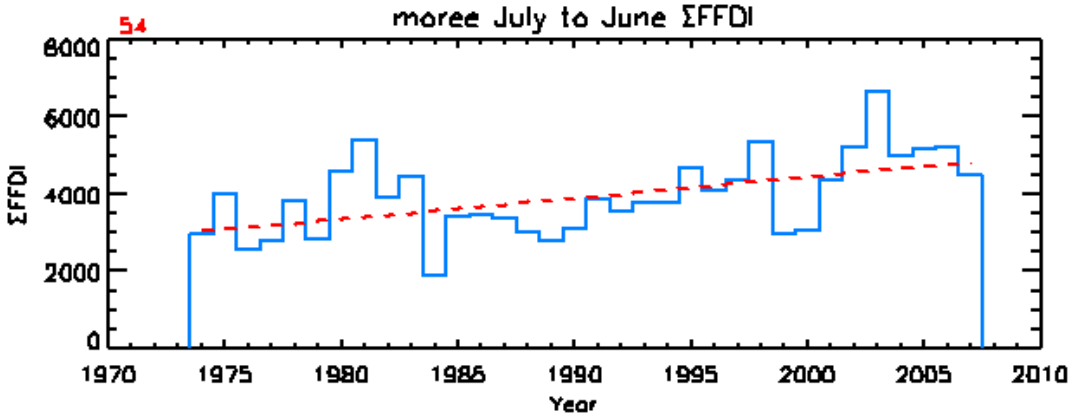

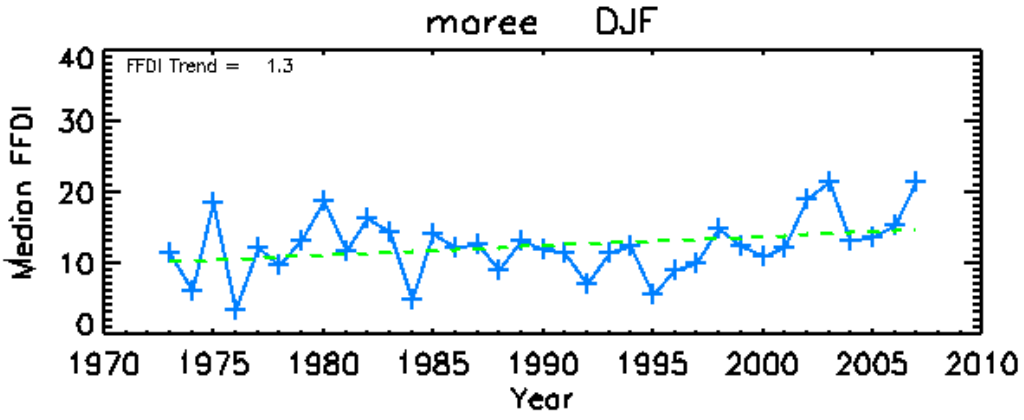

Mt Gambier

variable	now	2020				2050			
		low2	low3	high2	high3	low2	low3	high2	high3
ΣFFDI	1910	1	2	3	5	2	3	11	18
VHE	11.5	11.6	11.8	12.3	12.8	12.0	12.3	14.0	15.4
%	0.0	1.3	2.9	7.4	11.6	4.5	7.1	22.2	34.0
xtrm	1.4	1.5	1.6	1.6	1.8	1.6	1.7	2.2	2.9
%	0.0	8.5	12.8	14.9	25.5	14.9	17.0	53.2	104.3
vxtrm	0.2	0.2	0.2	0.2	0.2	0.2	0.2	0.2	0.4
cata	0.1	0.1	0.1	0.1	0.1	0.1	0.1	0.1	0.2
DJF50	12.4	12.9	12.7	13.8	13.2	13.4	13.0	16.7	14.7
MAM50	9.6	10.0	9.9	10.5	10.2	10.2	10.0	12.2	11.3
JJA50	5.6	5.9	5.9	6.3	6.3	6.1	6.0	7.8	7.7
SON50	10.8	11.5	11.4	12.6	12.4	12.0	11.8	16.4	15.4
DJF90	27.9	29.0	28.8	30.9	30.2	29.8	29.4	36.5	34.4
MAM90	20.5	21.2	21.0	22.0	21.5	21.6	21.2	24.4	23.0
JJA90	12.4	13.0	13.0	14.0	13.9	13.5	13.3	17.5	17.1
SON90	27.9	29.6	29.5	32.3	32.3	30.9	30.8	41.0	40.6

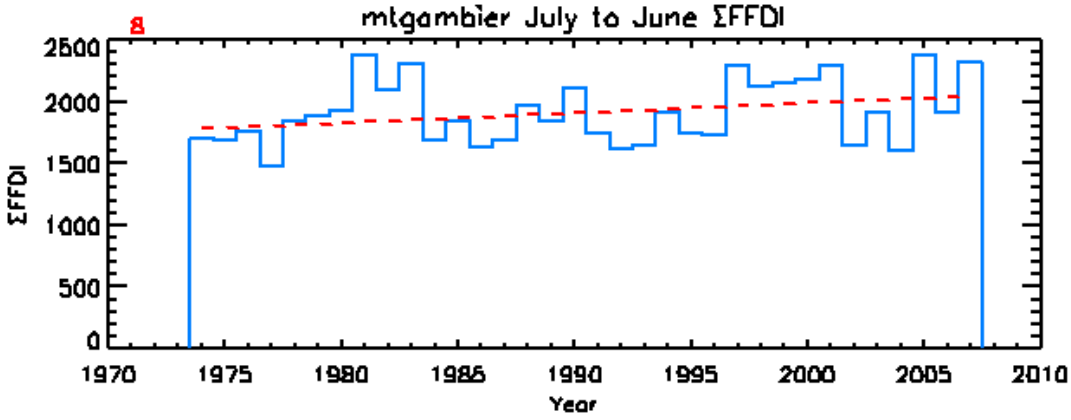

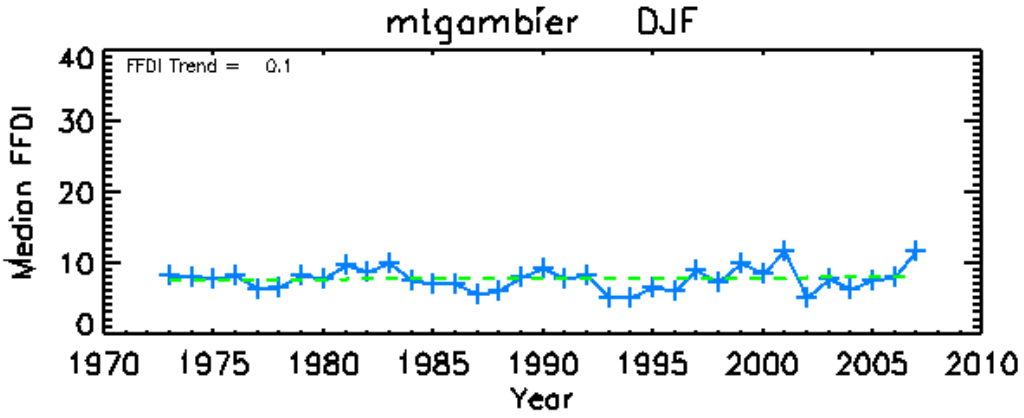

Nowra

variable	now	2020				2050			
		low2	low3	high2	high3	low2	low3	high2	high3
ΣFFDI	1768	0	1	2	7	0	4	12	29
VHE	8.8	8.7	9.1	9.2	10.3	8.9	9.6	10.8	14.7
%	0.0	-0.7	3.4	4.8	16.9	1.7	9.7	23.4	67.6
xtrm	1.1	1.0	1.2	1.2	1.6	1.1	1.5	1.9	4.0
%	0.0	-2.9	14.3	14.3	54.3	2.9	40.0	82.9	280.0
vxtrm	0.1	0.1	0.1	0.1	0.2	0.1	0.2	0.2	0.6
cata	0.1	0.1	0.1	0.1	0.1	0.1	0.1	0.1	0.1
DJF50	3.5	3.5	3.5	3.6	3.8	3.5	3.7	3.8	4.5
MAM50	2.8	2.7	2.8	2.7	2.8	2.7	2.8	2.7	2.9
JJA50	3.1	3.1	3.1	3.3	3.2	3.2	3.1	3.9	3.6
SON50	3.3	3.3	3.4	3.4	3.7	3.4	3.5	3.9	4.7
DJF90	11.7	11.7	11.9	11.8	12.5	11.7	12.1	12.2	14.6
MAM90	8.5	8.3	8.4	8.3	8.5	8.3	8.4	8.2	8.9
JJA90	8.8	8.8	8.9	9.2	9.5	8.9	9.2	10.5	11.4
SON90	14.5	14.6	14.8	15.1	16.3	14.9	15.5	17.5	22.2

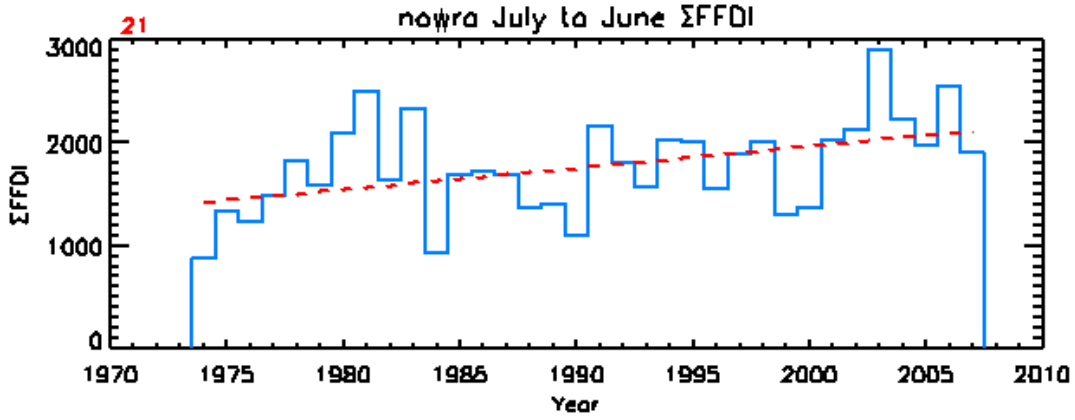

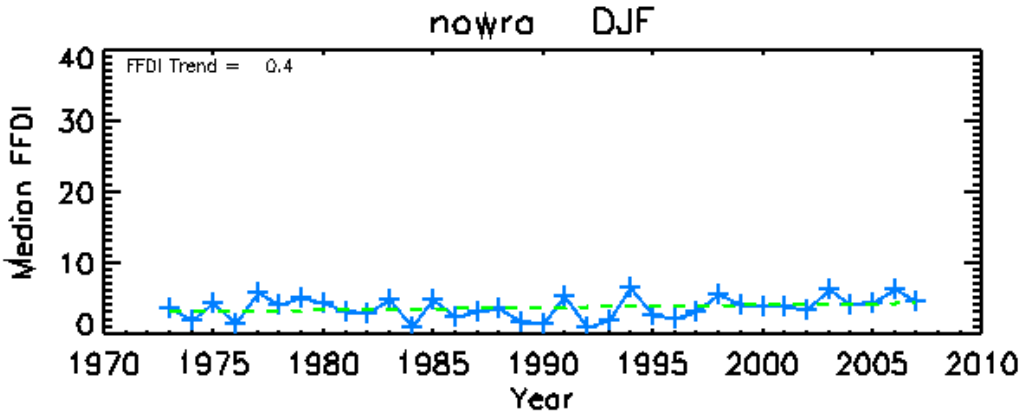

Richmond

variable	now	2020				2050			
		low2	low3	high2	high3	low2	low3	high2	high3
ΣFFDI	2152	1	2	6	8	3	5	20	26
VHE	13.3	13.8	14.2	15.2	16.3	14.5	15.1	20.3	23.6
%	0.0	4.1	6.4	13.9	22.8	9.3	13.2	52.6	77.4
xtrm	1.5	1.5	1.6	1.7	1.9	1.6	1.8	2.7	4.0
%	0.0	4.2	8.3	14.6	29.2	8.3	20.8	85.4	177.1
vxtrm	0.4	0.4	0.4	0.4	0.5	0.4	0.5	0.6	0.9
cata	0.0	0.0	0.0	0.0	0.0	0.0	0.0	0.1	0.2
DJF50	5.4	5.5	5.6	5.8	6.0	5.6	5.8	6.5	7.3
MAM50	3.9	3.9	3.9	4.0	4.0	3.9	3.9	4.3	4.4
JJA50	4.3	4.4	4.4	4.7	4.6	4.6	4.5	5.5	5.2
SON50	6.9	7.1	7.1	7.5	7.6	7.3	7.3	8.8	9.1
DJF90	21.2	21.3	21.7	22.1	22.8	21.7	22.2	24.0	26.6
MAM90	12.0	12.1	12.1	12.2	12.4	12.1	12.3	12.7	13.1
JJA90	11.9	12.3	12.2	13.1	12.8	12.6	12.4	15.2	15.0
SON90	22.4	23.0	23.5	24.5	25.6	23.6	24.5	29.1	32.3

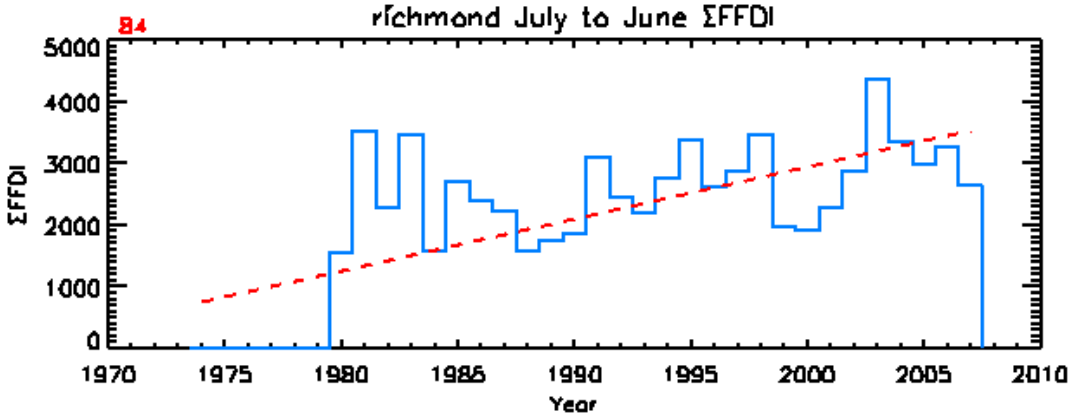

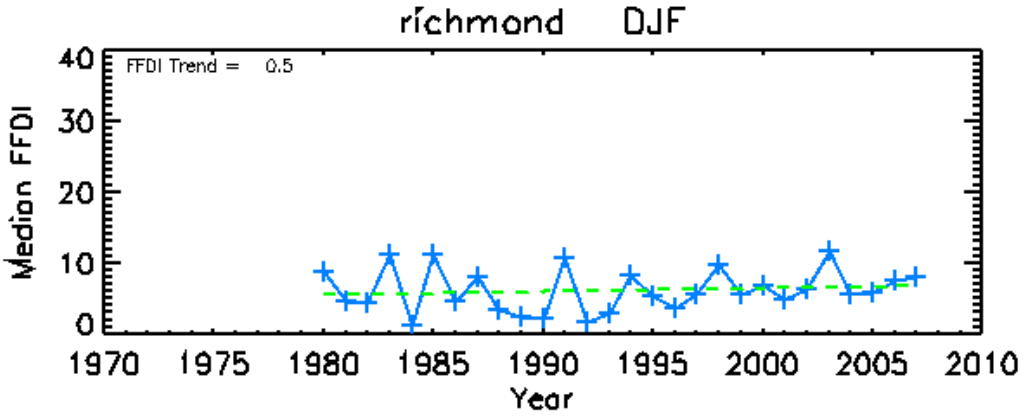

Rockhampton

variable	now	2020				2050			
		low2	low3	high2	high3	low2	low3	high2	high3
ΣFFDI	3166	2	2	6	7	4	4	21	22
VHE	11.2	12.0	11.9	13.2	13.5	12.4	12.8	18.6	19.4
%	0.0	6.5	5.7	17.0	19.7	10.2	13.5	65.8	72.8
xtrm	0.6	0.6	0.7	0.7	0.8	0.6	0.7	1.2	1.5
%	0.0	5.0	15.0	20.0	30.0	5.0	20.0	105.0	140.0
vxtrm	0.1	0.1	0.1	0.1	0.1	0.1	0.1	0.2	0.2
cata	0.0	0.0	0.0	0.0	0.0	0.0	0.0	0.0	0.1
DJF50	6.6	6.8	6.9	7.1	7.3	6.9	7.0	8.0	8.6
MAM50	7.3	7.3	7.4	7.6	7.7	7.4	7.6	8.4	8.7
JJA50	8.0	8.3	8.1	8.8	8.4	8.5	8.2	10.6	9.2
SON50	9.7	9.9	9.9	10.4	10.5	10.2	10.2	12.0	12.2
DJF90	14.4	14.6	14.8	15.0	15.7	14.8	15.2	16.2	18.1
MAM90	14.5	14.6	14.7	15.0	15.2	14.8	14.9	16.1	16.8
JJA90	17.2	17.7	17.4	18.7	17.9	18.2	17.6	22.3	19.5
SON90	20.7	21.1	21.3	21.9	22.4	21.5	21.8	23.7	25.6

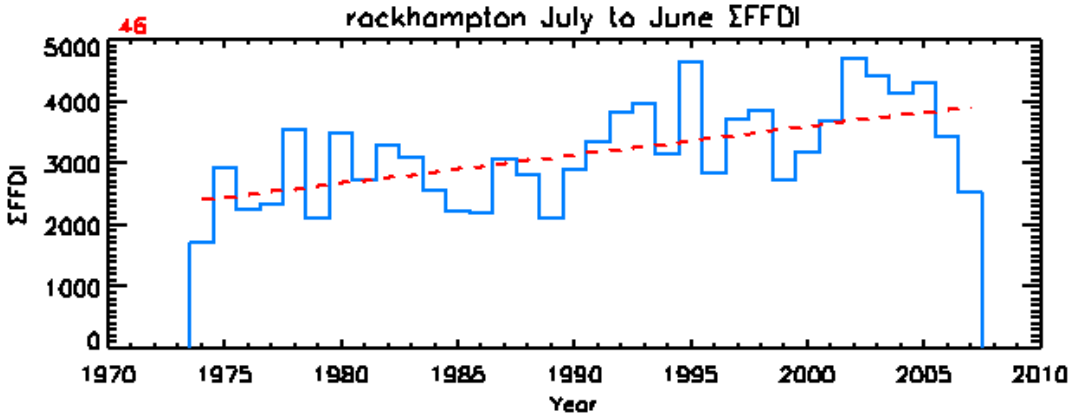

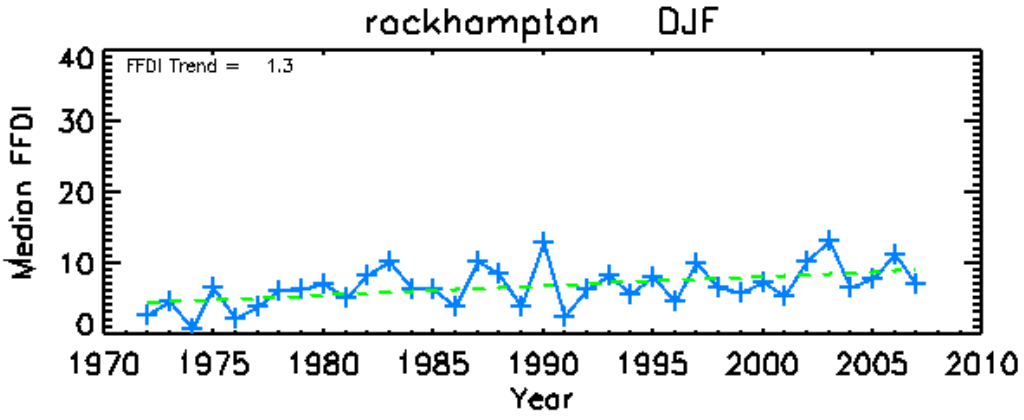

Sale

variable	now	2020				2050			
		low2	low3	high2	high3	low2	low3	high2	high3
ΣFFDI	1713	0	1	5	8	2	4	19	31
VHE	5.4	5.4	5.7	5.9	7.1	5.7	6.3	8.1	11.1
%	0.0	1.1	6.8	10.2	31.6	6.2	17.5	50.3	106.8
xtrm	0.6	0.6	0.7	0.7	0.9	0.6	0.8	1.1	1.9
%	0.0	5.0	10.0	15.0	45.0	5.0	30.0	80.0	215.0
vxtrm	0.2	0.2	0.2	0.2	0.2	0.2	0.2	0.2	0.2
cata	0.1	0.1	0.1	0.1	0.1	0.1	0.1	0.1	0.2
DJF50	5.3	5.3	5.4	5.5	5.9	5.5	5.6	6.1	7.2
MAM50	3.3	3.3	3.3	3.4	3.4	3.3	3.4	3.6	3.8
JJA50	1.9	1.9	1.9	2.1	2.0	2.0	1.9	2.4	2.2
SON50	2.7	2.8	2.8	3.1	3.0	2.9	2.9	4.0	4.0
DJF90	15.6	15.6	15.9	15.8	16.9	15.6	16.4	16.9	20.3
MAM90	10.0	9.9	10.0	10.1	10.3	10.0	10.1	10.6	11.0
JJA90	5.4	5.4	5.5	5.7	5.7	5.6	5.6	6.7	6.8
SON90	9.5	9.8	10.0	10.6	11.0	10.2	10.5	13.0	15.2

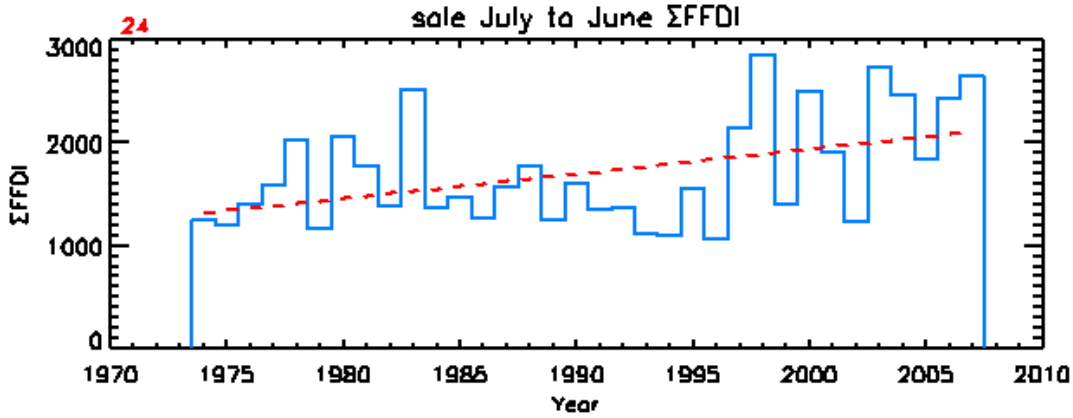

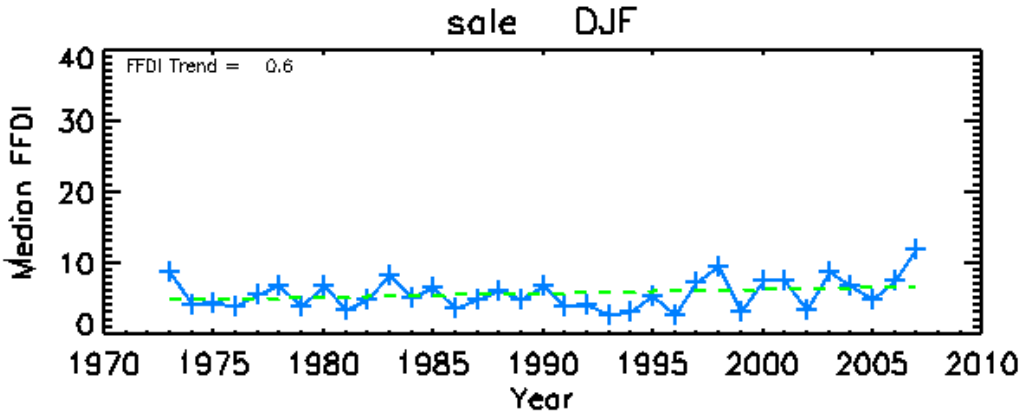

Sydney AP

variable	now	2020				2050			
		low2	low3	high2	high3	low2	low3	high2	high3
ΣFFDI	1897	1	3	4	10	2	6	11	31
VHE	7.6	7.8	8.1	8.3	9.4	8.0	8.7	9.8	14.2
%	0.0	1.6	6.0	9.1	23.4	4.4	13.9	27.8	86.5
xtrm	1.2	1.3	1.4	1.5	1.7	1.3	1.5	1.8	3.5
%	0.0	10.5	21.1	26.3	50.0	13.2	34.2	52.6	200.0
vxtrm	0.2	0.2	0.2	0.2	0.3	0.2	0.2	0.3	1.0
cata	0.0	0.0	0.0	0.0	0.0	0.0	0.0	0.0	0.2
DJF50	4.2	4.3	4.4	4.4	4.7	4.3	4.5	4.7	5.5
MAM50	2.8	2.8	2.9	2.9	2.9	2.9	2.9	2.9	3.1
JJA50	2.9	3.0	3.0	3.1	3.1	3.1	3.1	3.5	3.5
SON50	4.2	4.2	4.4	4.3	4.7	4.3	4.5	4.7	5.8
DJF90	12.6	12.7	13.1	12.9	13.8	12.8	13.4	13.4	16.2
MAM90	8.8	8.8	9.0	8.8	9.2	8.8	9.1	8.8	9.9
JJA90	10.1	10.2	10.5	10.6	11.3	10.4	10.8	11.7	13.3
SON90	14.4	14.7	15.3	15.1	16.6	14.9	15.9	16.9	21.7

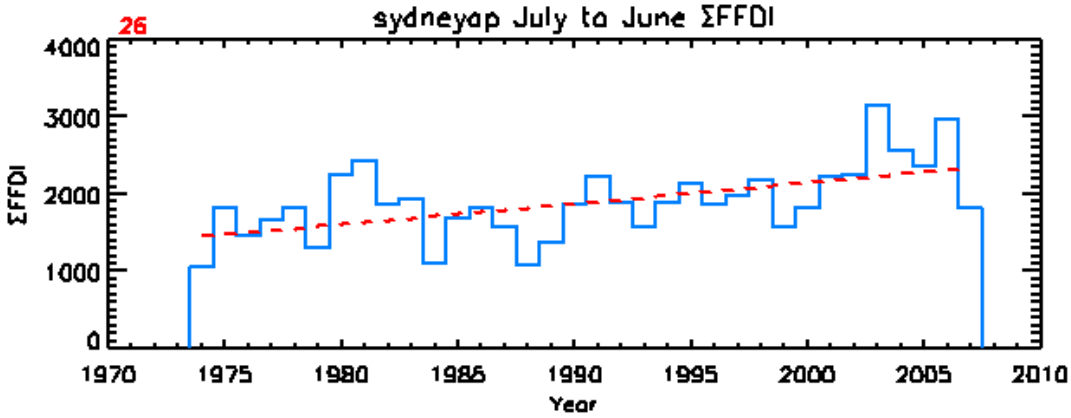

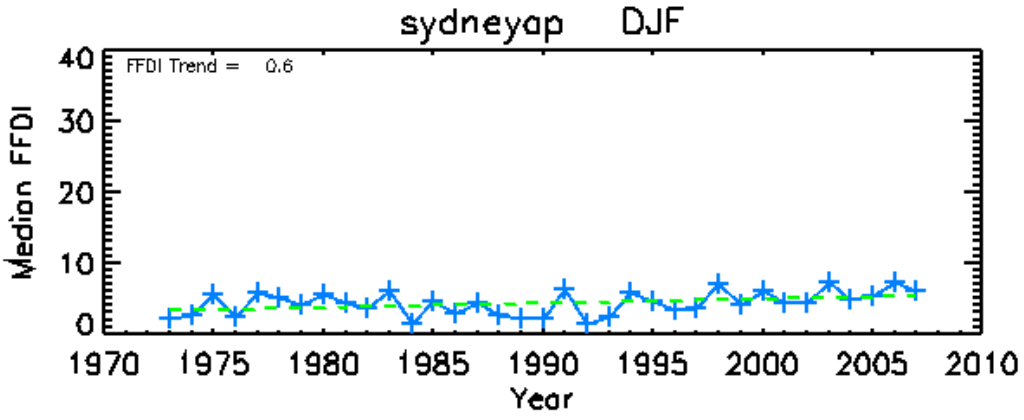

Wagga

variable	now	2020				2050			
		low2	low3	high2	high3	low2	low3	high2	high3
ΣFFDI	3319	3	3	9	10	6	6	29	33
VHE	32.6	34.8	35.0	39.7	40.3	37.1	37.2	56.3	57.6
%	0.0	6.8	7.3	21.8	23.5	13.8	14.0	72.7	76.8
xtrm	4.2	4.7	4.8	5.7	5.9	5.2	5.5	9.9	11.1
%	0.0	13.9	14.6	36.5	42.3	26.3	31.4	138.0	167.9
vxtrm	0.5	0.6	0.7	0.9	0.9	0.8	0.8	2.2	2.7
cata	0.1	0.1	0.1	0.1	0.2	0.1	0.1	0.3	0.5
DJF50	16.1	16.7	16.7	17.8	17.7	17.2	17.1	21.0	21.3
MAM50	7.1	7.2	7.2	7.4	7.5	7.3	7.4	8.0	8.2
JJA50	1.7	1.8	1.8	1.8	1.9	1.8	1.8	2.1	2.2
SON50	3.7	3.9	3.9	4.3	4.3	4.1	4.1	5.6	5.8
DJF90	36.5	37.4	37.7	39.3	39.7	38.3	38.6	45.8	47.2
MAM90	19.1	19.5	19.3	20.2	19.8	19.9	19.5	22.2	21.3
JJA90	4.9	5.1	5.2	5.2	5.5	5.1	5.3	5.8	6.7
SON90	17.6	18.7	18.9	20.6	21.2	19.6	20.0	28.1	30.4

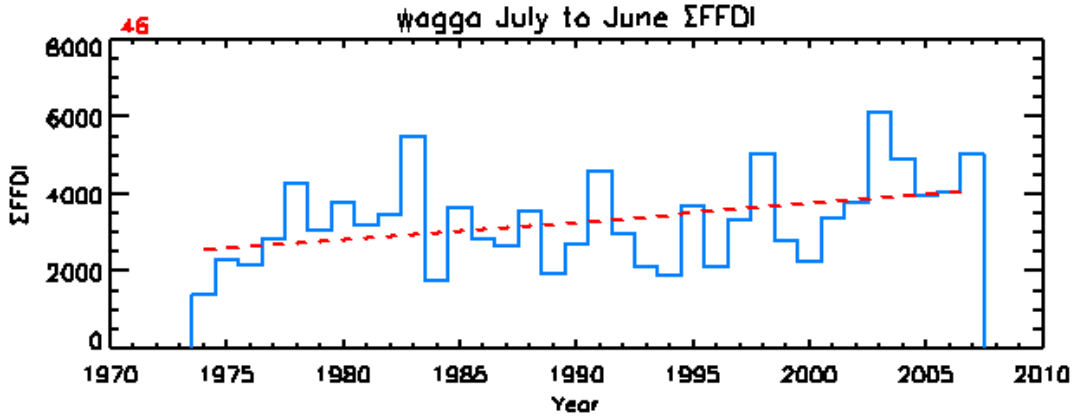

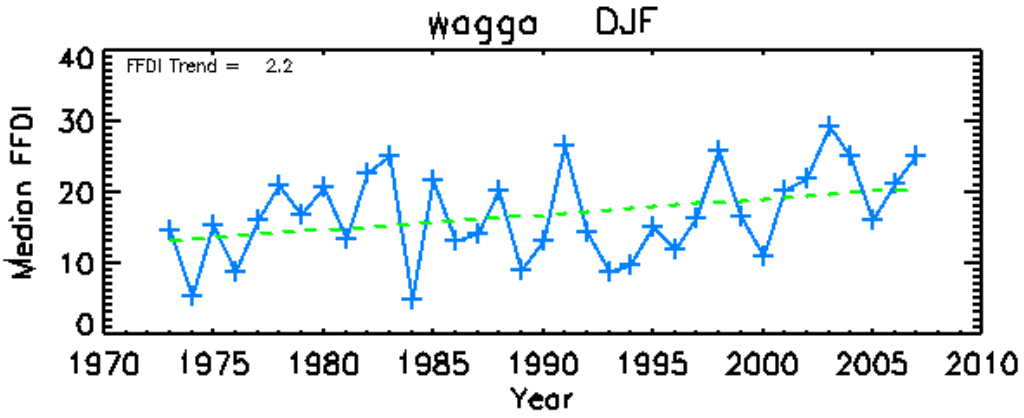

Williamtown

variable	now	2020				2050			
		low2	low3	high2	high3	low2	low3	high2	high3
ΣFFDI	1984	1	3	4	9	3	6	14	27
VHE	10.3	10.8	11.2	11.5	12.8	11.3	11.9	13.9	17.8
%	0.0	5.6	8.6	12.1	24.5	10.0	15.6	35.7	73.2
xtrm	1.4	1.6	1.7	1.7	2.3	1.6	1.9	2.4	4.1
%	0.0	10.6	17.0	17.0	61.7	14.9	36.2	66.0	189.4
vxtrm	0.2	0.3	0.3	0.3	0.5	0.3	0.4	0.5	1.1
cata	0.0	0.1	0.1	0.1	0.1	0.1	0.1	0.1	0.3
DJF50	4.5	4.6	4.7	4.8	5.0	4.7	4.8	5.2	5.8
MAM50	2.4	2.5	2.5	2.5	2.5	2.5	2.5	2.7	2.6
JJA50	2.5	2.6	2.6	2.7	2.6	2.7	2.6	3.0	2.8
SON50	4.3	4.3	4.4	4.4	4.7	4.4	4.6	4.7	5.6
DJF90	15.9	16.1	16.4	16.5	17.3	16.3	16.8	17.5	19.2
MAM90	8.9	9.0	9.1	9.0	9.5	9.0	9.3	9.2	10.3
JJA90	9.8	9.9	10.0	10.3	10.6	10.1	10.3	11.4	12.2
SON90	16.5	16.9	17.3	17.6	18.5	17.3	18.0	20.1	23.7

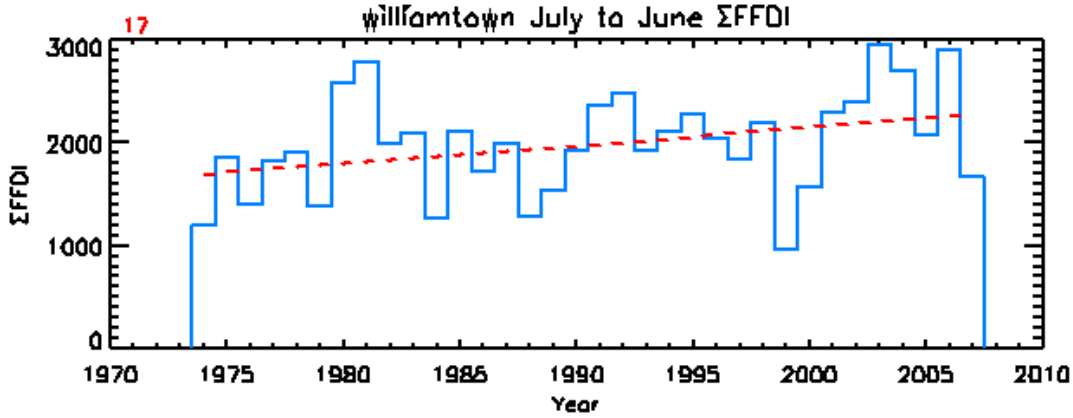

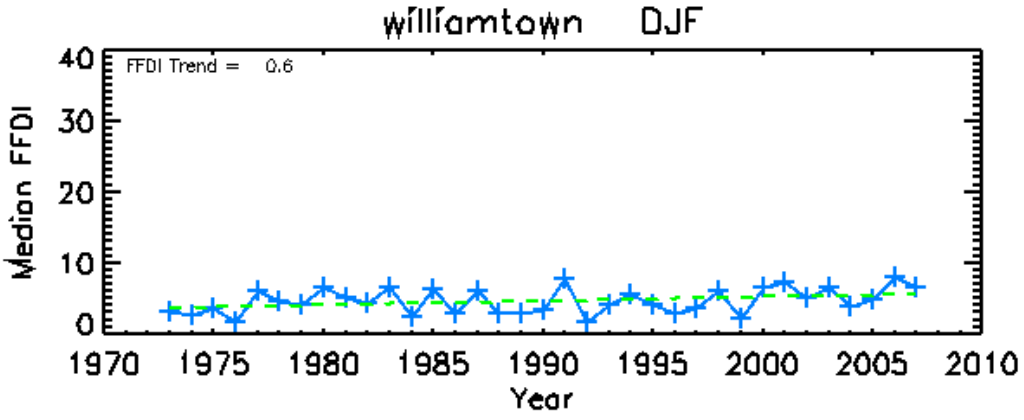

Woomera

variable	now	2020				2050			
		low2	low3	high2	high3	low2	low3	high2	high3
ΣFFDI	7249	1	2	5	6	3	4	15	20
VHE	109.1	112.3	112.8	118.1	119.4	115.2	115.9	135.4	139.1
%	0.0	3.0	3.4	8.2	9.5	5.6	6.3	24.1	27.5
xtrm	19.6	20.8	21.5	22.4	24.1	21.6	22.5	29.3	34.7
%	0.0	5.7	9.3	14.2	22.5	10.2	14.4	49.4	76.7
vxtrm	4.1	4.5	4.6	5.1	5.7	4.8	5.2	7.2	10.1
cata	0.9	1.0	1.1	1.3	1.5	1.2	1.3	1.9	2.9
DJF50	27.7	28.0	28.2	28.7	29.2	28.3	28.7	31.1	32.5
MAM50	14.7	14.9	14.9	15.2	15.3	15.1	15.1	16.3	16.7
JJA50	8.0	8.1	8.2	8.3	8.5	8.2	8.4	8.9	9.7
SON50	19.2	19.7	19.8	20.7	20.7	20.2	20.3	23.7	24.0
DJF90	50.5	51.1	51.7	52.3	53.7	51.7	52.7	55.9	60.5
MAM90	31.5	32.0	31.8	32.8	32.3	32.3	32.0	35.2	34.1
JJA90	20.0	20.5	20.5	21.3	21.5	20.8	20.9	24.0	25.0
SON90	46.4	47.6	47.9	49.4	50.2	48.3	48.9	55.4	58.3